

Mandibular Condyle Tissue Reaction to Low Intensity Pulsed Ultrasound  
in a Young Adult Rat Animal Model

by

Yasamin Hadaegh

A thesis submitted in partial fulfillment of the requirements for the degree of

Master of Science

in

Medical Sciences-Dentistry

University of Alberta

© Yasamin Hadaegh, 2014

## ABSTRACT

Mandibular condyle, especially in postnatal life, grows mainly by endochondral bone growth and has a pivotal role in development of the mandible and oro-facial complex as a whole. This important growth site of the mandible has unique adaptive remodeling in response to external stimuli even beyond natural growth. The mechanical stimulus produced by Low Intensity Pulsed Ultrasound (LIPUS) is osteoinductive and chondroinductive. It has been reported by previous studies that the application of LIPUS on the temporomandibular joint area can enhance mandibular growth in growing individuals. The aim of this thesis was to identify the effect of LIPUS on mandibular condylar remodeling in young adult rats.

Nineteen  $\approx$ 120-day-old female Sprague Dawley rats were allocated to experimental (n=10) and control (n=9) groups. The animals in the experimental group were sonicated bilaterally, 20 minutes each day for 28 consecutive days. The standard setting for LIPUS application used in the present study consisted of a 1.5 MHz sine wave repeated at 1 kHz at a spatial average temporal average intensity of  $30\text{mW/cm}^2$  with a pulsed width of 200  $\mu\text{s}$ . After euthanasia, gross morphological evaluation was performed on 2-dimensional photographs and 3-dimensional virtual models of hemi mandibles by means of AutoCAD and Geomagic QUALIFY software, respectively. Then, tissue reactions of the condylar head were assessed in the middle and posterior regions in sagittal plane. Evaluation of the mineralization and microstructure properties of subchondral cancellous bone was carried out with microcomputed tomography (micro-CT) scanning. Qualitative and histomorphometric analysis was performed on condylar cartilage and subchondral bone following Alcian-Blue Pas and Goldner's Trichrome staining. Vital fluorescent (calcein green) labeling was also utilized to determine the amount of endochondral bone growth in a time interval during the experimental period.

The two and three dimensional linear measurements of the mandibles were indicative of identical gross features of treated samples to untreated ones. However, a slight statistically non-significant increase in the condyle's growth direction (backward/upward) was detected in LIPUS group and the condylar cartilage was consistently thick and translucent in the most superior (middle) area in almost all experimental samples. In addition, comparing the average three-dimensional (computer generated) virtual models from experimental and control groups in the form of a 3-D deviation map was suggestive of enhanced periosteal bone apposition at the site of LIPUS application.

Histomorphometric and micro-CT analysis revealed that slight but statistically significant changes occurred at both cartilage and subcondral cancellous bone levels. In the posterior region, augmented total fibrocartilage, fibrous, and prechondroblastic layer thickness as well as increased cell population in the latter layer were detected. In the middle region, thickness as well as cell population in the chondroblastic layer also showed significantly higher values in the experimental group compared to that of the control group. Moreover, in subchondral cancellous bone, bone remodeling activity and active bone formation was increased in the middle region, which was detected by decreased bone volume fraction and increased percentage of newly formed bone and remnants of calcifying cartilage. In addition, osteoid thickness in trabecular bone subjacent to cartilage bone junction was 37% higher in the LIPUS group than in the control group. This was more evident in the middle region. The lower values of bone mineral density, bone volume fraction, trabecular thickness, and degree of anisotropy as well as higher values of bone specific surface and trabecular number obtained by micro-CT analysis in the LIPUS group compared to that of the control group also supported histomorphometric results. The changes in subchondral cancellous bone in the posterior region followed relatively the same trend but they

did not reach a statistically significant level. Even though we had technical difficulty in vital staining, the results were suggestive of a greater amount of endochondral bone formation in the experimental group compared to that of the control group.

In conclusion, LIPUS may stimulate both chondrogenesis and osteogenesis in young adult rat mandibular condyle and enhance endochondral bone formation and subcondral trabecular bone remodeling. This response is region specific probably due to differences in intrinsic maturity of the condylar cartilage in different regions (Middle versus Posterior). The middle region of the mandibular condyle maintains growth cartilaginous characteristic into the later stages and so it might be more responsive to LIPUS stimuli.

## **PREFACE**

This thesis is an original work by Yasamin Hadaegh. The research project, of which this thesis is a part, received research ethics approval from the University of Alberta Research Ethics Board, Project title: “The effect of low intensity pulsed ultrasound on mandibular condylar growth modification”, No. AUP00000381\_REN1, 11 June, 2013.

## **Dedication**

To:

*My parents and brother, who give me their endless support and love*

*My friends, who share with me their happiness and experiences*

## **Acknowledgement**

This work would not have been accomplished without the support and guidance from my estimable supervisors: Dr. T. El-Bialy and Dr. H. Uludag, to whom I am deeply indebted.

I wish to express my sincere gratitude to Dr. D. Douglas for his support and suggestions and Dr. S. Adeeb for giving me the opportunity to utilize their 3D software facilities.

I would also like to extend my heartfelt appreciation to Cezary kucharski and Harmanpreet Kaur for their generous cooperation.

I also deem it necessary to thank the respectable authorities of School of Dentistry, University of Alberta for their cooperation which made the accomplishment of this work possible.

This work was partially funded by fund for dentistry from university of Alberta (\$ 4500).

## TABLE OF CONTENTS

CHAPTER I:INTRODUCTION	1
I.I. Statement of the Problem	2
I.II. Literature Review	5
I.II.I. Growth Potential of the Temporo Mandibular Joint in Post puberty	5
I.II.II. Uniqueness of Mandibular Condylar Cartilage	9
I.II.III. Low Intensity Pulsed Ultrasound (LIPUS)	14
I.II.III.I. Osteogenic Potential of LIPUS	14
I.II.III.II. Chondrogenic and Fibrogenic Potential of LIPUS	19
I.II.III.III. Growth Modification of the Mandible with LIPUS	25
I.II.III.IV. Potential Mechanisms of Action of LIPUS	28
I.III. Objectives and Hypothesis	32
CHAPTER II: MATERIALS & METHODS	33
II.I. Experimental Design and Animals	34
II.II. LIPUS Application	35
II.III. Flourochrome Preparation and Injection	36
II.IV. Experiment Endpoint	36
II.V. Tissue Processing	37
II.VI. Gross Morphological Evaluation	37
II. VI.I. Morphometric Analysis on Two-Dimensional Photographs	37
II.VI.I.I. Statistical Analysis	38
II. VI.II. Linear Measurements on Three-Dimensional (3-D) Virtual Models	40

II.VI.II.I.	Statistical Analysis	42
II.VI.III.	3-D Visualisation	42
II.V.	Microscopic Histologic Evaluation	44
II.V.I.	Alcian Blue-Pas Staining	44
II.V.I.I.	Slide Preparation and Staining Protocol	45
II.V.I.II.	Quantitative and statistical analyses	45
II.V.II.	In vivo Flouochrome Labeling	48
II.V.II.I.	Slide Preparation	48
II.V.II.II.	Quantitative and Statistical Analyses	50
II.V.III.	Goldner's Trichrome Staining for Osteoid	51
II.V.III.I.	Staining Protocol	52
II.V.III.II.	Quantitative and Statistical Analyses	52
II.VI.	Micro Computed Tomography ( $\mu$ CT) Scanning	53
II.VI.I.	Quantitative and Statistical Analyses	54
CHAPTER III: RESULTS		56
III.I.	Body Weight	57
III.II.	Gross Morphological Evaluation	57
III.II.I	Morphometric Analysis on Two-Dimensional (2-D) Photographs	57
III.II.II.	Appearance of the Condylar Surface	61
III.II.III.	Linear Measurements on Three-Dimensional (3-D) Virtual Models	62
III.II.IV.	3-D Visualisation	63
III.III.	Histological Observation and Histomorphometric Analysis	64

III.III.I.	Condylar Cartilage	64
III.III.II.	Subchondral Cancellous Bone	66
III.IV.	Micro-CT Analysis	71
CHAPTER IV:DISCUSSION		76
REFERENCES		93
APPENDICES		125

## LIST OF TABLES

2-1	Determining the Landmarks, Linear and Angular measurements	39
2-2	The size of method error and single measures values of ICC test for histomorphometric parameters	47
2-3	The size of method error and single measures values of ICC test for bone densitometric and morphometric parameters evaluated by micro-CT analysis	55
3- 1	Values of Linear (mm) and Angular (°) Measurements in experimental and control groups	58
3-2	Values of linear measurements (mm) on 3-D virtual models in experimental and control groups	63
3-3	The comparison of histomorphometric parameters evaluated on decalcified sections stained with Alcian blue-PAS in experimental and control groups	67
3-4	The amount of endochondral bone growth ( $\mu\text{m}$ ) in experimental and control groups	69
3-5	The comparison of osteoid thickness ( $\mu\text{m}$ ) in experimental and control groups	70
3-6	The comparison of bone densitometric and morphometric parameters of subcondral cancellous bone in experimental and control groups evaluated by micro-CT analysis	75

## LIST OF FIGURES

2-1	Experimental set up	36
2-2	Determining the constant places on the lateral side of the mandible that each hemi-mandible sits on	37
2-3	Illustration of landmarks and measurements	39
2-4	One hemi mandible after aligning to the world coordinate system	41
2-5	Linear measurements on 3-D virtual model	41
2-6	Determining the most posterosuperior point of the condyle on 3-D mandible in Geomagic QUALIFY	42
2-7	Demonstration of averaging following best fit alignment of left hemi mandibles of the control group	43
2-8	An overview of a rat's mandibular condyle in the experimental group stained with Alcian Blue-PAS	46
2-9	3 reference points of the condylar head	49
2-10	Photomicrographs of undecalcified sections of mandibular condyle at mid sagittal plane	50
2-11	Measuring the distance between calcein labels	51
2-12	Demonstration of evaluated regions for osteoid thickness	53
2-13	1 Demonstration of measuring the osteoid thickness along the osteoid surface	53
2-14	Illustration of the method for locating the region of interest for micro-CT analysis	55
3-1	The change of weight of the animals in the control and LIPUS groups during acclimatization and experimental periods.	57
3-2	Demonstration of main linear variables for evaluating the size of the mandible	59
3-3	Demonstration of linear variables for evaluating condylar growth in different directions	59
3-4	Demonstration of increment in the degree of Alpha and geometrical reason...potential hypothetical regional changes in mandibular condyle	61

3-5	Condylar surface with dark (bone like) and translucent (thick cartilage) appearance	62
3-6	The comparison of linear measurements (mm) on 3-D virtual models for control and experimental groups	62
3-7	Lateral view of the virtual models of 3-D deviation map	63
3-8	Varied response of mandibular condyle in experimental animals and comparison to control , Alcian Blue PAS staining	64
3-9	Demonstration of increment in the thickness of chondroblastic layer at the middle region of the condyle, Alcian Blue PAS staining	65
3-10	Potential emergence or augmented chondroblastic layer in posterior and anterior end of the cartilaginous cap	66
3-11	Subchondral cancellous bone in the middle and posterior region of the condyle from control and experimental group, Alcian Blue PAS staining	66
3-12	The comparison of control and experimental groups with and without considering different regions for various histomorphometric parameters	68
3-13	The amount of endochondral bone growth in experimental and control groups	69
3-14	The comparison of Osteoid thickness ( $\mu\text{m}$ ) in experimental and control groups, Goldner's Trichrome staining.	70
3-15	Osteoid structure in subchondral cancellous bone in 148 days old rats, Goldner's Trichrome staining.	71
3-16	The comparison of the densitometric and morphometric parameters of the condylar subchondral bone between control and experimental groups with and without considering regions	74

## LIST OF ABBREVIATIONS

- $\mu$ CT: micro-computed tomography
- 2-D: two-dimensional
- 3-D: three-dimensional
- ALP: alkaline phosphatase
- ATP: adenosine 5'-triphosphate
- bFGF: basic fibroblast growth factor
- BMP: bit map
- BMPs: bone morphogenic proteins
- BS/BV: bone surface to volume ratio, bone specific surface
- BSP: bone sialoprotein
- BSSO: bilateral sagittal split osteotomy
- BV/TV: bone volume/tissue volume or percentage bone volume or bone volume fraction
- CBCT: cone beam computed tomography
- Cbfa1: core binding factor subunit alpha-1
- cDNA: complementary DNA
- COL2A1: collagen, type II, alpha 1
- COX2: cyclooxygenase-2
- CPC: chondrogenic progenitor cells
- CT: computed tomography
- CTGF: connective tissue growth factor
- DA: degree of anisotropy
- DI H<sub>2</sub>O: distilled water
- DNA: deoxyribonucleic acid
- ECM: extra cellular matrix

EtOH: ethanol

FAK: focal adhesion kinase

FDA: food and drug administration

FGF: fibroblast growth factor

Flt-1: fms-related tyrosin kinase 1 is VEGFR-1: vascular endothelial growth factor 1

FMA: functional mandibular advancer

FRD: forsus<sup>TM</sup> fatigue-resistant device

G protein: guanin nucleotide binding protein

Gdf5: growth differentiation factor 5

GEE: generalized estimating equation

HU: hounsfield unit

Hz: hertz

ICC: intraclass correlation coefficient.

ICP: iterative closest point algorithm

IGF: insulin like growth factor

IHH: indian hedge hog

IL- : interleukin

iNOS: inducible nitric-oxide synthase

IQR: inter-quartile range

IVC: individually ventilated caging

KDR/FLK-1: kinase insertdomain receptor/fetal liver kinase 1 is VEGFR-2: Vascular endothelial growth factor 2

L: left

LIPUS: low intensity pulsed ultrasound

LO: lysyl oxidase

L-SOX5: long form SRY (Sex determining region Y)-box5

M: middle region

MARA: mandibular anterior repositioning appliance

MARK: mitogen activated protein kinases, originally called, ERK: extracellular signal-regulated kinases

MCC: mandibular condylar cartilage

MDO: mandibular distraction osteogenesis

MP: mandibular plane

MRI: magnetic resonance imaging

mRNA: messenger RNA

MSCs: mesenchymal stem cells

Myf6: myogenic factor 6

NP: nucleus pulposus

NZ: New Zealand

OC: osteocalcin

OSAS: obstructive sleep apnea syndrome

P: posterior region

PAS: periodic acid and Schiff's reagent

PDGFs: platelet-derived growth factors

PGE2: prostaglandinE2

PI3K/Akt: phosphatidylinositol 3 kinase/ threonine protein kinase pathway

PI3K: phosphatidylinositol 3 kinase

PTHrp: parathyroid hormone-related peptide

R: right

RANKL: receptor activator nuclear kappa-B ligand

Ranx2: runt-related transcription factor 2

rGH: recombinant growth hormone

RNA: ribonucleic acid

RT: room temperature

SATA: spatial average temporal average

Shox 2: short stature homeobox2

SOX9: SRY (Sex determining region Y)-related HMG (high mobility group) box9

STL: stereolithograph

SUS: sabbagh universal spring

Tb. Sp: trabecular separation

Tb.N: trabecular number

Tb.Th: trabecular thickness

TFBC: twin force bite corrector

TGF-  $\beta$ : transforming growth factor  $\beta$

TMD: temporomandibular joints dysfunction

TMJ: temporomandibular joint

TNF: tumor necrosis factor

VEGF: vascular endothelial growth factor

W: Watt

# CHAPTER I: INTRODUCTION

---

## **II. STATEMENT OF THE PROBLEM**

Underdevelopment of the lower jaw is one of the most common deformities of craniofacial region (Mc Namara J. 1981; Proffit W. et al., 1998; Cozza P. et al., 2006; Kaneyama K. et al., 2008; Pirttiniemi P. et al., 2009). This malformation not only affects functional occlusion and aesthetic appearance of the face (Pirttiniemi P. et al., 2009; Proffit W.R., 2013c) but also may lead to upper airway obstruction (Azgara-Calero E. et al., 2012; Flores-Mir C. et al., 2013). Thus, the consequences of this deformity can adversely affect the quality of life of the patients (Seehra J. et al., 2011; Proffit W.R., 2013c).

Over the last decades, we have witnessed an ever-increasing number of young adult patients with mandibular deficiency who are demanding cost-effective, non-surgical, and high-quality treatment with increased efficiency (Khan R.S. and Horrocks E.N., 1991; Vanarsdall R.L. and Musich D.R., 2005; Sood S., 2010). Despite this, surgical interventions for advancing the mandible such as sagittal split osteotomies and distraction osteogenesis remain as the choice remedy especially in severely affected patients (Pancherz H., 2000; Ruf S. and Pancherz H., 2004; Kinzinger G. et al., 2008; Ow A.T.C. and Cheung L.K., 2008; Randerath W.J. et al., 2011). Unfortunately, such procedures are costly and risky in essence, and also suffer from limitations and unclear stability (Kersey M.L. et al. 2003; Ow A.T.C. and Cheung L.K., 2008; Ow A. and Cheung L.K. 2009; Tucker M.R. and Farrell B.B., 2014). In recent years, however, fixed bite-jumping appliances such as the Herbst appliance has been utilized for treating young adult patients with mandibular deficiency, and favorable skeletal response and improved facial profile have been reported (Ruf S. and Pancherz H., 1999a; Ruf S. and Pancherz H., 2006; Chaiyongsirisern A. et al., 2009; Kinzinger G. et al., 2009).

Mandibular condyle, especially in post natal life, grows mainly by endochondral bone growth and has a pivotal role in development of the mandible and oro-facial complex as a whole (Von den Hoff J.W and Delatte M., 2008; Sperber G.H. et al., 2010; Patil A.S. et al., 2012). The growth of the condyle is known to be highly adaptable to functional factors, or in other words altered mechanical loading (Shen G. and Darendeliler A., 2005; Meikle M.C., 2007; Von den Hoff J.W and Delatte M., 2008; Owtad P. et al., 2011; Puricelli E. et al., 2012). This distinctive characteristic of the condyle is the fundamental rationale for therapies with different bite-jumping appliances (Shen G. and Darendeliler A., 2005; Shen G. et al., 2006). Similar to

growing condyle, several studies on primates, rodents, and humans have demonstrated growth adaptation in adult condyle in response to continuous forward positioning of the mandible (Mc Namara J.A. Jr. et al., 1982; Woodside D.G. et al., 1983; Hinton R.J. and Mc Namara J.A. Jr., 1984 a and b; Woodside D.G. et al., 1987; Mc Namara J.A. Jr. et al., 2003; Rabie A.B. et al., 2004b; Xiong H. et al., 2004, 2005a and b; Tagliaro M. L. et al., 2006 and 2009; Paulsen H.U. et al., 1995, 1998 and 2000; Konick M. et al., 1997; Ruf S. and Pancherz H., 1999b and 2004; Aidar L.A. et al., 2006; Maia S. et al., 2010). The treatment reactivates chondrogenesis in adult condylar cartilage which otherwise is at resting status and eventually leads to increased bone formation (Shen G. and Darendeliler A., 2005; Rabie A.B. et al., 2004b).

Final recommendation by the available clinical studies is that fixed bite-jumping appliances are the appropriate alternative for borderline<sup>1</sup> adult patients with under-developed mandibles that may require surgery (Ruf S. and Pancherz H., 1999 a, b, and 2006; Nalbantgil D. et al., 2005; Pancherz H. and Ruf S., 2008b; Bremaen J.V. et al., 2009; Chaiyongsirisern A. et al., 2009; Bock N.C. et al., 2010; Kabbur K.J. et al., 2012). It is undeniable that compared to the growth peak period, skeletal changes by this therapy in adults are slower and lesser which is due to lower growth and remodeling activity in adult mandibular condyle, (Ruf S. and Pancherz H., 1999a; Ruf S. and Pancherz H., 2006; Liu J. et al., 2009; Bremaen J.V. et al., 2009; Frye L. et al., 2009). However, it is noteworthy that repeated mechanical loading (i.e: stepwise mandibular advancement) compared to the one step method can increase new bone formation, condylar growth (Rabie A.B. et al. 2003a; Ng T.C. et al., 2006a and b), and hence skeletal changes (Purkayastha S.K. et al., 2008; Chaiyongsirisern A. et al., 2009). This shows that by exploiting more efficient techniques the potential of bone formation and remodeling can be enhanced further even in adult mandibular condyle.

In recent years, for intensifying mandibular condylar growth, some novel techniques have been suggested by various research groups such as local application of mesenchymal stem cells (Oyonarte R. et al., 2013), variety of growth factors (Suzuki S. et al., 2004; Rabie A.B. et al., 2007; Kaur H. et al., 2014), growth hormone (Khan I. et al., 2013) , parathyroid hormone (Wana Q. et al., 2010; Liu Q. et al., 2012), low level laser (Seifi M. et al., 2010; Abtahi M. et al. 2012),

---

<sup>1</sup> Those patients who could have been treated by dentofacial orthopedic means during their active growth period (Ruf S. and Pancherz H., 2006).

light emitting diode (LED) (El-Bialy T. et al., 2014), and low intensity pulsed ultrasound (LIPUS) (El-Bialy T. et al., 2003; El-Bialy T. et al., 2006; Oyonarte R. et al., 2009; El-Bialy T. et al., 2010; Oyonarte R. et al., 2013; Khan I. et al., 2013; Kaur H. et al., 2014).

LIPUS is an acoustic pressure wave above the limit of human hearing with the capability to transfer mechanical energy into biological tissues and trigger biochemical events at the cellular level (Khanna A. et al., 2009). This safe, easy to use, and cost effective physical modality has been approved by the FDA (food and drug administration), USA for enhancing bone fracture healing (Kasturi G. et al., 2011; Bashardoust T. et al., 2012). LIPUS may have a direct effect on several cell lines including chondrocytes, endothelial cells, and osteoblasts, which are involved in inducing the cellular process of chondrogenesis, angiogenesis, and osteogenesis (Azuma Y. et al., 2001; Zhang Z.J. et al., 2003; Warden S.J. et al., 2006; Kobayashi Y. et al., 2009; Khanna A. et al., 2009; Katano M. et al., 2011). By stimulating chondrogenesis, cartilage hypertrophy, angiogenesis, and osteogenesis LIPUS may lead to earlier onset and enhanced endochondral bone formation than the natural process (Tsumaki N. et al., 2004; Rutten S. et al., 2008; Khanna A. et al., 2009; Katano M. et al., 2011; Coords M. et al., 2011).

Application of LIPUS on the Temporomandibular joint (TMJ) region has been shown to enhance condylar and mandibular growth in growing species especially under continuous mandibular advancement (El-Bialy T. et al., 2003; El-Bialy T. et al., 2006; Oyonarte R. et al., 2009; El-Bialy T. et al., 2010; Oyonarte R. et al., 2013; Khan I. et al., 2013; Kaur H. et al., 2014). In these studies, histologic and histomorphometric changes were to some extent able to delineate chondrogenic and osteogenic effects of LIPUS in growing mandibular condyle (El-Bialy T. et al., 2003; El-Bialy T. et al., 2006; Oyonarte R. et al., 2009; Oyonarte R. et al., 2013; Kaur H. et al., 2014). Nonetheless, the effect of LIPUS on adult condyle remodeling has yet to be investigated. Thus, in the present study we aimed to explore if LIPUS can stimulate cartilage and bone formation in the mandibular condyle of young adult rats. Our further objective was to evaluate if the potential stimulatory effect is great enough to enhance the efficacy of fixed bite-jumping appliances, i.e. increasing skeletal effect in young adults.

## **I.II. LITRATURE REVIEW**

### **I.II.I. Growth Potential of the Temporomandibular Joint (TMJ) in Postpuberty**

Endochondral as well as periosteal bone formation are important for growth of the mandible. The mandibular body becomes longer only through periosteal apposition of the bone on its posterior surface. However, the increase in the height of the mandibular ramus occurs by endochondral replacement of the condyle along with surface remodeling (Proffit W.R., 2013 a and b). The Temporomandibular joint, a bilateral synovial articulation between the mandible and temporal bone, is a critical contributor to the growth of the mandible in length and height (Hinton R.J., 2014). The proper conception is that the mandible is translated downward and forward while at the same time its size increases by growing upward and backward. The growth rate before puberty is relatively fixed at about 2-3 mm per year for body length and 1-2 mm per year for ramus height (Proffit W.R., 2013 a and b). It has been suggested that this growth rate in the growth peak period is more than before or after peak (Hagg U. and Pancherz H. et al., 1988). Nevertheless, the growth of the condyle and remodeling of the glenoid fossa (compartments of the temporomandibular joint) can continue or can be reactivated many years after the age of twenty (Pancherz H., 2000). The following research findings can support this statement.

It has been demonstrated in various studies that the growth of the craniofacial skeleton may continue to a substantial extent in both genders well into the third decade of life (Behrents R.G., 1985). The growth of the facial skeleton continues during adult life in all dimensions with vertical changes more prominent than anteroposterior changes and width changes least evident. There is a cephalocaudal gradient in the growth of the facial skeleton which means more mandibular than maxillary changes in adult life (Proffit W.R., 2013b).

Based on histologic findings, condylar cartilage matures with age to an adult form with no obvious hypertrophic layer. However, in the adult mandibular condyle, zones of unmineralized growth cartilage and undifferentiated mesenchyme are present (Blackwood H.J.J., 1966; Durkin J. et al., 1973; Ingervall B. et al., 1976; Hanson T. and Nordström B., 1977; Carlson D.S. et al., 1978; Oberg T. et al., 1985; Luder H.U. and Schroeder H.E., 1992; Bathia S.N. and Leighton B.C., 1993; Paulsen H.U., 1999). The presence of remnants of mesenchymal cells opens the possibilities of re-activating growth and the remodeling potential of the condyle (Rabie A.B., 2004b). In addition, adult mandibular condylar cartilage, unlike the epiphysial articular cartilage,

displays continuous turnover of chondrocytes during the process of endochondral ossification<sup>2</sup> (Tajima Y. et al., 1998).

Observations associated with mandibular osteotomies, condylar fracture therapy, and mandibular repositioning in disc displacement therapy have shown that the adult TMJ is able to remodel (Jacobsen P.U. and Lund K., 1972; Hollender L. and Ridell A., 1974; Lindahl L. and Hollender L. 1977; Edlund J. et al., 1979; Hellsing G. et al., 1985; Westesson P.L. and Lundh H., 1988; Yattani H. et al., 1991; Sato H. et al., 1997).

It is reported that the adult TMJ retains the ability to adapt to alterations in the mechanical equilibrium of the joint, regardless of the cessation of skeletal growth (Lubsen C.C. et al., 1985). Preliminary mandibular protrusion experiments on adult animals showed negligible or no adaptive changes in the temporomandibular joint area (Hiniker J.J. and Ramfjord S.P., 1966; Ramfjord S.P. and Enlow R.D., 1971; Ramfjord S.P. et al., 1971; Mc Namara J.A. Jr., 1972 and 1973; Adams C.D. et al., 1972; Mc Namara J.A. Jr. et al, 1975; Ramfjord S.P. and Blankenship J.R., 1981). However, more recent experimental studies on adult monkeys (Mc Namara J.A. Jr. et al., 1982; Woodside D.G. et al., 1983; Hinton R.J. and Mc Namara J.A. Jr., 1984 a and b; Woodside D.G. et al., 1987; Mc Namara J.A. Jr. et al., 2003) and rats (Rabie A.B. et al., 2004b; Xiong H. et al., 2004, 2005a and b) have clarified that condylar growth can be stimulated and the glenoid fossa remodeled by the continuous mechanical strain from using bite jumping appliance. The adaptive process in the adult condyle and glenoid fossa are qualitatively similar to that of growing animals but quantitatively they are lessened.

Mandibular advancement by trimming lower incisors resulted in condylar growth in one month in 16 month old female mice (Tagliaro M.L. et al., 2006) as well as 7 and 15 month old male mice (Tagliaro M.L. et al., 2009). The authors concluded that functional orthopedic therapy in mature and old individuals can result in favourable mandibular respond.

In two well controlled prospective longitudinal studies conducted by Ruf and Pancherz, the successful treatment of young adults with class II malocclusion by a Herbst appliance has been demonstrated. In all individuals, mandibular protrusion was successfully achieved and as a result skeletal and soft tissue profile convexity was diminished. Condylar and glenoid fossa remodeling in almost all temporomandibular joints has been detected through magnetic resonance imaging

---

<sup>2</sup> This is mediated by the basic fibroblast growth factor-heparan sulphate complex.

(MRI) (Ruf S. and Pancherz H.; 1999a and b). However, it is noteworthy that in both histological animal experiments and in MRI Herbst studies, the signs of condylar remodeling appeared later during mandibular protrusion in older individuals than in younger ones (Ruf S. and Pancherz H.; 1999a).

In patients after pubertal growth spurt, subsequent to treatment with Herbst appliances, Computed Tomography (CT) evaluation demonstrated remodeling of the glenoid fossa and condyle, TMJ adaptation and airway widening (Paulsen H.U. et al., 1995, 1998 and 2000; Konick M. et al., 1997; Ruf S. and Pancherz H., 2004; Aidar L.A. et al., 2006; Maia S. et al., 2010).

Upon application of mechanical strain as a result of mandibular advancement in adult individuals, IHH (Indian Hedgehog morphogen), which is a mechanotransduction mediator, is expressed by cells within the condylar tissue. In turn, IHH increases cellular replication and cartilage formation in the condyle, resulting in condylar growth. The suggested mechanism is that IHH, in the condyle, activates the Parathyroid hormone-related peptide (PTHrP) pathway in response to mechanical strain. The transcription factor SOX9 (SRY (Sex determining region Y) box9) is the target for PTHrP signaling and is also the factor that regulates the differentiation of replicating mesenchymal cells to chondroblasts. Furthermore, SOX9, expressed by chondrocytes, regulates the synthesis of type II collagen, the major component of the condylar cartilage matrix (Xiong H. et al., 2005a). The cells constituting this newly formed cartilaginous matrix in the condyle would undergo hypertrophy and synthesize hypertrophic matrix. The framework of the hypertrophic matrix is type X collagen, whose expression precedes the onset of endochondral ossification in mandibular condyles. Indeed, the up regulation of type II and X collagen followed by increased new bone formation has been observed in adult condyle following mandibular advancement (Rabie A.B. et al., 2004b). On the other hand, as a result of mandibular advancement of the adult condyle, the angiogenic mediator Vascular Endothelial Growth Factor (VEGF) is also expressed. Neovascularization is the crucial step in endochondral ossification and marks the onset of ossification (Xiong H. et al., 2005b). Increased replication of undifferentiated mesenchymal cells in the erosive zone has also been reported as a result of mandibular advancement. One explanation for this increase is that newly formed blood vessels are rich in undifferentiated mesenchymal cells and the larger the population size of mesenchymal cells, the

more the possibility of osteoprogenitor cells (Rabie A.B. 2003b; Xiong H. et al., 2005a; Pukayastha S.K. et al., 2008).

Local periodic injection of IGF-I (Insulin like Growth Factor-I) (50µg/ml) into articular capsules of mandibular condyles in the 15-week-old (mature) male rats also led to an increase in the thickness of the cartilaginous layer, a decrease in the percentage bone area in the subchondral cancellous bone layer of the condyle, and a larger endochondral bone growth. These observations proved that local injection of IGF-I into the mature condyle reactivated the process of endochondral bone formation and induced an actual bone growth in the mature condyle (Suzuki S. et al., 2004).

IGF-I is a crucial regulator in many tissues while their postnatal development via promoting mitogenesis, cell migration, survival and protein synthesis by autocrine, paracrine, and endocrine mechanisms. There is strong evidence to show that IGF-I plays a major role in the regulation of skeletal growth and development (Chen Y. et al., 2012). IGF-I has a significant effect on the bone by stimulating proliferation and promoting differentiation of osteoblastic tissues (Maki R.G. et al., 2010). In the growth plate of longitudinal bone, IGF-I is a key growth factor for stimulating proliferation and differentiation of chondrocytes (Wu S. et al., 2008). IGF-I regulated adaptive remodeling of mandibular condylar cartilage by a commencement or enhanced proliferation of chondrocytes through the MARK-ERK pathway<sup>3</sup> (Shen G. and Darendeliler M.A., 2005). Strong immunostaining of IGF-I has been observed in the proliferative chondrocyte layer mainly, as well as in the hypertrophic chondrocyte layer of condylar hyperplasia (Meng Q. et al., 2011). IGF-I promoted the expression of type II Collagen, alpha 1 in chondrocytes and therefore enhanced the cartilage growth augmenting the matrix synthesis capacity of chondrocytes (Chen Y. et al., 2012). It has been shown that IGF-I plays a role in cartilage growth by promoting the proliferation and differentiation of chondroblasts (Visnapuu V. et al., 2001). Seemingly, IGF-I has an especial role in the expression of  $\beta$ 1 integrins ( $\alpha$ -1,  $\alpha$ -3,  $\alpha$ -5 subunits) through which several physiological sub-processes of chondrogenesis take place (Patil A.S. et al., 2012).

---

<sup>3</sup> MARK-ERK pathway is a series of intracellular proteins that organize a signal from a receptor on the surface of the cell to the DNA in the nucleus of the cell. The pathway includes many proteins, including MARK (mitogen activated protein kinases), originally called ERK (extracellular signal-regulated kinases), which communicate by adding phosphate groups to the neighboring protein, which acts as an “on” or “off” switch (Orton R.J. et al, 2005).

### **I.II.II. Uniqueness of Mandibular Condylar Cartilage (MCC)**

The Mandibular condyle, especially in post natal life, grows mainly by endochondral bone growth and has a pivotal role in development of the mandible and oro-facial complex as a whole (Von den Hoff J.W. and Delatte M., 2008; Sperber G.H. et al., 2010; Patil A.S. et al., 2012). The growth of the condyle is known to be highly adaptable to functional factors or in other words altered mechanical loading (Von den Hoff J.W. and Delatte M., 2008; Shen G. and Darendeliler M.A., 2005; Shen G. et al., 2006). This distinctive adaptability of the mandibular condyle is the fundamental rationale for therapies with different mandibular forward positioning devices (Shen G. and Darendeliler M.A., 2005; Gong F.F. et al., 2011). In the process of TMJ's growth and development and its adaptive response to mandibular advancement, the role of the mandibular condyle is strikingly higher than that of glenoid fossa, which grows by intramembranous ossification. This greater adaptability of mandibular condyle means that the rate of proliferation and hypertrophic activities and hence morphological changes are much higher in the mandibular condyle than in the glenoid fossa (Owtad P. et al., 2010; Barnouti Z.P. et al., 2011; Owtad P. et al., 2013). Therefore, in the present study, explained in the succeeding chapters, we only focused on the effect of LIPUS, as a form of mechanical loading, on the mandibular condyle.

Mandibular condylar cartilage does not look or act like an epiphyseal cartilage during orthopedic treatment (Voudouris J.C. and Kuftinec M.M., 2000) or during LIPUS therapy (please see sections I.II.III.II. and I.II.III.IV). Hence, in this section we emphasise the documented differences of these two structures to partially explain why their mode of action varies so greatly.

MCC is a unique cartilage classified as secondary cartilage<sup>4</sup>, and differs from the primary cartilage found in long bones in various ways:

Primary cartilage forms early in prenatal development and has two dissimilar forms: articular cartilage and growth plate cartilage. These are formed following the emergence of the secondary ossification centre in the epiphysis. Articular cartilage, in different joints, acts as load bearing cartilage, while growth plate cartilage serves as the template of longitudinal growth in long

---

<sup>4</sup> Secondary cartilage can also be seen in the structures of the maxilla, the mandibular symphysis, and the angular and coronoid processes (Litsas G. et al., 2010). Contrary to these secondary cartilages that are transient, mandibular condyle develops partly to permanent articular cartilage (Von den Hoff J.W. and Delatte M., 2008).

bones. Mandibular condylar cartilage forms later in prenatal development and plays both of these roles during growth. After growth is completed, the hypertrophic chondrocytes disappear from the ossification front of MCC which becomes articular cartilage (Takahashi I. et al., 1996).

The primary epiphysial cartilage reacts while in development, primarily to systemic growth stimuli such as hormones. In addition, tissue-separating force is the main factor in determining the length of long bones. The primary epiphysial cartilage has relatively little adaptive potential over the short-term to local stimuli, since it is covered by a thin perichondrium and has no fibrocartilaginous cap (Voudouris J.C. and Kuftinec M.M., 2000).

In contrast, the mandibular condyle does not have significant tissue-separating force, but condylar cartilage has a unique multidirectional capacity for growth and remodeling and has a significant adaptive growth with short term mechanical stimulation. In fact, compared with epiphyseal chondrocytes, condylar prechondroblasts are not surrounded by an intracellular matrix to isolate them from local factors (Johnston L.E. Jr., 1987; Voudouris J.C. and Kuftinec M.M., 2000). The most intriguing biological aspect of condylar cartilage that differs from synovial or epiphysial cartilage lies in its capability of adaptive remodeling to external stimuli (e.g.: condylar repositioning, articular functioning, and mechanical loading) during or after natural growth. This adaptive capability can be achieved by altering or reactivating chondrogenesis and subsequently endochondral ossification in growing and adult individuals respectively (Kantomma T. and Ronning O., 1997; Nakano H. et al., 2003; Shen G. et al., 2003; Rabie A.B. et al. 2003e; Chayanupatkul A. et al., 2003; Rabie A.B. et al., 2004a). In fact, unlike epiphysial cartilage with only a thin perichondrium, MCC is covered by a fully developed mesenchymal tissue layer. This mesenchymal covering of the condyle is responsible for the crucial characteristic of the condylar cartilage or in other words significant adaptive growth to external stimuli (Delatte M. et al., 2005).

While extreme phenotypic changes can be observed in the epiphysial cartilage after pubertal growth, condylar cartilage chondrocytes are existent all through postnatal life and their biological features remain unchanged (Shen G. and Darendeliler M.A., 2006). Moreover, these two structures differ in modes of proliferation and differentiation, cell alignment, invading capillary pattern, and extracellular matrix production, as has been observed (Wang L. and Detamore M.S., 2007).

The mandibular condylar cartilage, in contrast to the primary cartilages, derives from alkaline phosphatase-positive cells of the periosteum (Shibata S. et al, 2002) or as a condensation separate from the developing bone (Vinkka H. et al., 1982; Anthwal N. et al., 2008). There is a seamless conversion from a periosteum on the ramus to a perichondrium in the force bearing mandibular condyle. This seamless conversion is reflected in the spatial continuity of the fibrous and osteogenic layers of the periosteum with the articular and prechondroblastic layers of the perichondrium (Hinton R.J., 2014). Mandibular condylar cartilage as a secondary cartilage is dissimilar to primary cartilages, especially in its superficial layers. These layers consist of a perichondrium in which prechondroblastic cells that are relatively undifferentiated secrete a matrix rich in type I collagen rather than the type II collagen matrix usually secreted by chondrocytes (Mizoguchi I. et al., 1990). These relatively undifferentiated cells by their proliferation and differentiation are responsible for the growth at the mandibular condylar cartilage (Carlson D.S. et al., 1980). However, chondrocytes in the mandibular condylar cartilage secrete typical cartilage specific products such as type II collagen, aggrecan, and type X collagen (Shibata S. et al., 2006). Another notable differing characteristic of these proliferative cells compared to that of primary cartilage is that they have a dual potential for differentiation to either cartilage or bone, depending on the mechanical forces affecting them. This dual potential can be explained by their ability to express both Sox 9 and Runx2 (Runx-related transcription factor 2) ribonucleic acid (chondrogenic and osteogenic markers, respectively) and by the preferential localization of the cell fate mediators Notch and Twist to these cells (Serrano M.J. et al., 2011). Based on the above mentioned capability of differentiation to either cartilage or bone, localized transformation of perichondrium to periosteum can occur in regions subjected to biomechanical forces or low oxygen tension (Hall B.K., 1972). Thus secondary cartilages can shrink or be replaced by bone if the mechanical stimulus is altered. Placement in a non-functional environment, lack of movement, or reduced loading can result in reduction or loss of the cartilaginous phenotype (Hinton R.J., 1988).

In brief, primary and mandibular condyle cartilages differ in their biochemical composition, histological organization, metabolism and growth pattern in response to the growth factors and biomechanical stimuli (Visnapuu V. et al., 2001). The growth of this cartilage is partially determined genetically and robustly influenced by two types of epigenetic factors: systemic

factors (hormones and vitamins) and local factors (growth factors and mechanical stimuli) (Von den Hoff J.W. and Delatte M., 2008). MCC as highlighted above has an unusual manner of development and has distinctive characteristics; thus molecular determinants of development and growth of the TMJ could be different from those in the primary cartilaginous joints.

A diversity of biomolecules has been suggested as regulators for TMJ remodeling. These include IHH; PTHrP (a critical component of the IHH regulatory loop) (Rabie A.B. et al., 2003d; Shibukawa Y. et al., 2007); Shox 2 (Short stature homeobox2) (Gu S. et al., 2008); Sox 9 (Rabie A.B. et al. 2003c); L-Sox 5 (long form SRY [Sex determining region Y]-box5) (Chu F.T. et al., 2008); Runx2, also known as Cbfa1 (Core binding factor subunit alpha-1) (Hinton R.J., 2014; Rabie A.B. et al., 2003e and 2004a); type II collagen (Rabie A.B. et al. 2003c); type X collagen (Shen G. et al., 2006); IGF-I and II (Haijar D. et al., 2003; Patil A.S. et al., 2012); VEGF (Rabie A.B. et al., 2007; Owtad P. et al., 2010); FGFs (Fibroblast Growth Factors) (Owtad P. et al., 2010; Hinton R.J., 2014); TGF- $\beta$  (Transforming growth factor  $\beta$ ) (required for both proliferation of osteoprogenitor and chondroprogenitors) (Hinton R.J., 2014); and BMPs (Bone Morphogenic Proteins) (Barnouti Z.P. et al., 2011); Notch signaling pathways<sup>5</sup> (Serrano M.J. et al., 2014); and Wnt/  $\beta$ -catenin pathway<sup>6</sup> (Hinton R.J., 2014).

Between mandibular condylar cartilage and cartilage of the limbs, there are distinct differences in gene expression. Some of them are as follows:

The presence of extremely overlapping expressions of type I collagen, type II collagen, and type X collagen in mandibular condylar cartilage, all of which indicates rapid chondrocyte hypertrophy (Shibata S. et al., 1997). Thus, the cell cycle is exited and the differentiation to hypertrophic chondrocytes, which is a crucial step in osteoblast induction, is rapid. This rapid differentiation leads to pre-hypertrophy and IHH up regulation (Buxton P.G. et al., 2003). Gdf5 (growth differentiation factor 5) and Gdf6 proteins that have been observed in the joint cavities of the developing limb are absent in mandibular condylar cartilage (Purcell P. et al., 2009). Osteopontin and bone sialoprotein expression in these two structures are different (GU S. et Al.,

---

<sup>5</sup> The notch signaling pathway is important for the cell-cell communication that encompasses gene regulation mechanisms, which, in turn, control the multiple cell differentiation process for embryonic as well as adult life (Oswald F. et al., 2001).

<sup>6</sup> The Wnt/ $\beta$ -catenin pathway regulates stem cell pluripotency and cell fate decisions during development. This developmental cascade integrates signals from other pathways, including retinoic acid, FGF (fibroblast growth factor), TGF- $\beta$ , and BMP, within different cell types and tissues (Angers S. and Moon R.T., 2009).

2008). Responses to gene inactivation in limbs compared to those responses in mandibular condylar cartilage are qualitatively different (Yasuda T. et al., 2010). In limb bud development, Sox-9 expressing osteochondroprogenitors give rise to Runx2- expressing osteogenic cells (Akiyama H. et al., 2005). Nonetheless, studies showed that in secondary cartilages the reverse is correct: chondrocytes form by means of an up-regulating of Sox-9 in a precursor population expressing Runx2 (Shibata S. and Yokohama-Tamaki T., 2008). Current evidence suggests that the nature of the prechondroblastic cells of the mandibular condylar cartilage is not undifferentiated mesenchymal stem cells as previously believed, but (already differentiated) Runx2-expressing periosteum-like cells that are bipotent between osteogenic and chondrogenic lineages (Shibata S. et al., 2006). VEGF-B, VEGF receptors Flt-1, and kinase insert domain receptor/Flk-1-KDR are expressed, respectively, twice, three times and four times as high in the perichondrium as in the cartilage (Hinton R.J. et al., 2009). A nine fold enrichment of myogenic factor 6 (Myf6) in the perichondrial sample has been also reported (Hinton R.J., 2014). The degree of unsuspected plasticity in this bipotent cell population derived from an osteogenic lineage can be understood from the high expression of above mentioned genes. It has been hypothesized that Osterix, which is a crucial zinc-finger transcript factor for osteoblast differentiation, rather than Runx2 may have a direct interaction with Sox9 in condylar cartilage formation (Shibata S. and Yokohama-Tamaki T., 2008). From a considerable increase in the level of expression of Wnt5, prior to such an increment in the expression of Sox9, it can be understood that Wnt5a has an important role in recruiting the mesenchymal cells to enter into the chondrogenic route in the condyle (Al-kalaly A. et al., 2009). This especial role of Wnt5a is another unique aspect of secondary cartilage, as in the primary cartilage of the long bone Wnt5a may down regulate the Sox9 transcription activity (Yang Y. et al., 2003). As the chondrocytes in the hypertrophic zone become highly mature; however, it is important to note that hypertrophic chondrocytes do not lose proliferative activity (Suda N. et al., 1999). The impact of PTHrP on condylar chondrocytes appear to be different to that on long bones. In the tibial diaphysial cartilage, PTHrP is present in the proliferative zone but absent from hypertrophic zone. In contrast, PTHrP has been detected in both cell layers in condylar cartilage (Deng Z. et al., 2014).

### **I.II.III. Low Intensity Pulsed Ultrasound (LIPUS)**

Ultrasound<sup>7</sup>, an acoustic wave, is a form of mechanical energy. The acoustic energy engendered from ultrasound is produced from a piezoelectric crystal within a transducer. This transducer produces high-frequency acoustic pressure waves (1-12 MHz). These waves convey through body tissues by molecular vibrations and collisions. Pressure waves produce micromechanical strains in body tissues that can lead to biochemical events at the cellular level (Speed C.A., 2001; Baker K.G. et al., 2001).

The medical applications of ultrasound encompass therapeutic, operative, and diagnostic procedures (Ziskin M.C., 1987). Operative and therapeutic ultrasound has intensities ranging from 0.2 to 100 W/cm<sup>2</sup> and its biological results, such as muscle pain relief and decrease of joint stiffness, are achieved by noticeably increasing the temperature of the tissue (Wells P.N.T., 1985). In contrast, intensities for diagnostic imaging are much lower (0.5-50 mW/cm<sup>2</sup>), which considered nonthermal stimuli (St John Brown B., 1984).

Low intensity pulsed ultrasound (LIPUS) is ultrasonic waves applied at low intensity<sup>8</sup> ( $\leq 0.1$  W/cm<sup>2</sup>) with spatial average temporal average [SATA], in a constant frequency (1-1.5 MHz) and in a pulsatile manner. Therefore, LIPUS uses intensities low enough to be considered neither thermal nor destructive (Xavier C.A.M. and Durate L.R., 1983). The official setting for LIPUS application considered as standard is 20 min treatment per day of a 1.5 MHz sine wave repeated at 1kHz at  $I_{SATA} = 30 \text{ mW/cm}^2$  with a pulsed width of 200  $\mu\text{s}$  (Claes L. and Willie B., 2007; Pounder N.M. and Harrison A.J., 2008).

#### **I.II.III.I. Osteogenic Potential of LIPUS**

Mechanical strain, placed on bone or other cells, is one of the most important physiologic factors for maintaining skeletal system function and regulating a variety of bone cell functions (Rubin C.T. et al., 1985). Mechanoreceptors convert biophysical stimuli as a result of physical loading into biochemical responses that change gene expression and cellular adaptation. (Chen

---

<sup>7</sup> Ultrasound is sound waves with frequencies above 20 kHz (the hearing range for human is between 20 Hz and 20kHz).

<sup>8</sup> Intensity is the rate at which energy is delivered per unit area; it is expressed in units of watts per square centimeter (W/cm<sup>2</sup>).

Y.J. et al., 2003) The nature of the LIPUS-induced anabolic response might be similar to that in a physically loaded bone, based on Wolff's law (Naruse K. et al., 2000; Rutten S. et al., 2008). The strain induced by LIPUS at tissue level is far lower than the peak strains generated by functional load bearing (Rubin C.T. et al., 1984). However, high frequency low magnitude strains can lead to strong regulatory signals in bone tissue (Bacabac R.G. et al., 2006; Rubin C. et al., 2002).

The first beneficial effect of LIPUS on accelerating the bone growth was reported in 1983. In this initial experiment by Duarte, ultrasound treatments were applied with frequencies of 1.65 and 4.93 MHz with intensities of 49.6 and 57 mW/cm<sup>2</sup>, respectively. The transducers were pulsed at 5µs, and a repetition frequency of 1 kHz. The treatment was applied on fractured rabbit fibula and femur for 15 min each day, and the area of bone growth increased more rapidly for the first 10-12 days (Durate L.R., 1983). The effect of LIPUS on bone healing was clinically established and approved by the United States FDA (Food and Drug Administration) in 1994 for fresh fractures and in 2000 for non unions and delayed unions (Claes L. and Willie B., 2007). Since 1983 until today, there are several in vitro, in vivo, and clinical studies that provide evidence that LIPUS application stimulates osteogenesis.

In vitro studies have demonstrated that LIPUS generates considerable multifunctional effects that are directly related to bone formation and resorption (Wu C.C. et al., 1996; Ryaby J.T., 1989; Parvizi J. et al., 1999; Li J.K. et al., 2003). Significant increase in the osteoblast cell counts, while significant decrease in the osteoclasts cell counts has been reported as a result of low-intensity pulsed ultrasound stimulation to rat alveolar osteoclast-osteoblast co-culture system (Sun J.S. et al., 2001). Ultrasound exposure could enhance the osteoblast's population together with an increase in TGFβ1 secretion in a culture medium that has a stimulatory effect on osteoblast proliferation. In addition, LIPUS stimulation can cause a decrease in the concentration of IL (interlukin)-6 and TNF (tumor necrosis factor) α in the culture medium, which probably means that it could down-regulate the formation of osteoclasts and prevent bone resorption (LI J.K. et al., 2003). LIPUS stimulation increased the cellular proliferation of skull bone osteoblasts and the expression of various genes involved in differentiation and transcription of stem cells into osteoblasts (Gleizal A. et al., 2010; Sena K. et al., 2011). LIPUS also reportedly regulates proliferation and differentiation of osteoblasts through osteocytes; increased secretion of Prostaglandin E2 (PGE2) from osteocytes may play a role in this effect (Li L. et al., 2012).

Cellular level studies using primary osteoblasts or osteoblast-like cell lines have shown that LIPUS enhances osteoblast activity through a number of mechanisms. This enhancement includes stimulation of PGE<sub>2</sub>, probably through up-regulation of COX2 (Cyclooxygenase-2) (Kokubu T. et al.,1999; Naruse K. et al., 2003); ATP (Adenosin 5'-triphosphate) release (Hayton M.J. et al, 2005); and elevation in c-fos<sup>9</sup>, Runx2, ALP (Alkaline phosphatase), OC (osteocalcin), BSP (bone sialoprotein), IGF-I, TGF-β1, VEGF, and BMP-2 expression (Doan N. et al.,1999; Warden S.J. et al., 2001c; Azuma Y. et al., 2001; Li J.G. et al., 2002; Naruse K. et al., 2003; Leung K.S. et al., 2004a; Sant'Anna E.F. et al., 2005; Ikeda K. et al., 2006; Takayama T. et al., 2007; Hou C.H. et al., 2009). LIPUS up-regulated lysyl oxidase mRNA expression and elevated the total amount of cross-link formation of collagen. LIPUS also induces chemokines and RANKL (Receptor activator nuclear kappa-B ligand) through the angiotensin II type 1 receptor in these cells (Reher P. et al., 1999; Saito M. et al., 2004; Bandow K. et al., 2007). LIPUS stimulation has been demonstrated to activate Integrin / FAK (focal adhesion kinase) / P13K (phosphatidylinositol-3 kinase) /Akt (protein kinase B) complex and MARK-ERK pathways leading to increased osteoblastic activity and differentiation in osteoblast cells (Yang R.S. et al., 2005; Tang C.H. et al., 2006 and 2007; Takeuchi R. et al., 2008). LIPUS exposure can increase collagen in the extracellular matrix, leading to increased cellular adhesion and matrix mineralization (Uddin S.M.Z. and Qin Y.X., 2013).

In addition, when LIPUS is applied to bone-marrow-derived stromal cells (ST2 cells), it induced the transient expression of the immediate-early response gene c-fos and eminent mRNA levels for IGF-I, OC and BSP (Naruse K. et al., 2000; Chen Y.J. et al., 2003). Another study in which LIPUS was applied for 20 min to ROS cells (rat clonal cell line) demonstrated that ALPase activity was increased and a significant increment occurred in the expression of mRNA for the transcription factors important for osteoblast differentiation, i.e., Runx2, Msx2 (Msh homeobox 2), Dlx5 (distal less homeobox 5), Osterix, and Bone sialoprotein (Takayama T. et al., 2007). Increased Runx2, ALP, type 1 Collagen, and integrin beta 1 expression in LIPUS treated MSCs (mesenchymal stem cells) have also been shown in recent studies (Lai C.H. et al., 2010).

---

<sup>9</sup> C-fos is a symbol of FBJ murine osteosarcoma viral oncogen homolog. C-fos encodes a protein that participates in the formation of the AP-1 (Activator protein-1) complex, which binds DNA to AP-1 specific sites at the promoter and enhancer regions of target genes and converts extracellular signals into changes of gene expression (Chiu R. et al.,1988).

LIPUS has been broadly found to stimulate bone fracture healing in controlled animal models (Durate L.R., 1983; Pilla AA et al., 1990; Wang S.J. et al., 1994; Yang K.H. et al., 1996; Azuma Y. et al., 2001; Rawool N.M. et al., 2003; Shakouri K. et al., 2010; Coords M. et al., 2011) and in clinical treatments (Cook S.D. et al., 1997; Heckman J.D. et al., 1997; Cook S.D. et al., 2001a; Leung K.S. et al., 2004b; El-Mowafi H. and Mohsen M., 2005; Jinguishi S. et al., 2007; Lubbert P.H. et al., 2008; Rutten S. et al., 2008; Miyabe M. et al., 2010; Naruse K. et al., 2010). Particularly, LIPUS reportedly shortens the healing period of fresh fractures, distraction osteogenesis, refractory fractures (such as pseudoarthrosis), and delayed union fractures. Azuma et al. reported that LIPUS shortened the bone fracture healing period by beneficially affecting three processes: cartilage formation, endochondral ossification, and bone remodeling (Azuma Y. et al., 2001). Nevertheless, Katono et al. reported that in aged mice, acceleration of delayed fracture healing occurs only through promotion of endochondral ossification and bone remodeling. LIPUS application can enhance endochondral ossification through improved neovascularization through the following means: VEGF expression, endothelial cell migration, and COX2 –derived PGE2 expression. The latter may enhance production of chondroclasts/osteoclasts, which are key contributors to endochondral ossification (Katano M. et al., 2011).

Two studies have demonstrated a positive effect of LIPUS treatment on noncritical size cortical defects in long bones with (Walsh W.R. et al., 2008) and without (Durate L. et al., 1983; Yang K. et al., 2001) bone graft. In rats with critical sized femoral segmental defects, LIPUS enhances rhBMP-2 induced bone formation at suboptimum doses (1.2µg and 6 µg) and callus maturation at optimum doses, delivered on absorbable collagen sponge for bone repair. Increased bone formation in the former study can be explained by the direct effect of LIPUS on the osteogenic activity of the stromal cell population or indirect effect by enhancing blood flow, which provides needed growth factor and cells. In the latter study, callus maturation and remodeling occurred at a faster pace by a direct effect of LIPUS on osteoclast-like cells or, again, by indirect enhanced blood flow (Angle S.R. et al., 2014).

Fractures and bone defects provide a unique environment dominated by acute inflammation and distorted bone geometry. As mentioned above, there is growing evidence that LIPUS

accelerates their healing by affecting bone cells. However, there is conflicting evidence regarding the use of LIPUS on intact bone.

Spadaro et al. found no differences in BMD (bone mineral density) at the femur/ tibia between treated and untreated four week old rats (Spadaro J.A. et al., 1998). Similarly, LIPUS application was ineffective in preserving BMD and BV/TV (bone volume/tissue volume, bone volume fraction) in the proximal tibia and distal femur at the intensity of, respectively, 30 and 125 mW/cm<sup>2</sup> in a study by Warden et al. and Yang et al. (Warden S.J. et al., 2001a and b; Yang K.H. et al., 2001). On the other hand, as a result of a 30mw/cm<sup>2</sup> LIPUS treatment, a qualitative increase in new bone formation in the cancellous region of the proximal femur has been reported by Carvalho et al. (Carvalho D.C. et al., 2004). Lim et al. showed that low-intensity ultrasound at 30 mW/cm<sup>2</sup> was capable of new bone formation or prevention of bone loss in young adult ovariectomized mice (Lim D. et al., 2011). In the same way, Ferreri et al., noted significant improvement in cancellous bone microstructure and subsequent improvement in the structural integrity in the lumbar spine of 4-5 months old ovariectomized rats, especially when LIPUS was applied at the intensity of 100 mW/cm<sup>2</sup> (Ferreri S.L. et al., 2011).

In an organ culture system, Witlink et al. used a short application of 770 mW/cm<sup>2</sup> (SATP:spatial average intensity over the one period), 100-Hz pulsed, 1-MHz ultrasound to fetal mouse long bone rudiments and found that this energy level increases longitudinal growth over control by 10% in four to seven days. The proliferative cartilage zone was stimulated selectively without affecting the hypertrophic cartilage (Witlink A et al., 1995). In an in vivo study using four-week-old SD (Sprague Dawley) rats; however, 28 days of LIPUS (intensity of 30 mW/cm<sup>2</sup>) application, produced no detectable longitudinal growth of the long bone (Spadaro J.A. et al., 1998).

LIPUS treatment (at the intensity of 30 mW/cm<sup>2</sup> for 7 days) of fetal mouse metatarsal rudiments in vitro has been demonstrated to stimulate endochondral ossification. This was the result of a direct effect of LIPUS on osteoblasts and hypertrophic chondrocytes by stimulation of cell activity and/or differentiation. However, as a result of treatment there was no change in the total length of the rudiments, which may suggest that there was no effect on chondrocyte proliferation (Korstjens C.M. et al., 2004; Nolte P.A. et al., 2001).

In a more recent organ culture study, LIPUS application for 15 days did not result in additional longitudinal growth of the femur. Zones of epiphyseal cartilage and hypertrophic and calcified cartilage did not exhibit any differences. In contrast, metaphyseal periosteum showed accelerated mineralization perpendicular to the ultrasound path. This acceleration of ossification was revealed using alizarin red staining, micro-CT, and immunostaining by osteocalcin (Naruse K. et al., 2009).

An interesting experiment by Perry et al. in 2009 demonstrated that the effects of low-intensity pulsed ultrasound stimulation mimic to a degree the actions of physiological mechanical loading when applied to bone in a non-fracture environment in vivo. In this study, physiological mechanical loading, LIPUS and the combination of both were experimented on ulna of adult female wistar rats. All three treatments induced a significant periosteal response, increasing the proportion of periosteal bone surface with double label from <10% in control limb to >80% in treated limbs. Moreover, the increase in the mineral apposition rate of experimental ulna versus the contralateral control were 2.9 ( $\pm$  0.9), 8.6 ( $\pm$  2.4) and 8.7 ( $\pm$  3.2) for the ultrasound only, ultrasound and load, and load only groups, respectively. Significantly, in this experiment LIPUS at the intensity of 30 mW/cm<sup>2</sup> on the surface of the bone was applied for only 7min per section, repeated 3 times weekly for two weeks (Perry M.J. et al., 2009).

De Gusmao C.V.B. et al. in their 2010 study suggested that long-term LIPUS acts on mechanotransduction and growth factor pathways in a noncumulative manner. The LIPUS effect on mechanotransduction pathway is through increased FAK and ERK1/2 activation and expression. The effect of LIPUS on growth factor pathway is via increased insulin receptor substrate-1 (IRS-1) expression, perhaps due to IGF-1 mechanically induced increased expression. These effects show that LIPUS applied to intact bone acts on proteins involved in osteogenesis; however, the osteogenic effect might be temporary due to the possible presence of a major inhibitory mechanism for FAK activation and IRS-1 expression (De Gusmao C.V.B. et al. 2010).

### **I.II.III.II. Chondrogenic and Fibrogenic Potential of LIPUS**

Even though these procedures are still debated as delineated below, a number of invitro and in vivo studies demonstrated that mechanical stimulus produced by low intensity pulsed ultrasonic energy (spatial average temporal average intensities between 2-100 mW/cm<sup>2</sup>) promotes

chondrogenesis in bone fracture healing, isolated cell cultures, cartilage explants, engineered cartilage and cartilage injuries.

The primary effect of LIPUS seems to be on the chondrocyte population in the healing fracture, as LIPUS increases soft-callus formation. LIPUS enhances the endochondral ossification, an effect possibly achieved through inducing chondrocyte proliferation (Witlink A. et al., 1995; de Albornoz P.M. et al., 2011). The acceleration of fracture healing has also been linked to the promotion of cartilage-related gene expression, earlier synthesis of extracellular matrix proteins, such as proteoglycan and aggrecan in cartilage, as well as to the consequent chondrocyte maturation and earlier endochondral bone formation (Klug W. et al. 1986; Pilla A.A. et al. 1990; Wang S.J. et al. 1994; Yang K.H. et al.1994; Yang K.H. et al. 1996; Tanzer M. et al. 1996). In addition, as a result of LIPUS application, up-regulation of VEGF in the early fracture healing phase has been revealed, followed by chondrogenesis (Lu H. et al., 2008).

LIPUS is a form of dynamic compression that generally increases the synthesis of cartilage matrix macromolecules (Irrechukwu O.N. et al., 2011). Initially, in an in vitro study using rat chondrocytes, increased aggrecan mRNA levels and proteoglycan synthesis were reported, while alpha type II procollagen mRNA remained unaffected (Parvizi J. et al., 1999). Subsequently, several in vitro studies evaluating the effect of LIPUS on chondrocytes in both monolayer and 3-D model systems reported the up-regulation of aggrecan and type II collagen genes (Zhang Z.J. 2002 and 2003; Mukai S., 2005; Tien Y.C. et al., 2008); proteoglycan synthesis in the chondrocytes embedded in the type I collagen scaffold (Nishikori T. et al., 2002; Irrechukwu O.N. et al., 2011); scaffold-free cartilage construct (Uenaka K. et al., 2010); as well as GAG synthesis in different culture models (Nishikori T. et al., 2002; Kopakkala-Tani M. et al., 2006; Irrechukwu O.N. et al.,2011). Nevertheless, some other observations suggested limited or only transient changes on the above-mentioned ECM (extracellular matrix) compartments (Yuan L.J. et al.2014).

The effect of LIPUS stimulation is dependent on the cell's microenvironment and does not alter the cartilage phenotype. LIPUS increases type X collagen (a marker for endochondral ossification) by stimulating hypertrophic chondrocytes in the ossifying (proximal) sternum. This effect suggests that LIPUS may augment bone formation by stimulating hypertrophy in chondrocytes that are developing toward terminal differentiation. However, LIPUS did not

stimulate type X collagen in non ossifying (distal) sternum and does not induce chondrocyte hypertrophy (Zhang Z.J. et al, 2002). LIPUS delayed the appearance of type X collagen mRNA expression and maintained the higher expression levels of type II collagen and aggrecan mRNA of chondrocytes isolated from distal femurs (resting zone of the growth plate) of two- day- old rats in the aggregate culture (Mukai S. et al, 2005). In chondrocytes isolated from bovine stifle joint articular cartilage seeded into type I collagen scaffolds, LIPUS increases type II collagen synthesis but does not stimulate type I collagen (the marker for chondrocyte dedifferentiation and abundant in fibrocartilage) production. It also inhibits the production of type X collagen and MMP (matrix metalloproteinase)-13 (up regulate during cartilage destruction) (Irrechukwu O.N. et al., 2011).

Ultrasound stimulation of chondrocyte proliferation has been evaluated in a number of experimental models. In an osteoarthritis model, the chondrocyte density in the superficial and middle zones of the articular cartilage increased subsequent to US with a spatial and temporal peak intensity of 2.5 W/cm<sup>2</sup> (Huang M et al, 1997). Six weeks daily US application (2.2 W/cm<sup>2</sup>, 20 min) to the left knee of 6-week-old New Zealand rabbits lead to a nearly 1.7 fold increase in the proliferative zone and a 2.8 fold increase in the reserve zone (Lyon R. et al., 2003). In an organ culture system, LIPUS at the intensity of 0.77 W/ cm<sup>2</sup> increased chondrocyte proliferation in 16-day-old metatarsal rudiments of mice (Wiltink A. et al.1995).

In a 1999 preliminary in vitro study by Parvizi et al., no influence on cell proliferation of rat chondrocytes in monolayer culture has been observed as a result of 50 and 120 mW/cm<sup>2</sup> LIPUS exposure (Parvizi J. et al., 1999). Similarly, LIPUS application has had no reported significant increase in the cell number of rabbit chondrocytes in an in vitro atelocollagen culture model (Nishikori T. et al., 2002). More recently, however, Zhang and colleagues irradiated cultured chick embryo chondrocytes in alginate beads at 2mW/cm<sup>2</sup> and 30mW/cm<sup>2</sup>, and measured the cell count and volume of the extracellular matrix over time. Interestingly, at 2mW/cm<sup>2</sup> they observed a significant but transient increase on day three of culture, in comparison with the control group (Zhang Z.J. et al., 2003). In an even more recent experiment, LIPUS (30mW/cm<sup>2</sup>) application for 15 days promoted the proliferation and retained the differentiation state of chondrocytes from the distal femurs of neonatal rats in the aggregate culture. This study also revealed that TGF- $\beta_1$  plays an important role in mediating the LIPUS effects in chondrocytes (Mukai S. et al., 2005).

Significant increase in chondrocyte proliferation has been also reported by Ikeda et al. (Ikeda K. et al., 2006). LIPUS (18 mW/cm<sup>2</sup>-98 mW/cm<sup>2</sup>) application for 14 days on isolated chondrocytes of young children's articular cartilage of ablated polydactylia leads to increase aggrecan and type II collagen synthesis. Nevertheless, LIPUS has no significant effect on cell proliferation. Moreover, human chondrocytes which were isolated from older donors were less responsive to LIPUS (Tien Y.C. et al, 2008). In contrast, for human chondrocytes obtained from the osteoarthritis cartilage (degenerative or collateral compartment) of senile patients (57-71 yrs), LIPUS (30 mW/cm<sup>2</sup>-6 days) was found to promote cell proliferation and matrix production (Hsu S.H. et al., 2006; Korstjens C.M. et al., 2008). Increases in the number and size of glycosaminoglycan-positive lacunae and cellular organelles following LIPUS application have been also observed in human articular chondrocytes isolated from osteoarthritis patients (Miyamoto K. et al., 2005; Choi B.H. et al., 2006). In a study by Takeuchi R. et al., LIPUS promoted the proliferation of cultured chondrocytes (from 6 month old pig's metatarsophalangeal joints) and the production of type IX collagen (involved in promoting chondrocyte proliferation and cartilage layer expansion), but not type II collagen in a three-dimensional culture using a collagen sponge following 14 days. The rate of increase in the cell number was slightly but significantly higher in the LIPUS group. The Ki-67 (a very reliable marker of proliferation) index of the chondrocytes exposed to LIPUS was significantly higher compared to that of control (Takeuchi R. et al., 2008).

The main integrin found on the chondrocyte membrane, integrin  $\beta$ 1, regulates the proliferation and differentiation of chondrocytes via mechanochemical transduction through ECM, integrins, cytoskeletal proteins and focal adhesion molecules. LIPUS increases integrin expression through mechanical stress, phosphorylation of FAK, activation of PI3K /Akt pathway and increase of the expression of type II collagen and aggrecan, which leads to the proliferation of chondrocytes (Korstjens C.M. et al., 2008; Takeuchi R. et al., 2008). Application of LIPUS to osteoarthritis (OA) chondrocytes activates the same integrin-FAK-PI3K/Akt mechanochemical transduction pathway, inhibits the increase in MMP-1 and MMP-13 and decreases the degradation of type II collagen and aggrecan. Thus, LIPUS can promote the repair of cartilage damage and delay the degeneration of articular cartilage that leads to OA (Cheng K. et al., 2014).

There are structural similarities between chondrocytes and nucleus pulposus (NP) cells important for intervertebral disc integrity (Iwashina T. et al., 2006). TGF- $\beta$ 1 promotes intervertebral disc cell proliferation and matrix synthesis. It also has a role in chondrocytes regulation (Hiyama A. et al., 2007). Increased expression of the transforming growth factor-beta type 1 receptor (TGF- $\beta$ 1) gene has been observed in NP cells following exposure to LIPUS. LIPUS application can increase collagen synthesis (16-19%) in cells isolated from the intervertebral disc. In the human nucleus pulposus cell line (HNPSV-1), LIPUS stimulates proliferation, proteoglycan synthesis, and gene expression of growth factors and their receptors (BMP2, FGF8, TGF $\beta$ 1, EGFRF1, and VEGF) (Kobayashi Y. et al., 2009). LIPUS can stimulate the extracellular matrix (aggrecan and type II collagen) of degenerative human nucleus pulposus cells cultured in calcium alginate beads through activating the P13K/Akt pathway (Zhang X. et al., 2013).

LIPUS has also been proposed as a tool to induce both human and animal mesenchymal stem cells (MSCs) to differentiate into chondrocytes or enhance their chondrogenic differentiation in monolayer as well as three dimensional culture systems (Schumann D. et al., 2006; Lee H. J. et al., 2007; Cui J.H. et al., 2007; Park S.R. et al., 2007; Gurkan I. et al., 2010; Lai C.H. et al., 2010; El-Bialy T. et al., 2010).

A 2010 experiment examined a LIPUS treatment to implanted tissue-engineered mandibular condyle (combined chondrogenic differentiated-cell-loaded sponge and osteogenic differentiated-cell-loaded sponge in an extracellular matrix scaffold) in skeletally mature NZ rabbits. The results demonstrated better structural formation (i.e., new osteogenic and chondrogenic tissue formation) and better integration of newly formed tissues and original condylar bone in LIPUS treated condyles compared to those without LIPUS treatment (El-Bialy T. et al., 2010).

As a result of LIPUS application, accelerated healing of tendon graft-bone interface in rabbit models has been reported. It has been partially revealed that improvement of bone tendon junction healing is achieved through regulation of the VEGF expression in the early healing phase and subsequent chondrogenesis (Lu H. et al., 2008; Papatheodorou L.K. et al., 2009).

In vivo studies in adult NZ rabbit (Cook S.D. et al., 2001b, Jia X.L. et al., 2005) and canine (Cook S.D. et al., 2008) models with full thickness osteochondral defects have demonstrated

that LIPUS can accelerate the repair of injured articular cartilage. In the canine model, LIPUS therapy significantly improves the quality of the interface repair tissue around autologous osteochondral plugs. The results were more hyaline-like interface repair tissue and improved bonding between the osteochondral plug and the adjacent cartilage compared to the contralateral untreated control. The interface repair tissue of LIPUS treated sites also had a more normal translucent appearance than the control sites. Ultrasound treatment improved the cell morphologic characteristic of the interface repair tissue and increased subchondral bone regeneration.

In a rat osteoarthritis with anterior cruciate ligament and meniscus transaction model, LIPUS increased type II collagen synthesis via induction of type II collagen mRNA expression and activation of chondrocytes (Naito K. et al, 2010). Another in vivo experimental rat osteoarthritis model also demonstrated efficacy in cartilage restoration (Huang M.H. et al, 1997). However, LIPUS treatment has no significant effect on severe articular cartilage in the rabbit model. Only proliferative tissue with less up take under Alcian blue stain has been observed after a LIPUS treatment with no deposition of type II collagen or proliferation of chondrocytes (Yang S.W. et al, 2014).

At a clinical level there are only limited studies in which the efficacy of LIPUS on the cartilage repair has been evaluated. In a 2001 clinical trial, as a result of LIPUS therapy enhancement in cartilage repair in patients with mild and moderate osteoarthritis has been reported. In this study, an indirect measurement of knee cartilage injury, i.e.: (99m) Tc bone scintigraphy has been used for evaluations (Huang M.H. et al, 2001). Recently, one double-blinded, randomized, placebo-controlled pilot study dealing with the same issue has been conducted. Age-adjusted analyses, including only subjects who attended 20 sessions or more, were indicative of an increase (90µm-95% confidence interval) in the medial tibia cartilage thickness in the active LIPUS therapy group (Loyola-Sanchez A. et al, 2012).

A recent study revealed that some of the beneficial effects of LIPUS on cartilage repair may be mediated by increased focal adhesion kinase activation, which is a major process in relaying signals from integrins to downstream factors, in chondrogenic progenitor cells (CPC). CPCs greatly enhance the repopulation of hypo cellular cartilage after an injury. However, whether this

LIPUS application can improve cartilage repair depends on the ability of CPCs to re-establish a functional cartilage matrix in situ, a scenario that remains unproven (Jang K.W. et al, 2014).

Therefore, collectively, exposure to LIPUS could significantly affect chondrocyte viability, metabolism, proliferation, phenotype expression, and cartilage formation, maturation and extracellular matrix production. However, as mentioned above, scientists still observe inconsistent effects.

Information regarding the effect of LIPUS on fibroblasts is limited, but briefly presented as follows:

It has been demonstrated that LIPUS exposure can increase ERK  $\frac{1}{2}$  activation, trigger DNA (deoxyribonucleic acid) synthesis, and hence cell proliferation of human foreskin fibroblasts (Zhou S. et al 2004). LIPUS can stimulate fibroblasts to synthesize more collagen and favour the maturation of collagen, possibly through the stimulation of calcium influx and a change in membrane permeability (Dyson M., 1987; Webster D.F. et al, 1978 and 1980, Zhou S. et al. 2004, Mendonca A.C. et al. 2006). LIPUS stimulates fibroblast activity, which alters the function of the cell membrane, amplifies endoplasmic reticulum activity, raises intracellular calcium levels, and increases protein synthesis (Lai J. And Pittelkow D.M.P., 2007, Pires Oliveria D.A.A. et al, 2009).

### **I.II.III.III. Growth Modification of the Mandible with LIPUS**

Until today, seven published experiments evaluated the possibility of growth modification of the mandible with LIPUS. These studies were conducted by two different research groups.

In the first experiment, LIPUS (200 microsecond burst of 1.5 MHz sine waves repeating at 1 kHz with the intensity of 30 mW/cm<sup>2</sup>) was applied for 20 minutes daily for 4 weeks to the left temporomandibular joint area of eight growing, ten-week-old NZ male rabbits, where the contralateral side served as a control. Significantly higher values for condylar height, ramus height, and mandibular length were reported for the treated hemi mandible compared with the untreated ones. Histologic findings in the LIPUS- treated side compared to that of control included a thicker fibrocartilaginous layer, hypertrophy of chondrocytes, excessive bone formation lined with active osteoblasts, and dilated blood capillaries. The authors concluded that the findings strongly support the enhancement of mandibular condylar endochondral bone

growth as a result of daily LIPUS application with above mentioned setting (El-Bialy T. et al., 2003).

In 2006, El-Bialy T. et al. conducted the second study on growing male baboons (n=14), which have a closer phylogenetic affinity to humans. These scientists combined this newly proposed treatment with a conventional bite-jumping appliance to evaluate the potential synergetic effect of the two treatments. LIPUS stimulation with the same setting as the previous study led to increased mandibular length, especially when accompanied with the anterior bite-jumping appliance after four months LIPUS application. Similarly, bone scintigraphy showed a higher <sup>99m</sup>Tc uptake in stimulated condyles, particularly when treatment combined by functional therapy indicative of higher bone metabolism and remodeling activity. Moreover, histomorphometric analysis evaluating the bone trabeculae surface area confirmed the results. The results again proved that LIPUS, per se, can induce growth modification of the mandibular condyle (El-Bialy T. et al., 2006).

The third study by the same authors was performed on five children (age range 3-11 years; both genders) with hemifacial microsomia and reported in 2010. The patients were treated with hybrid jaw orthopedic functional appliances, and LIPUS, with the same parameters as previous studies, was applied on the affected mandibular condyle. Clinical and radiographical results after a year of treatment revealed significant improvement of the underdeveloped side of patients' faces and mandibles. The growth pattern of the affected sides was normalized to a greater extent in mild to moderate cases and particularly in younger patients. The treatment shortened the conventional non invasive treatment for patients with hemifacial microsomia since the results were comparable to that of a previously reported study using hybrid jaw orthopedic functional appliances (Kaplan R.G., 1989), albeit following a five year treatment (El-Bialy T. et al., 2010).

Oyonarte et al. examined the stimulatory effect of LIPUS (30 mW/cm<sup>2</sup>, 1MHz, 500-microsecond pulses) on condylar growth in growing (22 days old) male rats. In this 2009 experiment, 16 animals were stimulated with LIPUS in the TMJ region for ten minutes, four animals were stimulated for 20 minutes a day on 20 occasions and 10 rats were considered as control. Several qualitative and quantitative histologic changes occurred as a result of LIPUS stimulation, which differs in anterior and posterior regions of the condyles. These scientists observed some tendencies in proliferative, maturation, and total cartilage, as well as a significant

modification in relative layer thickness in the anterior region. In the maturation zone, increased matrix secretion, more hypertrophic chondrocytes, changes in both cellular arrangement and subchondral bone region, elongation of the trabecular distribution, and significant increase in the bone marrow perimeter were evident in the stimulated condyles. Changes were more prominent in the 20-minute group, however. In this experiment, the authors suggested that scarce significant differences in the linear histologic measurements were related to the small sample size for the 20-minute group and possibly to failure to achieve a certain threshold level of mechanical stimulation that up-regulates cellular metabolism in the case of the 10-minute group (Oyonarte R. et al., 2009).

Recently, the same research group evaluated the effect of an intra-articular injection of Mesenchymal Stem Cells (MSCs) ( $1 \times 10^5$  cells/kg) and/or LIPUS stimulation (50 mW/cm<sup>2</sup>, 1MHz, 0.2 millisecond pulses, 20 minutes daily) on the mandibular condyles of growing (23 day old) rats (n=5 per group). Cone Beam Computed Tomography (CBCT) and histology was performed following a 21-day experimental period. Imaging results demonstrated that LIPUS and MSC application to the TMJ region of growing rats significantly favoured transverse condylar growth (wider condyles), while LIPUS application alone may enhance sagittal condylar development (significantly greater condylar length and lower midline shift to unstimulated side). Moreover, histology revealed increased vascularity in the erosive cartilage zone in LIPUS treated groups (Oyonarte R. et al., 2013).

Another recently published article by the first research group evaluated the effect of local injection of recombinant growth hormone (rGH) (5µg/day) into temporomandibular joint and/or local application of therapeutic LIPUS on mandibular growth of growing (8-week old) male rats (n=6 per group). Following 21 consecutive days of the experimental period, the results from the micro-CT analysis were as follows: hemimandibular bone volume and surface area increased significantly with rGH and/or LIPUS application in comparison to control. The combination therapy resulted in a significant increase in the mandibular head length and a significant decrease in the bone mineral density (Khan I. et al., 2013).

The most recently published article is a pilot study evaluating the effect of non viral plasmid delivered basic fibroblast growth factor (bFGF) and/or low intensity pulsed ultrasound on mandibular condylar growth in “so called” late adolescent-adult (the age of the animals were not

clearly mentioned) male SD rats (n=3 per group). The condylar process length and ramal height reported to be significantly greater in the LIPUS group compare to that of the control group. For the same evaluations, combination therapy and bFGF groups were located in the subsequent places. The similar trend has been observed when the number of proliferative cells was compared between groups. Moreover, the chondroblasts were more hypertrophic in the LIPUS group. A micro-CT analysis of the trabecular bone of the whole condyle showed a significant increase in the BV/TV in the combination therapy (Kaur H. et al., 2014).

Among the biomolecules that are known or suggested to play a role in mandibular condylar growth, in vitro and in vivo studies revealed that in a variety of cells, LIPUS can up-regulate the expression of Runx2/Cbfa1 (Chen Y.G. et al, 2003; Takayama T. et al, 2007; Lai C.H. et al, 2010; Uddin S.M. and Qin Y.X., 2013; Yue Y. et al, 2013); Osterix (Uddin S.M. and Qin Y.X., 2013); Sox9 (Lai C.H. et al, 2010); VEGF (Reher P. et al,1999; Doan N. et al. 1999; Wang W. et al, 2004, Leung K.S. et al,2004a; Lee H.J. et al,2007; Walsh W.R., 2008; Lu H. et al, 2008; Kobayashi Y. et al, 2009; Katano M. et al, 2011; Sawai Y. et al, 2012; Santana L.A. et al, 2013); IGF and especially IGF receptors (Naruse K. et al, 2000; Naruse K. et al, 2003; Sant'Anna E.F. et al, 2005; Lu H. et al, 2009; Tabuchi Y. et al, 2013); FGF(Kobayashi Y. et al, 2009); TGF $\beta$  (Li J.K. et al, 2003; Mukai S. et al,2005; Lu H. et al, 2009; Kobayashi Y. et al, 2009; Kosaka T. et al, 2011); PDGFS (platelet-derived growth factors) (Ito M. et al, 2000); CTGF(connective tissue growth factor) (Shirashi R. et al, 2011); BMPs (Lu H. et al, 2009; Kobayashi Y. et al, 2009; Suzuki A. et al.2009; Xue H. et al, 2013; Ishihara Y. et al, 2014); Cyclin D1 (El-Bialy T. et al, 2012); and type II and X collagen (Mukai S. et al 2005). LIPUS also activates the Wnt/  $\beta$  catenin (Olkku A. et al, 2010) and PI3K/Akt pathways <sup>10</sup>(Tang C.H., 2006 and 2007; Takeuchi R. et al, 2008; Watabe H. et al, 2011; Sawai Y. et al, 2012; Zhang X. et al, 2013; Cheng K. et al, 2014).

#### **I.II.III.IV. Potential Mechanisms of Action of LIPUS**

LIPUS has received increasing attention as a means of mechanical force. However, the precise molecular mechanisms by which cells translate mechanical forces into biological signals remain largely unknown (De Albornoz P.M. et al., 2011; Bashardoust Tajali S. et al., 2012).

---

<sup>10</sup> These pathways are suggested to be a potential target for PTHrp in condylar cartilage and play a crucial role in the proliferation and differentiation of condylar chondrocytes (Deng Z. et al., 2014).

Various theories for biophysical and biological triggers currently exist, which are briefly mentioned below.

It has been proposed that ultrasound acts as a mechanical wave and produces local pressure gradients. This premise is based on the biophysical mechanism of wave mode conversion. LIPUS produces a longitudinal pressure wave, a portion of which is converted to a transverse or shear wave when it encounters at the soft tissue-bone interface (Leung K.S. et al., 2004a). As a result, anabolic shear forces on cell membranes or alterations in local solute concentration may happen. The gradients could make local fluid flow, which may result in an anabolic signal (Ferrerri S.L. et al., 2011).

Another biophysical mechanism of action is nanoscale motion, as proposed by Claes L. and Willie B., 2007. Local changes in pressure may produce a biophysical environment that mimics Wolff's law on a microscopic scale (Claes L. and Willie B., 2007). LIPUS stimulation also produces fine vibrations in local tissues. This vibration causes increased capillary blood flow and cell membrane permeability (Omi H. et al., 2008).

Bone is piezoelectric in nature (Erdogan O. and Esen E., 2009). Ultrasound may generate an electric field that could then constrain an osteogenic adaptation (Pilla A.A., 2002). One in vitro study demonstrated the generation of an electric field in the range believed to be anabolic for bone tissue (Montalibt A. et al., 2001).

When ultrasonic waves transmitted through the tissue, its energy is absorbed at a rate proportional to the density of the tissue. Ultrasound signal absorption can lead to energy alteration to heat. This effect is very small (the temperature change is far below 1<sup>o</sup> C). Nevertheless, some enzymes like matrix metalloproteinase-1 and collagenase are strongly responsive to even such small changes in temperature. Therefore, profound biological effects can be expected (Welgus H.G. et al., 1981; Dee C. et al., 1996). The nonthermal effect of LIPUS on tissues can be explained as cavitation due to training and concentration of bubbles (O'Brien Jr, W. D., 2007).

Mccormick et al. demonstrated that exposure to LIPUS alone does not alter cell morphology (Mccormick S.M. et al., 2006). Based on this work, Pounder and Harrison suggest that since the cell itself does not change morphology under LIPUS treatment, it must be mechanoreceptors on the cell surface that induce changes (Pounder N.M. and Harrison A.J., 2008). There is growing

evidence that integrins<sup>11</sup> are promising candidates for sensing extracellular matrix-derived mechanical stimuli occasioned by LIPUS and then convert them into biochemical signals (Ingber D.E. et al, 2003). For instance, the up-regulation of inducible nitric-oxide synthase (iNOS) through an integrin receptor in osteoblast has been demonstrated in an in vitro study (Tang C.H. et al., 2007). The integrin receptors on osteoblasts served as mechanotransducers to transmit acoustic pulsed energy into intracellular biochemical signals through cytoskeleton systems. Integrin-associated signaling pathways featured an increase in tyrosine phosphorylation of several signaling proteins, an activation of serine/threonine kinases, as well as alterations in cellular phospholipid and calcium levels (Giancotti F.G. et al., 1999). These events were related to the formation of focal adhesions, which acted as a bridge to link integrin cytoplasmic domains to the cytoskeleton and to activate integrin-associated signaling pathways, such as the MAPK pathway (Schlaepfer D.D. et al 1998) and the Rho pathway (Riveline D. et al. 2001) that are both important in different cell functions. LIPUS also have a significant effect on cell function: cytoskeleton organization and stimulation of mitochondrial activity and the plasma membrane (Dyson M. 1987).

Even though, any of the abovementioned scenarios are possible, most likely ultrasound mechanism is a combination of many factors both biological and biophysical. The positive effects of LIPUS on differentiation, gene expression, mineralization, and proliferation of various cells under in vitro cell culture conditions have been reported. Some of these experiments have been mentioned in previous sections. Global-scale micro array analysis to reveal gene expression in some cell types has also been performed and reported in the literature, as it will be discussed here.

A single LIPUS exposure (30 mW/cm<sup>2</sup> for 30 min) in human osteoblastic osteosarcoma MG-63 cells resulted in two-fold up-regulation of 377 genes. These genes are involved with the

---

<sup>11</sup> Integrins are heterodimeric transmembrane glyco- proteins consisting of one  $\alpha$ - and one  $\beta$ -subunit. The  $\beta 1$  subfamily of integrins consists of many ECM receptors, including those for fibronectin, collagens and laminin. For example, integrin  $\alpha 2\beta 1$  is the preferential receptor for type II collagen (Loeser R.F. et al., 2000). Integrin binding stimulates intracellular signaling which can affect gene expression and alter cellular expression and affinity of integrins (Loeser R.F. et al., 2000). Many integrins are not constitutively active; in fact, they are normally expressed on the cellular surface in an inactive or “OFF” state, a state in which they do not bind ligands and do not signal (Hynes R.O., 2002). It is hypothesized that LIPUS must somehow activate integrins, perhaps by facilitating a mechanical change in the conformation of the integrin molecule (Lai C.H. et al., 2010).

cellular membrane and regulation of transcription, but not with osteoblast differentiation (Leskinen J.J. et al, 2008).

A single LIPUS (30 mW/cm<sup>2</sup> for 20 min) exposure to human osteoblastic osteosarcoma SaOS-2 cells lead to more than two-fold changes in 165 genes. These genes belonged to more than ten protein families, including integrins and cytoskeleton genes, transforming growth factor-beta family, insulin-like growth factor family, Mitogen-activated protein kinase pathway, ATP-related genes, Guanin nucleotide binding protein (G protein), Lysyl oxidase (LO) gene, and genes associated with cell apoptosis (Lu H. et al, 2008).

A cDNA (complementary DNA) microarray analysis revealed that a LIPUS (30 mW/cm<sup>2</sup> for 20 min) application once daily for three days significantly induced 114 genes including their growth factor-related proteins, proteoglycan, collagens, and matrix metalloproteinases in human nucleus pulposus cell line (Kobayashi Y. et al., 2009).

By using a Gene Chip microarray system in human lymphoma U937 cells treated with a single LIPUS (300 mW/cm<sup>2</sup> for 1 min), scientists observed that 193 genes were down regulated and 201 genes were up regulated more than 1.5 fold (Tabuchi Y. et al., 2008).

In a more recent study, a micro array analysis revealed that 38 genes were upregulated (including insulin-like growth factor 2) and 37 genes were down regulated (including transforming growth factor, beta induced) by 1.5 fold or more in preosteoblast MC3T3-E1 cells at 24 h after LIPUS (30 mW/cm<sup>2</sup> for 20 min) exposure (Tabuchi Y. et al., 2013).

### **I.III. OBJECTIVES AND HYPOTHESIS**

#### **General Objective**

- The goal of this thesis is to determine the effect of LIPUS on stimulation of mandibular condylar remodeling in young adult rats.

#### **Applied Objective**

- The long term goal of this work is to introduce LIPUS as a potential adjunct non invasive modality to fixed functional therapy with the aim of enhancing such therapy's efficacy, i.e., increasing skeletal effect, in young adults.

#### **Specific Objectives**

- The initial objective of the present study is to investigate the potential morphological changes in the condyle and the mandible subsequent to short term LIPUS therapy in young adult rats.
- The second objective is to detect the changes in the thickness of different mandibular condylar fibrocartilage layers, as well as changes in cell population in prechondroblastic and chondroblastic layers following short term LIPUS therapy in young adult rats.
- The third objective is to identify the changes in bone mineral density and microarchitecture of subchondral cancellous bone as a result of short term LIPUS therapy in young adult rats.
- The fourth objective is to determine the amount of active bone formation, osteoid thickness, and actual endochondral bone growth in subchondral cancellous bone as a result of short term LIPUS therapy in young adult rats.

#### **General Hypothesis**

- First hypothesis:  
LIPUS enhances chondrogenesis in mandibular condyle of young adult rats through enhancing cartilage hyperplasia, hypertrophy and extracellular matrix secretion.
- Second hypothesis:  
LIPUS enhances osteogenesis in the mandibular condyle of young adult rats through an anabolic effect on the activity of osteoblasts and increasing osteoid apposition.
- Third hypothesis:  
LIPUS stimulates mandibular condylar remodeling in young adult rats by acting at the cartilage and bone level.

# CHAPTER II: MATERIALS & METHODS

---

### **II.I. Experimental Design and Animals**

This experiment was approved by the animal care and use committee for health sciences, University of Alberta, Canada (AUP: 000000381-REN1). All the animal procedures were performed according to the guidelines of the Canadian Council on Animal Care.

In the present study, to be able to compare the results with those of other studies, especially Xiong H. et al. (2004, 2005a and b) and Rabie A.B. et al. (2004b) approximately 120-day-old “adult” female rats were used. Rats can be handled easily, need small space for living, are reasonably inexpensive and routinely have been used in mandibular condylar growth modification studies (Meikle M.C., 2007; Farias-Neto A. et al., 2012). 120-day-old rats are considered to be no longer growing (Luder H.U.1996; Gebhard A. et al., 2003), because their weight has stopped increasing at the age of 100 days, whereas 20 days is the reserve time. This age of SD rats falls in the young adult (twenties) stage for human beings (Losken A. et al., 1992; Jiao K. et al., 2010). Female rats have been used in the present study, because most of the adult patients with underdevelopment of the lower jaw who are seeking a kind of treatment are dominantly women (Chaiyongsirisern A. et al., 2009), and also, this gender of rats has been used in previous similar studies.

Nineteen 104 to 111 day old female Sprague Dawley (CD) rats have been purchased from Charles River Laboratories (Wilmington, MA, USA). The mean weight of the animals was 347.30 grams  $\pm$  14.41 SD (range 319.2- 374.5 grams) at the beginning of the study.

Each pair of animals has been caged in bottle top ventilated cages known as IVC or individually ventilated caging from Techniplast, Italy and were kept under standardized conditions of regulated light (12/12 on at 6 am, off at 6 pm), room humidity (40-70%) and room temperature (18-23<sup>0</sup> C) in the Health Sciences Laboratory Animal Facility, University of Alberta. They were provided with water at libitum and normal rat pellets (Lab Diet, St. Louis, MO, USA).

Following a 10 day acclimatization period, animals were allocated to control (n=9) and experimental (n=10) groups. To keep the experimental conditions as similar as possible for both groups, allocation has been performed based on the average weight of the rats during the acclimatization period and the cage-mate pairs consisted of one control and one experimental

group member<sup>1</sup>. Cage numbering and ear notching, identified individual animals and group membership. In the experimental group, animals were treated by LIPUS application for 20 minutes for 28 consecutive days, performed under inhalation anesthesia (2.5 % Isoflurane with 100% oxygen). As daily general anesthesia might affect general health and consequently bone growth, all experimental and control animals were anesthetized for the same period of time and weight of animals was monitored as one indicative of the general health.

## **II.II. LIPUS Application**

The TMJ area of both sides of the experimental groups has been exposed to LIPUS daily for 20 minutes in a single application for the period of the study (4 weeks). A custom-built ultrasound device that provides adjustable output parameters and long-term operation stability (SmileSonica Inc., Edmonton, AB, Canada) has been utilized (Figure 2-a). The LIPUS device has been set to generate ultrasound pulses with a repetition rate of 1 KHz. Each pulse had a square envelope with a duration of 200 microseconds and a pulse frequency of 1.5 MHz. The ultrasound transducer has an emitting area of 1.1 cm<sup>2</sup>, generating a temporal average ultrasound power of 32mW±10% (or a temporal average ultrasound intensity of 30mW/cm<sup>2</sup>±10%). The transducer has been applied on the cheek area covering the region encompassing the temporomandibular joint following shaving, and a high viscosity gel (National Therapy Products Inc., Woodbridge, ON, Canada) was used between the transducer and skin as a coupling media (Figure 2-b). The region of sonication was constant in all occasions, that is, confined to the shaved area. During the 20 minutes LIPUS application, rats were under general anesthesia using Isoflurane (Pharmaceutical partners of Canada Inc. Richmond Hill, ON). To prevent hypothermia in the anesthetized animals, they were kept on circulating water warming pads. Before and at the end of the experiment, the LIPUS application device was calibrated for the consistency of the ultrasound waveforms (1 KHz modulation, 200 microseconds pulse duration, and 1.5MHz carrier frequency) using a digital oscilloscope and then calibrated for ultrasound intensity of 30mW/cm<sup>2</sup> using an ultrasound power-meter (model UPM-DT-1AV from Ohmic Instruments, Easton, MD, USA).

---

<sup>1</sup> One of the cages consisted of only one rat from the experimental group. Later, the other experimental rat was added to the cage after the death of one control rat.

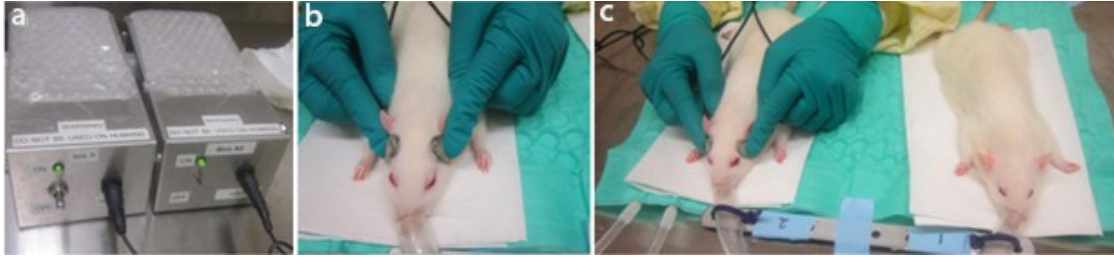


Figure 2-1; Experimental set up: a. LIPUS devices; b. Location of transducers; c. Rats from one cage: one from the LIPUS and another from control groups under inhalation anesthesia

### II.III. Flourochrome Preparation and Injection

To determine the potential actual endochondral bone growth in one to two sigma periods<sup>2</sup>, namely 21 days (Li X.J. et al., 1991), 7days and 28 days following the start of the treatment a solution of calcein green was injected into all the rats. The injection has been performed subcutaneously using 1ml syringe with 26 G1/2 precision glide needle (BD, Fanklin, NJ, USA). The calcein green solution was prepared immediately before injection at the dosage of 10 mg/kg by solving a 1- to 1.24 ml of 3g/l calcein green (C0875-5G, sigma Aldrich 3050 spruce street, St Loup. MO) in NaHCO<sub>3</sub> 2%.

NaHCO<sub>3</sub> 2%: 2 gr NaHCO<sub>3</sub> (All tech, Nicholasville, KY, USA ) has been weighed and solved in Milli-Q water to give a final 100 ml in a 100 ml erlenmeyer flask using a stir bar and stirring plate.

Calcein green Solution (3gr/l): Based on the weight of animals in the day of injection the approximate needed volume of NaHCO<sub>3</sub> 2% and the amount of calcein green to provide the final solution with the concentration of 3gr/l has been calculated. Calcein dissolved in NaHCO<sub>3</sub> 2% then solved by vortexing and filtered using MILLEX GS .22 μm filter. The solution has been sterile-filtered, poured in 15 ml falcon tubes and wrapped with aluminium foil.

### II.IV. Experiment Endpoint

One of the rats belonging to the control group died on the 11<sup>th</sup> day of the experiment as the initial exposure dosage of Isoflurane was higher than her tolerance in the induction phase. The rest of the rats were euthanized by intraperitoneal injection of 0.5 ml Euthansol (Virbac Corporation, Fort Worth, TX, USA) following inhalation anesthesia.

<sup>2</sup> One sigma period is the index of time taken to make a unit amount of bone in vivo at a cellular level (Galen S.M.V. et al., 2010).

## II.V. Tissue Processing

After euthanasia, animals' heads were carefully dissected along the middle sagittal plane. Hemi mandibles have been harvested and cleaned from any attached soft tissue and fixed in 20 ml of formaldehyde (Formalin Solution, Neutral buffered, 10%, Sigma Aldrich, Co. St Louis, MO, USA) at room temperature (RT) for 48 hrs in coded containers. Coding has been performed to address blinding in subsequent assessments. Following gross morphological evaluation and micro-CT scanning, the condylar process in each hemi mandible was separated at a height of about 5 mm. The left condyles have been used for undecalcified sections. The right condyles have been decalcified using Cal-ex II fixative-decalcifier (formaldehyde 1.03 M/L, formic acid 2.56 M/L) (Fisher Scientific, CS511-4D Fair lawn-New Jersey) for 3 weeks.

## II.VI. Gross Morphological Evaluation

### II. VI.I. Morphometric Analysis on Two-Dimensional (2-D) Photographs

It has been suggested that photographic analysis of the rat hemi mandible is more reliable than radiographic analysis (Levrini L. et al. 2003); however, standardizing the condition is of great importance. Positioning the hemi mandibles in a reproducible way was a challenge. Having at least 3 points or regions which can be stabilized for any rat hemi-mandible was a must. Visually, it was noticeable that rat hemi mandibles can lie on their outer side in a reproducible and stable way. To confirm this, a number of mandibles were located on a paper tape coloured with a fresh paint. As is illustrated, all were coloured in similar regions (Figure-

2-2).

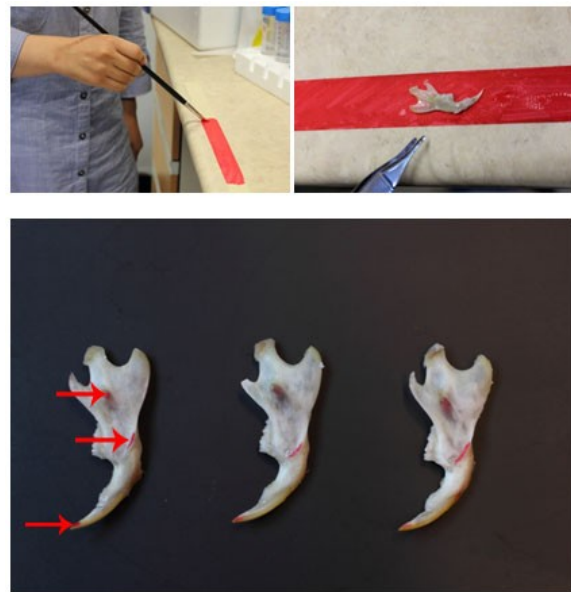


Figure 2-2; Determining the constant regions (arrows) on the lateral side of the mandible that each hemi-mandible sits on

Using a digital camera (Canon T2i, lens: Canon EF 50 mm f/25 Macro, program: aperture priority set to f/5.6) fixed on a steady mount with standardized configuration settings (aperture

f/5.6, shutter speed 1/30 s, and magnification of 2.6), digital pictures of the medial view of the right and left hemi mandibles were obtained and imported to Autodesk® AutoCAD® 2014 software (accuracy 0.0001 mm – measurements were calibrated by having a caliper in each photograph) to allow for accurate linear and angular measurements. The measurement of the condylar length ( $v_a$ ) and width ( $w$ ) has been performed directly on the dissected mandibles using a digital Vernier caliper (Accuracy 0.01 mm).

Morphometric measurements were performed using selected landmarks, distance, and angles based on a modified methodology utilized in previous studies (Xiong H. et al, 2004; Tagliaro M.L. et al, 2009; Taira k. et al, 2009) (Table, 2-1; Figure, 2-3).

### II.VI.I.I. Statistical Analysis

All measurements were performed twice with an interval of two weeks. There was no significant difference between the two registrations (using paired T-test) (for all  $p > 0.05$ ); thus, the mean value representing each hemi-mandible was used for statistical analysis.

Dahlberg's formula (Dahlberg G. 1940) has been used to calculate the error of measurement.

$$Me = \sqrt{\frac{\sum d^2}{2n}}$$

d: difference between two registrations

n: number of duplicate registrations

The size of method error was between 0.007 to 0.032 mm for linear measurements and 0.28° for angular measurement (Appendix 1).

Intra rater reliability for 6 randomly selected animals for each measured variable was tested using an intra class correlation coefficient ICC test. The results showed excellent absolute agreement (for all  $r > 0.9$ ) (Appendix 1).

Considering laterality (having both left and right hemi mandibles), Generalized Estimating Equation (GEE) was used to analyse the data. All statistical analysis was performed by SPSS (version 21.0, IBM Co., Chicago, IL). A P-value less than 0.05 was considered statistically significant.

Table 2-1; Determining the Landmarks, Linear and Angular measurements

LANDMARKS	LINEAR & ANGULAR MEASUREMENTS
1 The most anterior point of the lingual alveolar bone	i (1-2) The length of mandibular base
2 The midpoint of the mandibular foramen	ii (2-8) The length of condylar process 1 (condylar process axis)
3 The most anterior (superior) point of the condyle (determined as a tangent of 45° line and anterior border of the condyle)	iia (2-5) The length of condylar process 2
4 The most superior point of the condyle (determined as a tangent of parallel line to mandibular plane (MP)(9-10) and superior border of the condyle)	iii (1-8) The mandibular length 1
5 The posterosuperior point of the condyle (determined as a tangent of 45° line and posterosuperior border of the condyle)	iv (5-10) The mandibular length 2
6 The most posterior (inferior) point of the condyle (determined as a tangent of 45° line and posteroinferior border of the condyle)	v(va) (3-6) The length of the condyle
7 The middle point of 3 and 6	vi Ramus height (The distance from point 4 to MP)
8 Intersection point of 2-7 extension line and outer contour of the condyle	vii The distance from point 3 to MP
9 The most inferior point of lower border of the angular process	viii The distance from point 8 to MP
10 The posterior-inferior point of attachment of the digastrics muscle	viiiia The distance from point 5 to MP
	ix The distance from point 6 to MP
	x The distance from point 3 to perpendicular line from point 2 on MP
	xi The distance from point 8 to perpendicular line from point 2 on MP
	xia The distance from point 5 to perpendicular line from point 2 on MP
	xii The distance from point 6 to perpendicular line from point 2 on MP
	$\alpha$ Angle of condylar process axis to MP
	w The width of the condyle

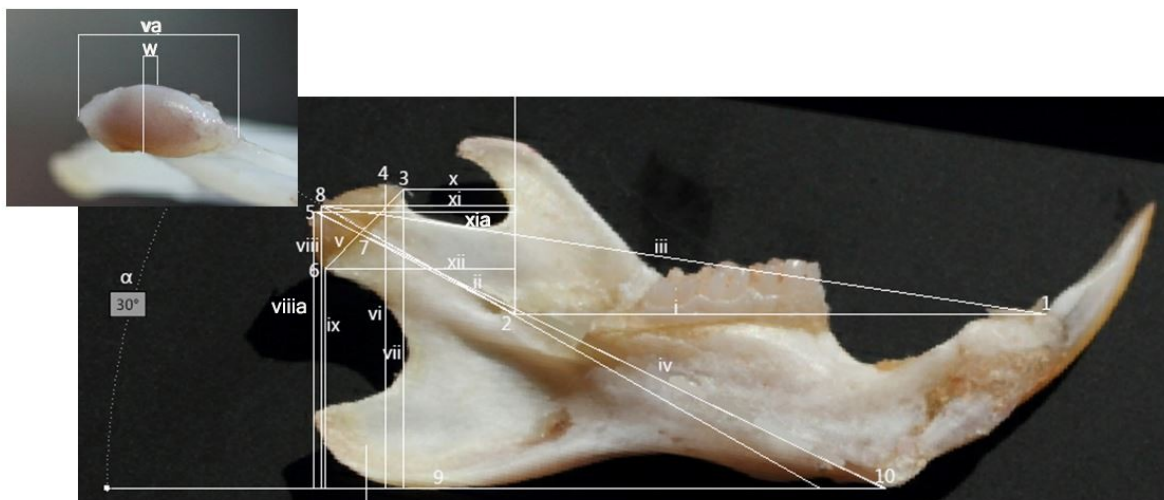


Figure 2-3; Illustration of landmarks and measurements

## II. VI.II. Linear Measurements on Three-Dimensional (3-D) Virtual Models

Micro-CT images of hemi-mandibles were used to create three dimensional visual models using the medical software package MATERIALISE MIMICS (Version 2013.16.0, Plymouth, MI, U.S.A). This package allows the creation of 3-D virtual models from threshold segmented images in the form of triangular mesh called an STL (steriolithograph). This procedure was performed as follows:

The initial geometric shape of mandibles were reconstructed using serial micro-CT scans including slices 18  $\mu\text{m}$  thick in horizontal, sagittal and coronal planes. The micro-CT scans, as BMP (Bit map) images, were opened directly in the MIMICS environment as a new project wizard.

In order to create a mask of the Mandible, the “Thresholding” tool was used while the threshold is determined manually in a way that encompasses the bony area which was mostly between 770 HU to 920 HU. In addition, “Fill holes” and “Keep largest” were selected. When applying this threshold, a mask was created for bony structures.

When the bony structure was masked, from a default menu in MIMICS a predefined high quality setting that preserved the integrity of the virtual models was used to calculate the 3-D objects. A grey value interpolation scheme was used to account for partial volume effects in the voxels. Then, the 3-D virtual models were smoothed using a voxel based technique with an existing MIMICS’ algorithm to preserve calculated volumes. The 3-D models were saved as STL files.

Later, STL files were imported into GEOMAGIC QUALIFY (Version 2014.1.0, Research Triangle Park, N.C., USA). This 3-D suite has been built for optimizing and comparing 3-D objects to a reference object. At this step, further removal of x-ray artifacts was performed manually. Next, alignment techniques (A and B) were performed to align the hemi mandibles to the environment of the program and to each other (clearly these procedures were performed for right and left hemi mandibles separately).

### A. Aligning an object (hemi mandible) to the world coordinate system:

Initially, the deepest point of coronoid notch (1), the most inferior point of the lower border of the angular process (2), and the posterior-inferior point of attachment of digastrics muscle (3) were determined. Then, a plate was made by these 3 points and a vector was created from point 2 to 3. Finally, using the “align to world” option in GEOMAGIC QUALIFY, the plate was

matched with x z plane, the vector paired with x vector and point 2 was used as origin (Figure 2-4).

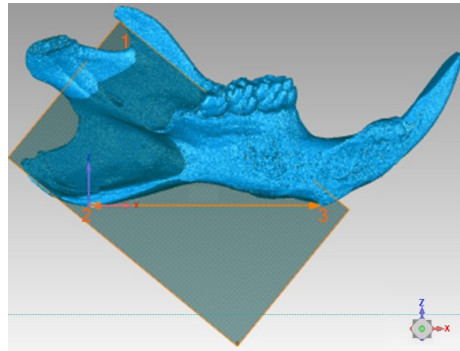


Figure 2-4; One hemi mandible after aligning to the world coordinate system

**B. Aligning the objects (all hemi mandibles) together:**

Using the built in algorithm for best fit (iterative closest point algorithm (ICP)), hemi mandibles (Test objects) from both groups were aligned to the one (Reference) which previously has been aligned to the world coordinate system. The algorithm works in two stages: the first stage fitting uses a small number of points (300) from similar locations on each object. The second stage uses a larger sample of points (1500) to make fine adjustments to best fit the models (analogous to a least squares best fit algorithm). In this way, all the mandibles were aligned to each other and to the world coordinate system.

To verify the results from two-dimensional comparisons, two main linear variables indicative of condylar and mandibular growth in the main direction of growth were measured on three-dimensional virtual models.

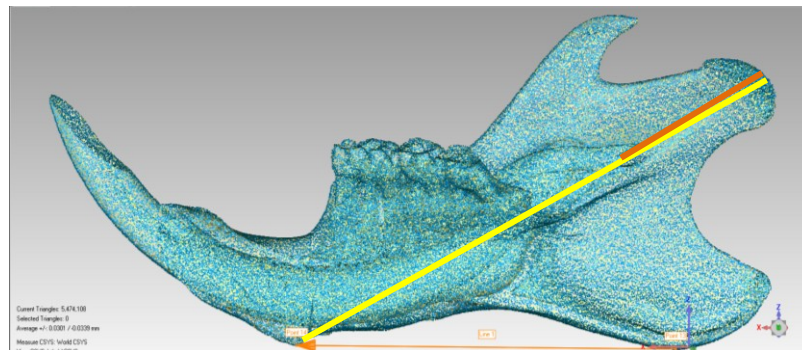


Figure 2-5; Linear measurements on 3-D virtual model; Condylar process length 2: distance from the midpoint of the mandibular foramen to the posterosuperior point of the condyle (orange line); Mandibular length 2: distance from the posterior-inferior point of attachment of digastrics muscle to the posterosuperior point of the condyle (yellow line)

As determining the most posterosuperior point of the condyle especially in 3-D mandibles is highly prone to visual illusion this point was determined as illustrated below:

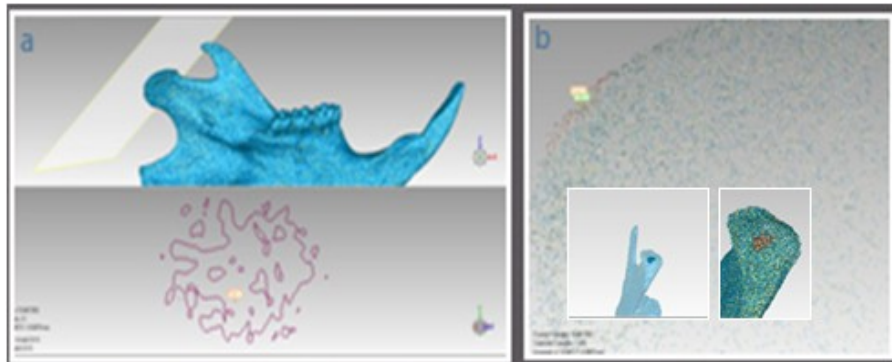


Figure 2-6; Determining the most posterosuperior point of the condyle on 3-D mandible in Geomagic QUALIFY; A 45° plane (using section through object (a)) up to the last possible location of the condyle has been moved. The area was selected and the centre was determined using a default option. If the point was not at the outer contour, the identical point at the outer contour was determined as the most posterosuperior point of the condyle (b)

### II.VI.II.I. Statistical Analysis

Both measurements were performed twice with an interval of two weeks. There was no significant difference between the two registrations (for both  $p > 0.05$ ); thus, the mean value representing each hemi-mandible was used for statistical analysis.

The size of method error based on Dahlberg's formula was 0.022 for mandibular length 2 and 0.015 for condylar process length 2.

Intra rater reliability for 6 randomly selected animals for both measured variables was tested using an intra class correlation coefficient ICC test. The results showed excellent absolute agreement ( $r = 0.999$  and  $0.998$  for mandibular length 2 and condylar process length 2 respectively).

Considering laterality, Generalized Estimating Equation (GEE) was used to analyse the data. All statistical analysis was performed by SPSS (version 21.0, IBM Co., Chicago, IL). A P-value less than 0.05 was considered statistically significant.

### II. VI.III. 3-D Visualisation

In an effort to objectively visualize potential morphological difference between experimental and control groups, mainly to detect any superficial remodeling, the two methods (A and B) previously reported in the literature were combined.

A. Averaging the hemi mandibles from each group:

In a study by Mavropoulos A. et al., (2004), digital tracings of 2-D photographs were combined to construct mean tracings from each experimental group. These were subsequently superimposed on the same reference plane to visualize morphological differences between them. The reference plane in the Mavropoulos study was defined by the mental and the mandibular foramina as it is considered to be minimally affected by growth (Kiliaridis S. et al., 1989).

In the present study, averaging the 3-D virtual models was performed through the following steps: Initially, STL files of all hemi mandibles were optimized by using the built in mesh-doctor feature. Then, superimposition using best fit alignment algorithm was done. This method resulted in the most constant results comparing superimposing on mental-mandibular foramina plane or mental region. The mental region is the area between the anterior end of the molar alveolar process and anterior border of mental foramen. This region is considered as a constant area in various species and is neither affected by forward growth of the incisor process in rodents nor backward growth (Manson J.D., 1968a). Lastly, averaging using a built in average polygon tool in GEOMAGIC QUALIFY was performed. The average object is the object made by points which are at the average spatial coordinates of identical points in test objects with respect to reference object. Averaging was possible using a default option, in which the closest object to the average could be used as a reference. Alternatively, to decrease the effect of normal variations and to imitate before and after treatment design (for the next procedure), one object (the mandible of the rat which died earlier) was used as reference object for both groups. Deviation of other objects was calculated with respect to this selected option.

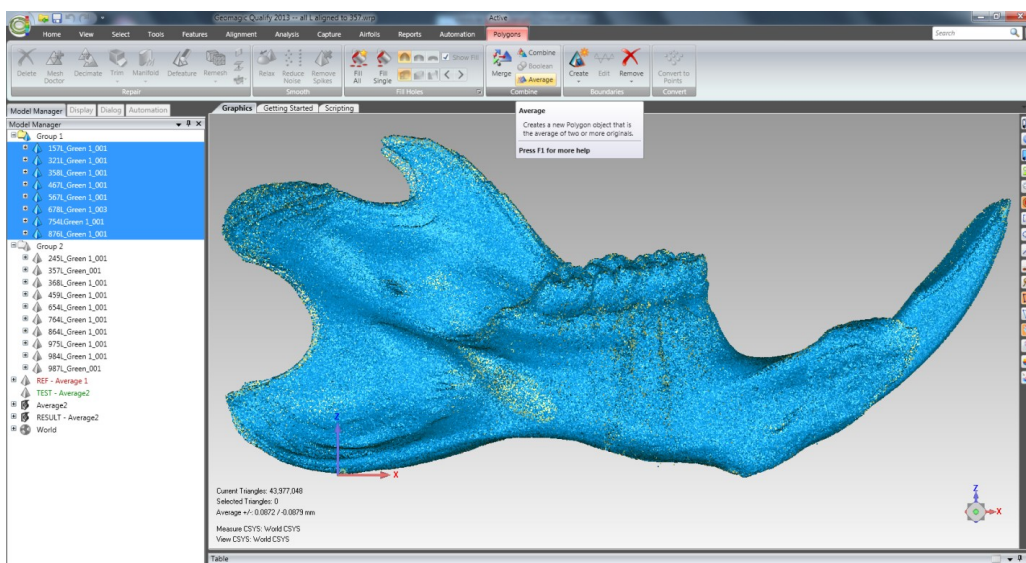


Figure 2-7; Demonstration of averaging following best fit alignment of left hemi mandibles of control group

The result was four 3-D virtual models representative of left and right hemi mandibles from control and LIPUS groups.

#### B. Producing 3-D Deviation map:

Reynolds M. et al. (2011) objectively visualized the magnitude of three dimensional growth of an adolescent human mandible over the period of one year by subtraction of the surfaces of 3-D virtual models made from two consecutive CBCT scans.

In the present study the same methodology and software were used to produce a deviation map from the average hemi mandibles representative of each group as follows: Firstly, to ensure that the triangles (the sub unit of objects) on each (left/right) pair (control/LIPUS) of virtual models were equal in size, which is important for comparing the models, their mesh were rewrapped with new triangles using a built-in feature of GEOMAGIC QUALIFY. Secondly, alignments of each pair of virtual models were performed using a built-in algorithm for best fit as previously mentioned. Thirdly, computing 3-D deviation maps for left and right hemi mandibles was done by measuring the orthogonal distance from vertices of the reference object (control) to the float object (LIPUS) utilizing a built-in feature of GEOMAGIC QUALIFY.

## **II.V. Microscopic Histologic Evaluation**

### **II.V.I. Alcian Blue-Pas Staining**

Based on previous studies by Rabie A.B. et al. (2001, 2004b) and Xiong H. et al. (2005a), combined Alcian blue-PAS (periodic acid and Schiff's reagent) staining can be used to distinguish acid and neutral mucins. While the former stained blue in cartilage, the latter stained distinct magenta in cartilage, which signify the calcifying cartilage matrix and new bone.

In the present study this technique has been utilized for two purposes. The first aim was to assist identifying various fibrocartilage cell layers (Xiong H. et al., 2005 a) (Figure 2-8-B). The most superficial layer is fibrous layer (articular tissue) which can be distinguished by negative staining of Alcian blue and is composed of dense fibroelastic connective tissue with several layers of fibroblast like flattened cells. Next is the proliferative layer (prechondroblastic cartilage layer) which stained positively with Alcian blue and encompasses densely packed undifferentiated mesenchymal cells. Last are the matured chondroblast and hypertrophic chondrocytes layers (chondroblastic cartilage layer); chondroblast layer whose extracellular matrix is stained with Alcian blue (blue color) and hypertrophic chondroblasts with calcifying

extracellular matrix and therefore positive PAS reaction (distinct magenta). The second objective was to discern newly formed bone (Rabie et al., 2004b) and remnants of calcifying cartilage (distinctive magenta) from mature bone (pale pink) (Figure 2-8-C & D).

#### **II.V.I.I. Slide Preparation and Staining Protocol**

After decalcification, the samples were embedded in paraffin. Serial sections of 5  $\mu\text{m}$  were cut through the condyles at the mid sagittal plane (please see section II.V.II.I for methodology) using a rotary microtome (Leica RM 2155; Wetzlar, Germany). Subsequent to dewaxing and hydrating in distilled water, the slides were placed in 3% acetic acid for 5 minutes and then in filtered Alcian Blue PH2.5 for 15 minutes. After rinsing in distilled water, the slides were placed in 0.5% periodic acid for 10 minutes and then washed well under tap then distilled water. Slides were placed in Schiff's reagent for 10 minutes, rinsed in distilled water for 5 minutes, stained in Harris Hematoxylin for 2 minutes and then washed well in tap water. Slides were dipped in 1% acid alcohol 3 times, and washed under tap water. The same procedure was performed in 1% Lithium Carbonate. Finally, the slides were dehydrated using 95% ethanol and 100% ethanol, mounted in Xylene and cover slipped using permount; a glass cover slip were added to the slides.

#### **II.V.I.II. Quantitative and Statistical Analyses**

Photomicrographs were taken using a Leica Fluorescent Digital Microscope with a (CCD) Digital camera (Leica, Wetzlar, Germany) and the image processing analyses were done using RS Image software (Version 1.73) (Photometrics, Roper Scientific, Inc, Tucson, AZ, USA). From each specimen, three sections were determined for histomorphometric analysis. On each section, the middle third of the posterior and middle regions of the condyle were evaluated (Figure 2-8-A).

The thickness of the fibrous, proliferative, chondroblastic, and total layers as well as the cell population in proliferative and chondroblastic layers were measured in a fixed measurement frame of 450 x 450  $\mu\text{m}$  at magnification of x560 (objective magnification x20). For measuring the thickness of fibrocartilage layers, six equally distributed lines parallel to each other and perpendicular to the outer contour of the articular surface were quantified and averaged for each region of each section (Figure 2-8-A and B). To quantify the bone remodeling activity (Suzuki et al., 2004, Xiong H. et al., 2005b) and the amount of active bone formation (Rabie et al., 2004b;

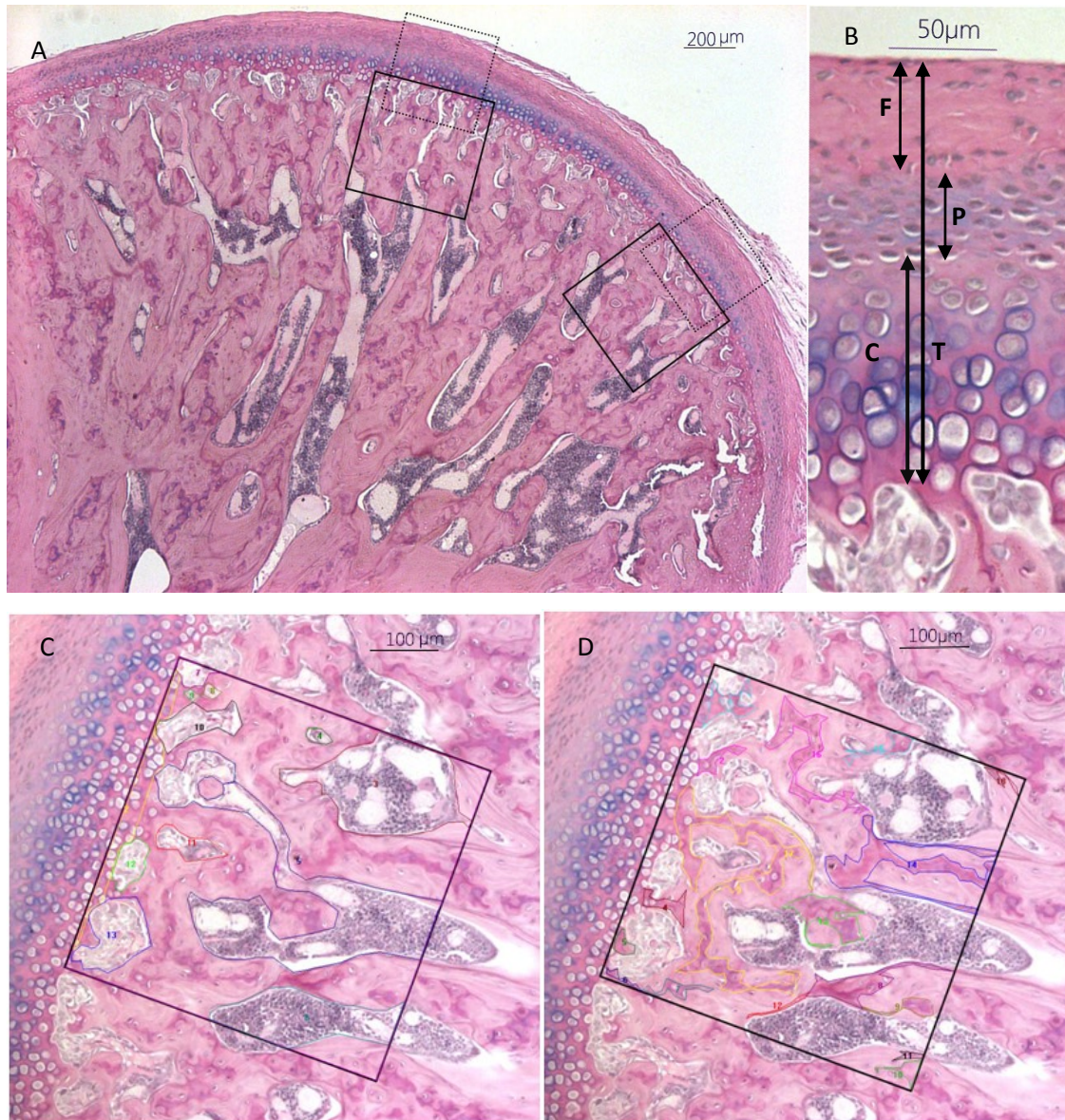


Figure 2-8; An overview of a rat's mandibular condyle in the experimental group (age: 148 days; experimental day: 28) stained with Alcian Blue-PAS: A) The surface of condylar cartilage was equally divided into three parts: anterior, middle and posterior. Two measurement frames were located at the middle third of the middle and posterior thirds. One for the measurement of layers and cell counting ( $450 \times 450 \mu\text{m}$ , dotted) and the other for calculating BV/TV and percentage of newly formed bone and calcifying cartilage area / bone area ( $500 \times 500 \mu\text{m}$ , solid). B) A section of the condyle showing the fibrocartilage layers; F: fibrous layer, P: proliferative layer, C: chondroblastic layer, T: total fibrocartilage layer. C) The hypertrophic area invaded in the erosive zone and the bone marrow areas were traced for calculating trabecular bone area. D) Distinctive magenta areas were traced to be representative of remnants of calcifying cartilage and new bone areas.

Mc Namara J.A. et al., 2003), BV/TV% ( $100 \times (\text{bone area}/\text{tissue area}^3)$ ) and the percentage of remnants of calcifying cartilage and newly formed bone areas/bone area ( $100 \times (\text{distinctive magenta areas}/ \text{bone area})^4$ ) were measured respectively. These evaluations were performed at magnification of X 280 (objective magnification x10) in a fixed frame of 500 x 500  $\mu\text{m}$  which was positioned in a way that its upper horizontal edge was located at the cartilage-bone junction (upper edge of the cartilage lacunae, which initially opened to the bone marrow) (Figure 2-8 A, C and D).

For all of the abovementioned histomorphometric parameters, the average of measurements obtained from three serial sections out of each sample were used for statistical analysis.

To present data mean, standard deviation, median and inter-quartile range (IQR) were used. To compare the groups when compensating for the correlation between the outcomes, Generalized Estimating Equations (GEE) was used. To perform two-by-two comparison when considering the multiple comparisons, Bonferroni method was employed.

Intra rater reliability for six randomly selected animals for all measured variables was tested using an intra class correlation coefficient ICC test. The method error was measured utilising Dahlberg's formula as previously described. Table 2-2 shows the size of method error (ME) for different histomorphometric parameters and intra class correlation values, which show the excellent absolute agreement (for all  $r > 0.9$ ).

	Thickness ( $\mu\text{m}$ ) of fibrocartilage layers				Percentage (%) of		Cell population in	
	Total	Chondro blastic	Proliferative	fibrous	BV/TV	Calcifying cartilage & newly formed bone area/ Total bone area	Chondroblastic layer	Proliferative layer
ME	6.667	3.900	2.528	2.442	1.808	0.729	4.743	6.467
r	0.928	0.953	0.981	0.967	0.983	0.958	0.978	0.912

Table 2-2; The size of method error and single measure values of ICC test for histomorphometric parameters

<sup>3</sup> Tissue area: 0.5 x 0.5 mm square – hypertrophic area invaded in erosive zone; Bone area: Tissue area- bone marrow area

<sup>4</sup> The presence of calcified cartilage matrix (the last morphologic stage of condylar cartilage before it ossifies in to trabecular bone) can be considered as a sign of active bone formation in mandibular condyle. (Mc Namara JA et al., 2003) Following PAS staining, both calcifying cartilage and newly formed bone take on a distinctive magenta color which can be distinguished from mature bone (Rabie A.B. et al., 2004b). In a series of mandibular condylar growth modification studies in which this staining has been performed, the amount of new bone formation has been calculated based on distinction in staining density using an automatic program. In the present study, manual tracing of distinctive magenta areas were utilized and due to the fact that it was not distinguishable whether these areas are newly formed bone or remnants of calcifying cartilage, both tissues were considered and calculated to be a sign of active bone formation.

All statistical analysis was performed by SPSS (version 21.0, IBM Co., Chicago, IL). A P-value less than 0.05 was considered statistically significant.

### **II.V.II. In vivo Fluorochrome Labeling**

In bone research, the use of fluorochrome is a relatively old but widely accepted technique (Galen S.M.V. et al., 2010; Andre T., 1956). Fluorochrome labels by binding to calcium ions can be integrated at any sites of mineralization and demarcates the mineralization front at time of administration. They can be detected in histologic sections without decalcification under a fluorescence microscopy.

The vital staining technique was used by Suzuki S. et al. (2004) to quantify the amount of endochondral bone growth (by measuring the distance between two labels) in mature (15 week old) rats following local injection of IGF-I. The aim was to determine whether histological changes are temporary or are accompanied by actual growth of the condyle. The marker interval (the time interval between the bone labels) was 21 days which covers the whole experimental period.

In the present study, the above mentioned vital stain technique has been used. Even though our experimental period was 28 days, the label interval was kept at 21 days (injections were performed at 7 days and 28 days following the start of the treatment) which is also one to two sigma periods and suggested as the most appropriate to investigate directed bone formation (Galen S.M.V., 2010). A longer time was avoided to decrease the chances for label escape (Frost H.M., 1969). As previously mentioned, calcein green (10 mg/kg in sodium bicarbonate 2%) has been used as a fluorochrome label and was injected subcutaneously into all the rats.

### **II.V.II.I. Slide Preparation**

After fixation in formaldehyde at RT, left specimens (mandibular condyles at the height of 5mm) were rinsed in distilled water and transferred to 70% 2-propanol for 24 hrs. Samples were placed in an automated tissue processor for dehydration and clearing. Dehydration was performed through 2-propanol gradient of 80%, 95%, 95% and 100% with 4 hours for each step at RT. Clearing (defatting) was done by replacing 100% 2-propanol with two exchanges of methyl salicylate for 6 hrs.

Infiltration and embedding the samples in Methyl Methacrylate was performed as follows: After removing the samples from processor they were placed in to a Methyl Methacrylate monomer for 24 hrs. Then, the monomer was removed and replaced with a Methyl Methacrylate mixture containing plasticizer and catalyst for the same duration. This was removed and replaced with a Methyl Methacrylate mixture containing plasticizer and an additional catalyst for 24 hrs. Finally, the mixture was removed and samples were embedded in glass vials with a Methyl Methacrylate embedding mixture containing plasticizer and catalyst till their polymerization was completed. In each procedure vacuum pressure was applied for 1hour in 20-minute intervals.

Polymerized blocks were broken out of the embedding vials, shaped and 6-micon thick sections were cut at mid sagittal plane with a D-profile tungsten carbide knife using a heavy-duty rotary microtome. To assure that all the sections<sup>5</sup> are at mid sagittal plane and similar for all the samples they were measured in all directions and the thickness was noted prior to embedding. While sectioning, trimming was performed until the mid-point was determined based on the thickness of each particular sample.

In addition, three reference points using blue tissue marker dye (Shandon tissue marking dye Thermo scientific MI, USA) were marked directly on the condyle after fixation and prior to any procedure (figure 2-9). These points were a. the anterior edge between the cartilage and bone, b. Posterior edge point between the cartilage and bone, and c. midpoint of “a” and “b” on the upper most articular surface in the frontal dimension. Having these points on sections confirmed that they were at mid sagittal plane.

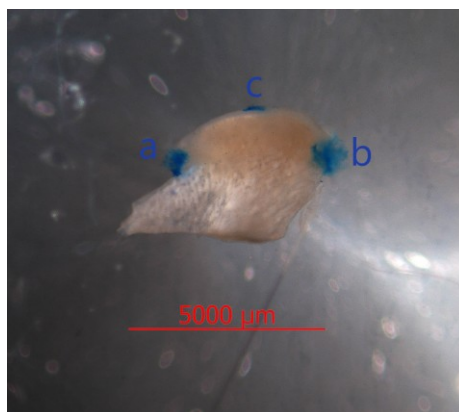


Figure 2-9; 3 Reference points of the condylar head: (a) anterior edge, (b) posterior edge between the cartilage and bone and (c) midpoint of “a” and “b” on the upper most articular surface in frontal dimension

<sup>5</sup> One sample from each group were sectioned wrongly and therefore deleted from the sample size.

Cut sections were adhered to pre-cleaned, silane-gelatin coated glass slides. Mounted sections were allowed to dry for 24 hours. Sections were deplasticized and cover slipped for fluorophore analysis.

#### II.V.II.II. Quantitative and Statistical Analyses

Photomicrographs were taken using an Olympus FluoView 1000 Inverted IX81 microscope and the image processing analyses was done using RS Image software (Version 1.73) (Photometrics, Roper Scientific, Inc, Tucson, AZ, USA). Excitation and emission wavelength filter settings for visualizing calcein labels were respectively 436-495 nm and 517-540 nm. From each specimen 3 sections were used for analysis.

To estimate the amount of endochondral bone growth in the condyle during 21 days of treatment, the distance between the calcein labels was measured. Evaluation was performed in a square of  $940\mu\text{m} \times 940\mu\text{m}$  at magnification of X 82 in the middle region of the condyle (Figure 2-10).

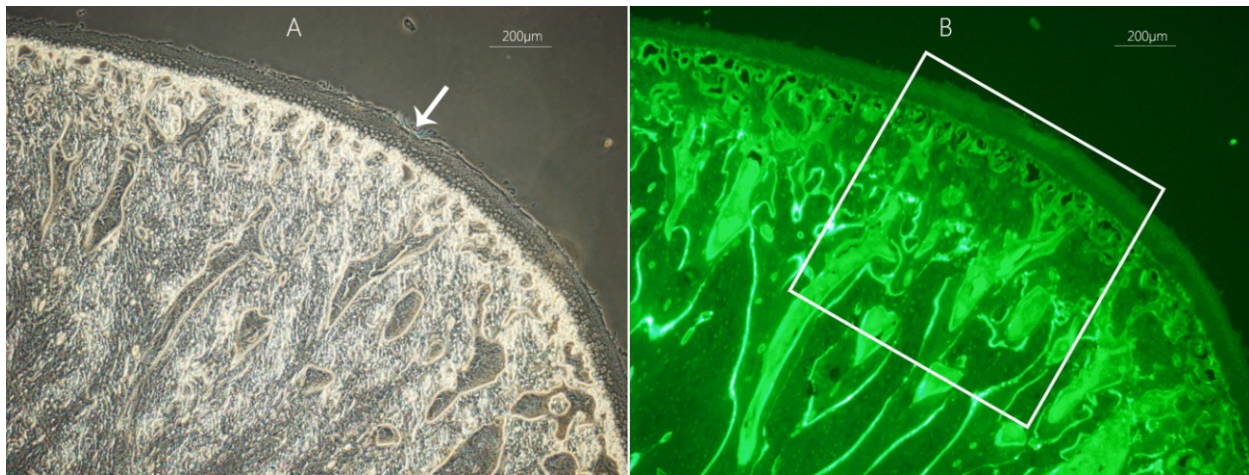


Figure 2-10; Photomicrographs of undecalcified sections of mandibular condyle at mid sagittal plane; A) midpoint of the condylar surface (arrow) demarcated with tissue marker dye as mentioned in the text; B) the section under epifluorescence illumination, region of evaluation: a square of  $940\mu\text{m} \times 940\mu\text{m}$  in the middle region

Due to the very irregular course of the fluorescent labels and in order to increase the accuracy of measurements, six parallel lines to each other were drawn equally distributed and perpendicular to the outer contour of the condyle between the upper most points of the first and second labels (Figure 2-11). The average measurements obtained from three serial sections out of each sample were used for statistical analysis.

Measurements were performed twice with an interval of two weeks. There was no significant difference between the two registrations ( $p > 0.05$ ), and the mean value for each sample was used for statistical analysis. The size of method error based on Dahlberg's formula was 5.262 and the single measure value ( $r$ ) was 0.968 using an intra class correlation coefficient ICC test. To present data mean, standard deviation, median and inter-quartile range (IQR) were used.

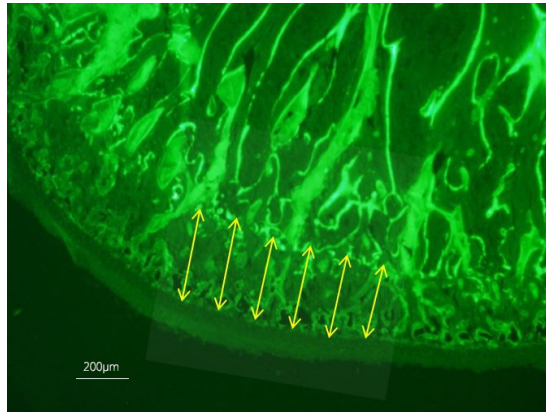


Figure 2-11; Measuring the distance between calcein labels

Considering two independent samples and the fact that equality of variance and normality were met, independent sample t-test was used.

All statistical analysis was performed by SPSS (version 21.0, IBM Co., Chicago, IL). A P-value less than 0.05 was considered statistically significant.

### **II.V.III. Goldner's Trichrome Staining for Osteoid**

This method was used to provide a sharp contrast between mineralized bone tissue [(greenish blue (light-green SF yellowish)] and newly formed non mineralized matrix of the bone, i.e.: osteoid [red (acid fuchsin-ponceau)] (Rutten S. et al., 2008; Leng K.S. et al., 2008).

Osteoblasts begin the process of forming bone tissue by secreting the osteoid. Under conditions of rapid bone turnover and growth, osteoblasts produce osteoid rapidly and in a disorganized fashion so woven bone is formed (Testori T. et al., 2013).

In the present study this technique has been utilized to determine whether LIPUS application has influence on osteoblast activity and osteoid formation in cancellous bone subjacent to condylar cartilage.

#### **II.V.III.I. Staining Protocol**

Staining was performed on two sections of each set of consecutive undecalcified sections (for details please see part II.V.II.I.) following the method described by Bemenderfer T.B. et al. (2014) as described below:

Slides were deplasticized using Xylene and plastic film was removed. Then they were placed in warm (40-60°C), Cool (at RT, with agitation) and warm Xylene for 40, 20, and 20 minutes, respectively. In each step, Xylene was discarded after use. Slides were rehydrated through graded series of ethanol (EtOH): 100 % EtOH for 2–5 min, 100 % EtOH for 2–5 min, 95 % EtOH for 2–5 min, 70–80 % EtOH for 2–5 min, and distilled water (DI H<sub>2</sub>O) for 2–5 min. Staining in a working solution of Weigert's iron hematoxylin for 15 min was also performed. Then slides were dipped in DI H<sub>2</sub>O, washed in gently running tap (basic pH) water for 15 min and again dipped in DI H<sub>2</sub>O. Slides were stained in a ponceau–acid fuchsin for 15 min. Following two times rinsing and shaking in 1 % acetic acid, they were quickly dipped in DI H<sub>2</sub>O to remove acid. The same procedure was performed after staining the slides in phosphomolybdic acid–Orange G for 8 min, and also, staining in Light Green SF Yellowish for 15 min. Then, slides were dehydrated through following graded ethanol immersions: 70–80 % EtOH for 2–5 min, 95 % EtOH for 2–5 min, 100 % EtOH for 2–5 min, and 100 % EtOH for 2–5 min, cleared in xylene for 2–5 min, and a cover slip was added.

#### **II.V.III.II. Quantitative and Statistical Analyses**

Photomicrographs were taken using a Leica Fluorescent Digital Microscope with a (CCD) Digital camera (Leica, Wetzlar, Germany) and the image processing analyses were done using RS Image software (Version 1.73) (Photometrics, Roper Scientific, Inc, Tucson, AZ, USA). From each specimen, two sections were used for analysis.

Evaluation was performed on two successive 240µm\*240µm squares (magnification x940) located at the interface of cartilage and subchondral cancellous bone in the middle and posterior regions of the condyle (Figure 2-12). For every measurement field, osteoid thickness was calculated by averaging the osteoid thickness values. 10 to 60 measurements were obtained at fixed intervals along the osteoid surface (Figure 2-13).

Measurements were performed twice with an interval of one week. There was no significant difference between two registrations ( $p > 0.05$ ) and therefore the mean value of measurements for

each sample was used for statistical analysis. The size of method error based on Dahlberg's formula was 0.192 and the single measure value (r) was 0.956 using intra class correlation coefficient ICC test. To present data mean, standard deviation, median and inter-quartile range (IQR) were used.

Considering two positions, Generalized Estimating Equations (GEE) was used to analyse the data. All statistical analysis was performed by SPSS (version 21.0, IBM Co., Chicago, IL). A P-value less than 0.05 was considered statistically significant.

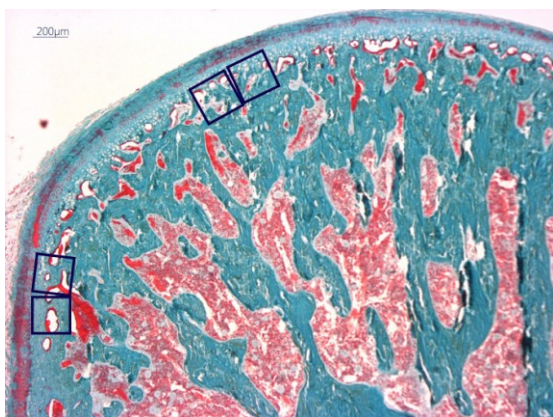


Figure 2-12; Demonstration of evaluated regions for osteoid thickness

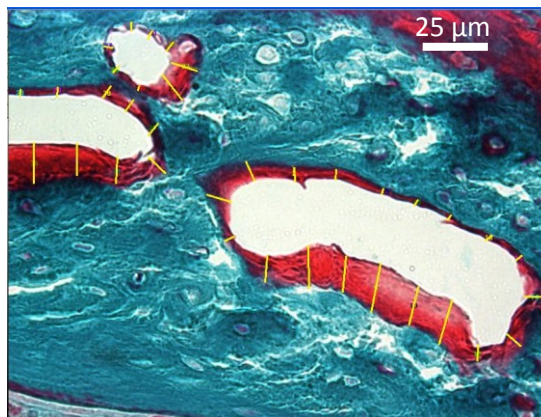


Figure 2-13; Demonstration of measuring the osteoid thickness along the osteoid surface

## II.VI. Micro Computed Tomography ( $\mu$ CT) Scanning

Mechanical loading can alter bone remodeling rate and therefore its microarchitecture and degree of mineralization. High resolution micro X-ray computed tomography is a non-invasive recently developed technique that can detect such changes precisely (Xiong H. et al., 2005b; Renders J.A.P. et al., 2007; Jiao K. et al., 2010). In evaluating the microarchitecture of cancellous bone, even though three dimensional morphometric indices can be derived from 2-D histologic images for the majority of parameters, a fixed structural model such as a plate model or rad model should be assumed while trabecular bone might change its structure incessantly. Using this technique, direct three dimensional morphometric analysis is possible without making an assumption about the structure type (Hildebrand T. et al., 1999).

The mandibles were mounted in cylindrical specimen holders (polypropylene, outer diameter: 29 mm, wall thickness: 1 mm), secured with synthetic foam and completely submerged in fixation fluid.

The specimens were scanned using a high-resolution compact fan-beam tomogram ( $\mu$ CT, SkyScan 1072, Aartselaar, Belgium) and associated software (Version 2.6.0) at a resolution of 18 $\mu$ m using an x-ray source potential of 85kV, amperage of 290 $\mu$ A, and power of 25W through 180° with a rotation step of 0.5°, to produce serial cross-sectional images. An aluminum filter of 1.0 mm thickness was used, and three projections for each scanned section were averaged. Scanned images were saved in \*.tiff format. Scion Image, beta 4.0.2 (Scion Image Corporation, USA), was used to median-filter the raw image data to reduce noise. The filtered image data was rendered in three dimensions. Using this orientation, the 2-D image stacks were exported to a commercial image analysis package (IP-PLUS, Media Cybernetics, Bethesda, MD, USA). Finally, the images were reconstructed using NRecon© (Version 1.4.4) from SkyScan®. Reconstructed images were analyzed using CT Analyser (Version 1.6.1.0, Skyscan N.V. Kontich, BE).

### **II.VI.I. Quantitative and Statistical Analyses**

To evaluate the changes of the trabecular bone subjacent to condylar cartilage at the middle and posterior areas of the condyle, a modified method which has been previously explained by Xiong et al. (2005b) was used. In brief, the first slice was determined at the section of the utmost point in the superior direction of the middle and posterior regions of the condyle in two separate actions. From the reference line, 80 slices with an increment of 18  $\mu$ m were scanned. In the middle and posterior regions the whole trabecular bone from slice 17<sup>th</sup> to 45<sup>th</sup> was selected manually as the volume of interest (Figure 2-14 A-C). Local adaptive threshold algorithms with pretresholding between 48 and 225 were used during the evaluation of all specimens. Standard bone microstructural parameters (Xiong H. et al., 2005b; Jiao K. et al., 2008; Teo JCM et al., 2006), namely Bone Volume Fraction (Bone Volume / Tissue Volume (BV/TV (%)), Bone Specific Surface (Bone Surface to volume ratio) (BS/BV) (mm<sup>-1</sup>), Trabecular Number (Tb.N) (mm<sup>-1</sup>), Trabecular Thickness (Tb.Th) (mm), Trabecular Separation (Tb. Sp) (mm), and Degree of Anisotropy (DA)(ratio), were evaluated using model independent, three dimensional morphometric analysis. In addition, to evaluate bone mineralization, Bone Mineral Density

(BMD) ( $\text{mg}/\text{cm}^3$ ) was determined based on the linear correlation between CT attenuation coefficient and bone mineral density using a calibrated phantom.

All the Parameters were quantified two times with an interval of two weeks. There was no significant difference between two registrations ( $p>0.05$ ) and therefore the average value from the measurements of each condyle was used for analysis. The size of method error (ME) has been determined using Dahlberg's formula (Table 2-3).

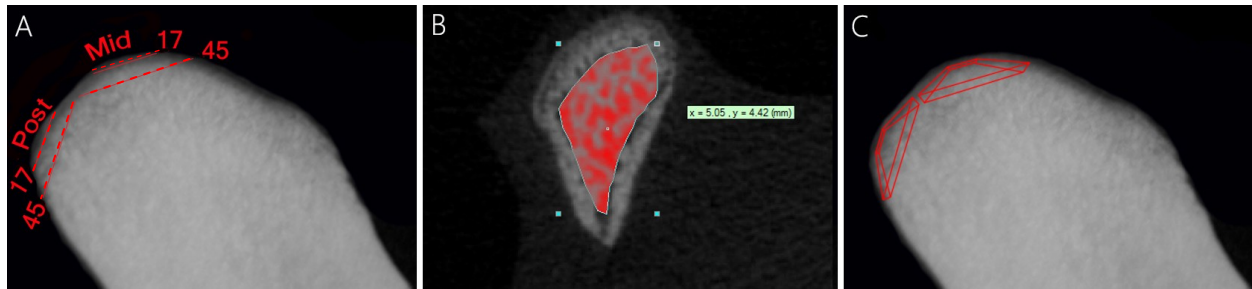


Figure 2-14; Illustration of the method for locating the region of interest for micro-CT analysis; A); the upper most point of the middle and posterior regions of the condyle were determined and the 17<sup>th</sup> to 45<sup>th</sup> slices were selected for each region; B) In each slice, the whole trabecular bone was selected manually; C) Final volume of interest evaluated for morphometric and bone mineral density analysis.

Intra rater reliability for six randomly selected animals for each measured variable was tested using an intra class correlation coefficient ICC test. The results showed excellent absolute agreement (for all  $r>0.9$ ). (Table 2-3)

Considering both laterality (Left and Right hemi mandibles) and position (Middle & Posterior), Generalized Estimating Equation was used to analyse the data. All statistical analysis was performed by SPSS (version 21.0, IBM Co., Chicago, IL). A P-value less than 0.05 was considered statistically significant.

	BMD ( $\text{mg}/\text{cm}^3$ )	BV/TV (%)	BS/BV ( $\text{mm}^{-1}$ )	TbTh (mm)	TbSp (mm)	TbN ( $\text{mm}^{-1}$ )	DA (ratio)
ME	0.034424	0.137648	0.34421	0.0005	0.003	0.035086	0.0606
r	0.997	0.986	0.985	0.993	0.956	0.996	0.968

Table 2-3; The size of method error and single measures values of ICC test for densitometric and morphometric parameters evaluated by  $\mu\text{CT}$  analysis.

# CHAPTER III: RESULTS

---

### III.I. Body Weight

The body weight of the species from both experimental and control groups were increased during the acclimatization period and then reduced about 5% following the start of the experiment. The average weight remained relatively on that reduced level till the end of the experiment for both groups.

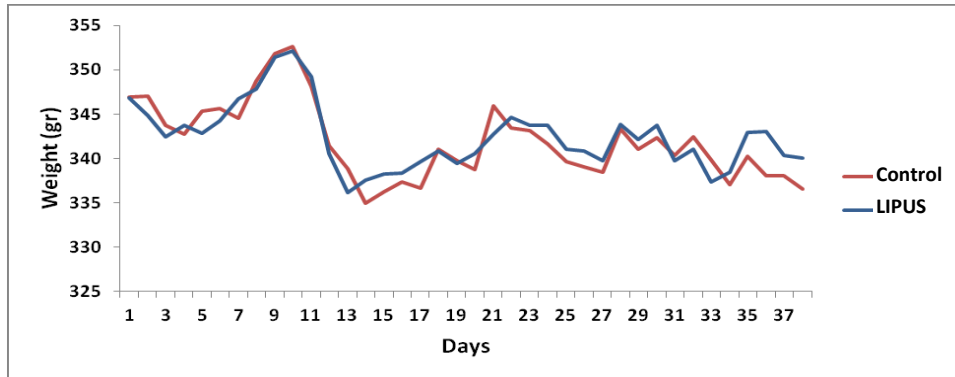


Figure 3-1; The change of weight of the animals in the control and LIPUS groups during acclimatization and experimental periods.

### III.II. Gross Morphological Evaluation

#### III.II.I Morphometric Analysis on Two-Dimensional (2-D) Photographs

The mean, standard deviation, and mean difference of the control and LIPUS groups for 16 linear and one angular measurement variables are presented in table 3-1, including comparison of the measurements between left and right hemi mandibles. Except for mandibular length 2 (iv) and condylar length (v) ( $p < 0.05$ ), there was no significant left-right differences in all other parameters.

Following the experimental period, no statistically significant difference was observed between the groups for ramus height (vi), a vertical linear variable, mandibular length 1 (iii), a horizontal linear variable, and mandibular length 2 (iv), the main linear variable in the direction of mandibular growth (upward, backward) (for all  $p > 0.05$ ). However, the latter showed 0.2 mm mean difference in favour of the LIPUS group (Control=  $24.08 \pm 1.13$ ; LIPUS=  $24.28 \pm 0.71$ ) (Figure 3-2; Table 3-1).

Table 3- 1; Values of Linear (mm) and Angular (°) Measurements (Mean ± SD) in experimental and control groups

Response Variable	Laterality	Control		LIPUS	Mean difference	P†	Response variable	Laterality	Control		LIPUS	Mean difference	P†	
		mean±SD							mean±SD					
i	L	20.91 ± 0.51	21.29 ± 0.63		0.16	0.471*	α	L	32.88 ± 2.66	36.05 ± 1.55		2.54	<0.001	
	R	21.52 ± 0.35	21.46 ± 0.55						R	32.5 ± 1.34	34.4 ± 2.51			
	Total	21.21 ± 0.53	21.37 ± 0.58						Total	32.69 ± 2.04	35.23 ± 2.2			
ii	L	8.14 ± 0.40	8.15 ± 0.26		0.03	0.893*	vii	L	12.25 ± 0.3	12.16 ± 0.44		-0.07	0.62	
	R	8.13 ± 0.44	8.19 ± 0.33						R	12.17 ± 0.46	12.13 ± 0.6			
	Total	8.14 ± 0.40	8.17 ± 0.29						Total	12.21 ± 0.38	12.14 ± 0.51			
iia	L	8.22 ± 0.18	8.23 ± 0.28		0.12	0.24*	viii	L	11.84 ± 0.34	11.91 ± 0.26		0.08	0.586	
	R	8.01 ± 0.38	8.25 ± 0.36						R	11.77 ± 0.5	11.84 ± 0.43			
	Total	8.12 ± 0.31	8.24 ± 0.31						Total	11.8 ± 0.42	11.88 ± 0.35			
iii	L	28.15 ± 0.56	28.24 ± 0.70		0.07	0.796*	viii a	L	11.62 ± 0.36	11.78 ± 0.43		0.09	0.499	
	R	28.59 ± 0.40	28.64 ± 0.56						R	11.56 ± 0.5	11.58 ± 0.37			
	Total	28.37 ± 0.52	28.44 ± 0.65						Total	11.59 ± 0.42	11.68 ± 0.40			
iv	L	24.10 ± 1.29	24.33 ± 0.62		0.20	0.034*	ix	L	9.54 ± 0.48	9.36 ± 0.38		-0.21	0.198	
	R	24.05 ± 1.03	24.23 ± 0.81						R	9.5 ± 0.45	9.26 ± 0.44			
	Total	24.08 ± 1.13	24.28 ± 0.71						Total	9.52 ± 0.45	9.31 ± 0.4			
v	L	4.57 ± 0.15	4.53 ± 0.32		0.02	0.033*	x	L	3.63 ± 0.16	3.22 ± 0.41		-0.2	0.121	
	R	4.45 ± 0.27	4.53 ± 0.32						R	3.4 ± 0.35	3.42 ± 0.42			
	Total	4.51 ± 0.22	4.53 ± 0.31						Total	3.52 ± 0.29	3.32 ± 0.42			
va	L	4.26 ± 0.14	4.23 ± 0.28		0.02	0.896	xi	L	6.8 ± 0.28	6.85 ± 0.26		0.07	0.532	
	R	4.21 ± 0.19	4.29 ± 0.28						R	6.64 ± 0.33	6.72 ± 0.2			
	Total	4.24 ± 0.16	4.26 ± 0.27						Total	6.72 ± 0.31	6.79 ± 0.24			
w	L	1.84 ± 0.10	1.82 ± 0.09		0.03	0.796*	xia	L	6.83 ± 0.37	6.96 ± 0.34		0.1	0.417	
	R	1.79 ± 0.15	1.88 ± 0.12						R	6.91 ± 0.27	7.04 ± 0.45			
	Total	1.81 ± 0.13	1.85 ± 0.11						Total	6.87 ± 0.31	6.97 ± 0.40			
vi	L	12.49 ± 0.3	12.47 ± 0.4		0.02	0.826	xii	L	7.27 ± 0.35	6.76 ± 0.41		-0.28	0.05	
	R	12.48 ± 0.49	12.42 ± 0.49						R	6.98 ± 0.39	6.94 ± 0.45			
	Total	12.48 ± 0.39	12.45 ± 0.43						Total	7.13 ± 0.38	6.85 ± 0.43			

\* Based on GEE, comparison of left and right laterality considering the correlation between responses.

† Based on GEE, considering the correlation between responses. L:Left, R:Right

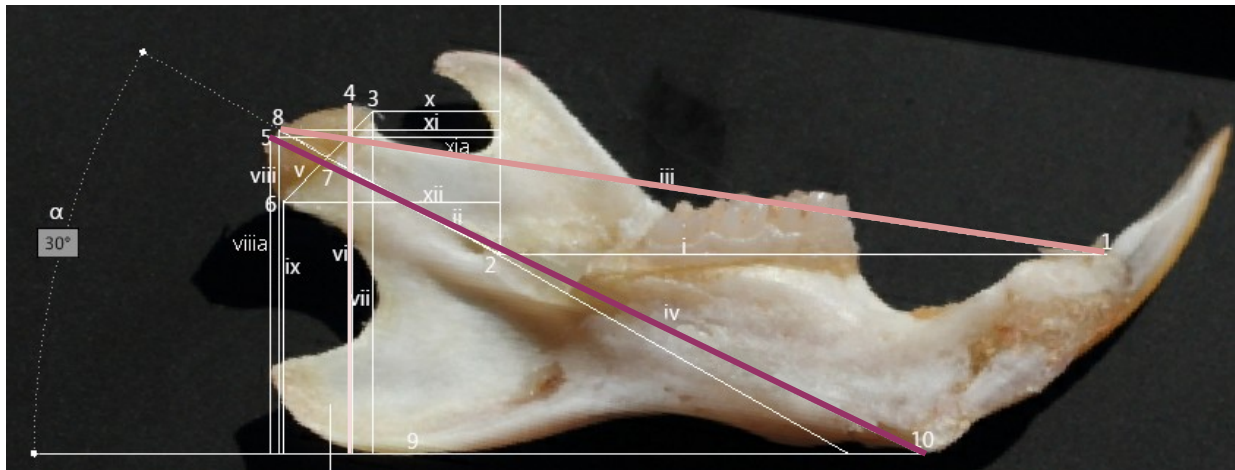


Figure 3-2; Demonstration of main linear variables for evaluating the size of the mandible

To examine the potential growth of the condyle in longitudinal, transverse, and sagittal (the main direction of condylar growth), condylar length ( $v/v_a$ ), width ( $w$ ), and condylar process length 1 and 2 ( $ii$  and  $ii_a$ ) have been evaluated and there was no significant difference between groups ( $p > 0.05$ ). Nonetheless, the mean difference for condylar process length 2 ( $ii_a$ ) was 0.12 mm (Control =  $8.12 \pm 0.31$ , LIPUS =  $8.24 \pm 0.31$ ) (Figure 3-3; Table 3-1).

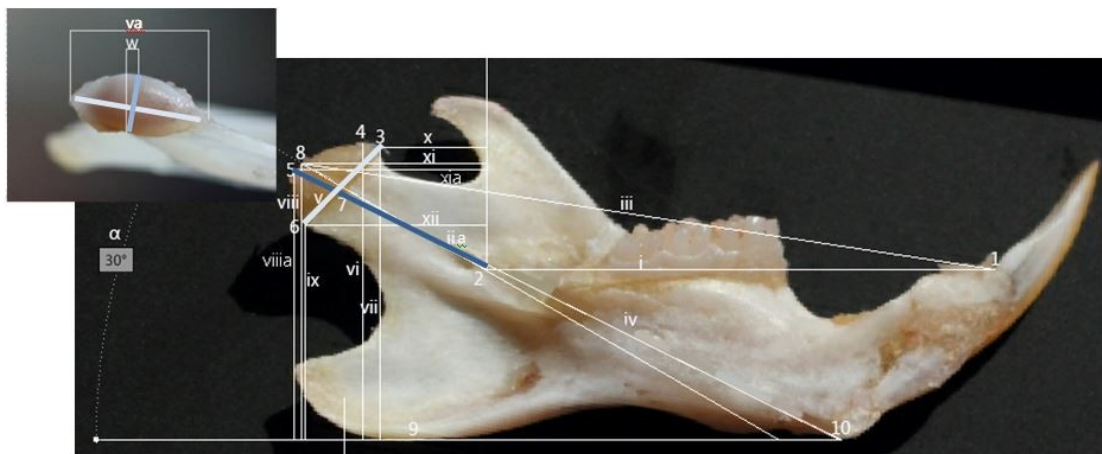


Figure 3-3; Demonstration of linear variables for evaluating condylar size in different directions

In the present study, condylar process length and mandibular length were measured in two different ways. In the first method following Xiong H. et al.(2004), mandibular length 1 ( $iii$ ) is the large side of the triangle made as well by mandibular base ( $i$ ) and condylar process axis ( $ii$ ). Since the mandibular base is not expected to be affected by the treatment mandibular length,

1(iii) is dependent on condylar process length 1 (ii), both of which are also affected by the degree of alpha (angle of condylar process axis to mandibular plane). Thus, this angle was measured as even previous studies recommend that the linear changes in the mandible must not be assessed in isolation, but always in relation to changes affecting the mandibular angle (Kinzinger G. and Diedrich P., 2005)<sup>1</sup>.

The degree of Alpha was significantly more ( $2.54^\circ$ ) in the LIPUS group ( $35.23 \pm 2.2$ ) in comparison to the control group ( $32.69 \pm 2.04$ ) ( $p < 0.001$ ). The mandibular plane (MP) is a reference line and therefore it is assumed to be invariant. The Condylar process axis is the line from point 2 (the midpoint of mandibular foramen) to point 8 (Intersection point of 2-7 extension line and outer contour of the condyle). The midpoint of mandibular foramen (2) has been considered as a reference point as it is constant and is not under the influence of growth or morphological changes (Xiong H. et al., 2004; Mavropolous A. et al., 2004). Thus, point 7 is the key point for changes in the degree of alpha which per se is dependent on the position of the most anterior superior (3) and posterior inferior (6) points of the condyle (point 7 is the midpoint of points 3 and 6). The distance of these points especially point 6 to MP (vii, ix) and particularly to the perpendicular line from point 2 on MP (x, xii) were less in the LIPUS group compared to the control group (Table 3-1). Therefore, the increment in the degree of Alpha geometrically can be attributed to more of an anterior inferior location of the most anterior superior and especially posterior inferior points of the condyle (Figure 3-4).

Despite the above mentioned changes which may imply a shorter mandibular condyle in the LIPUS group, point 8 was unchanged or even located more posteriorly superior in the experimental group. Moreover, the mean difference for condylar process length 1(ii) and mandibular length 1(iii), though negligibly, remained positive in favour of the LIPUS group. The distance of the most posterosuperior point of the condyle to MP (viii) and perpendicular line from point 2 on MP (xii) revealed that this point was also in a more posterosuperior location in the LIPUS group. In addition, condylar process length 2 (iia) and mandibular length 2 (iv),

---

<sup>1</sup> For instance, in the study in which the effect of continuous bite-jumping on mandibular and condylar morphology in adult rats (Xiong H. et al., 2004) was evaluated, the degree of alpha was significantly decreased and the condylar process and mandibular length significantly increased. This was attributed to the fact that bone apposition mainly happened in the posterior and superior of the condylar head and hence morphological changes of condylar head. It is suggested that these could happen as a result of the appliance's mechanics, or stronger pull of the supra hyoid musculature. These changes tend to relapse after treatment. Stable outcomes in the form of skeletal changes are due to a change in the condyle's growth direction (Kinzinger G. et al., 2008).

which are not dependent on the degree of alpha and are at the direction of condylar growth as previously mentioned, showed higher values in the LIPUS group; however, not to a significant degree (Table 3-1, Figure 3-4).

A potential explanation for the aforementioned observations could be progression of the cartilaginous cap in the perichondrial-periosteal junction and a slight enlargement in the middle region of the condylar cartilage and/or bone (most top areas of the condylar head in measurements were also determined as postro superior point of the condyle) consequent to LIPUS treatment (Figure 3-4). However, the majority of differences in the values was nonsignificant and therefore might be only due to normal variation and/or method error.

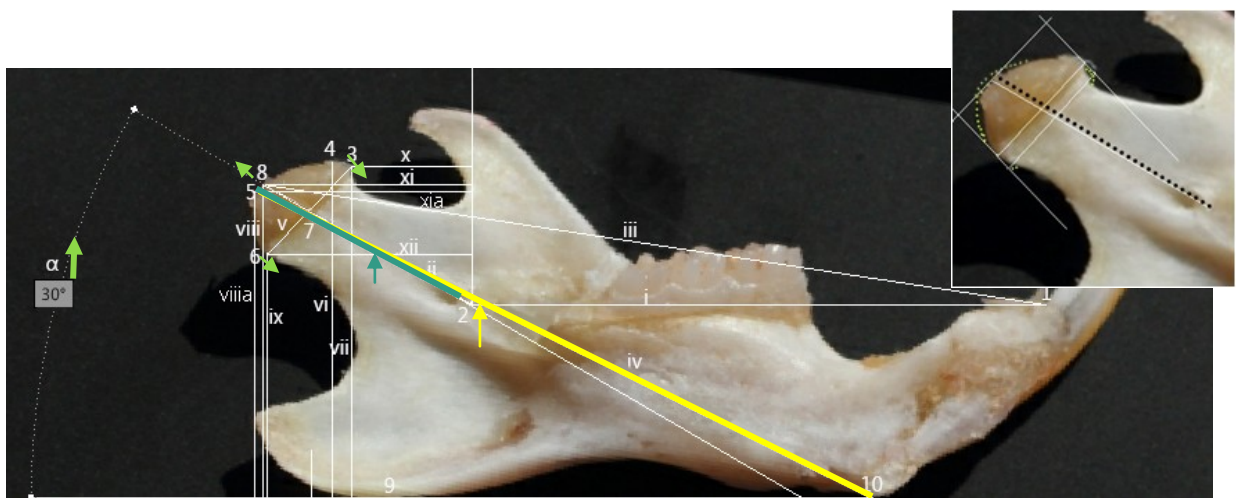


Figure 3-4; Demonstration of increment in the degree of Alpha and geometrical reason; slight increase in the middle region of the condyle as well as condylar process length (green line) and mandibular length (yellow line); potential hypothetical regional changes in mandibular condyle

### III.II.II. Appearance of The Condylar Surface

Xiong H. et al. (2004) reported that the surface of the mandibular condyle in adult rats is dark and more like bone due to a very thin covering cartilage layer. In contrast, when cartilage is formed as a result of treatment (fixed bite jumping appliance) in 30 days the thickness of the cartilage increased and the surface became translucent. Even though species, gender and age of the animals in the present experiment were the same as the previous study, such a darkness or translucency (Figure 3-5) was not a constant finding in the control or LIPUS groups. However, three pairs of the condyles in the LIPUS group had translucent, thick and large cartilage and such an appearance was absent in the control group. In addition, it was noteworthy that most superior

(middle) areas of the condylar cartilage were thick and translucent in almost all samples of the experimental group. This might suggest enlarged cartilage layer at this region as evidence of cartilage formation on the condyle surface.

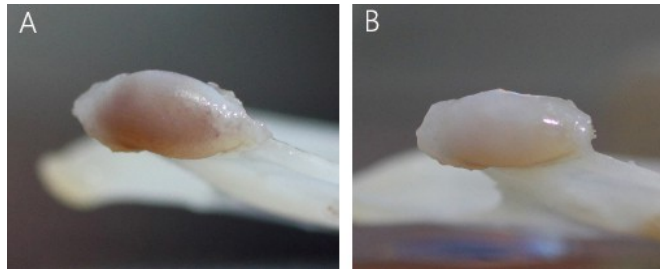


Figure 3-5; Condyle surface with A: dark (bone like) appearance  
B: translucent (thick cartilage) appearance both from LIPUS group

### III.II.III. Linear Measurements on Three-Dimensional (3-D) Virtual Models

Even though the values of condylar process length 2 and mandibular process length 2 were slightly higher in the LIPUS group, there was no significant difference ( $p>0.05$ ) between groups for the two linear measurements (Figure 3-6, Table 3-2). These results were consistent with that of linear measurements on 2-D photographs (Table 3-1).

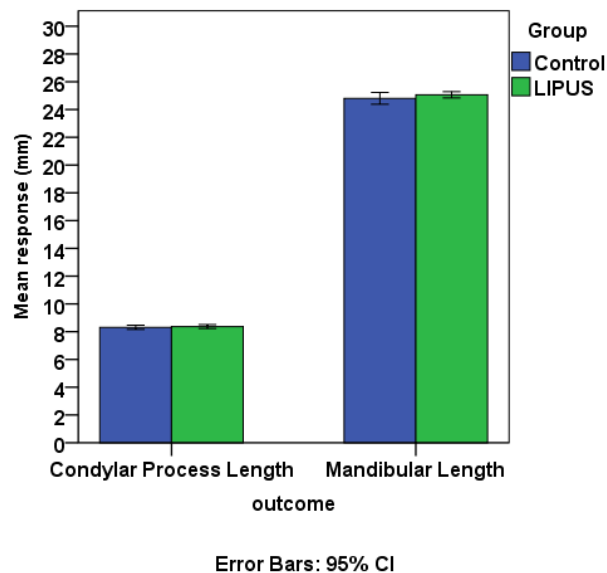


Figure 3-6; The comparison of Linear measurements (mm) on 3D virtual models for Control and Experimental group

Table 3-2: Values of linear measurements (mm) on 3-D virtual models in experimental and control groups

Response variable	Laterality	Control		LIPUS		P†
		Mean ± SD	Median (IQR)	Mean ± SD	Median (IQR)	
condylar process length2	R	8.22 ± 0.26	8.24 (8.01 to 8.35)	8.33 ± 0.39	8.41 (8.23 to 8.62)	0.448
	L	8.41 ± 0.3	8.35 (8.19 to 8.61)	8.41 ± 0.19	8.39 (8.28 to 8.55)	0.981
	Total	8.31 ± 0.29	8.26 (8.1 to 8.52)	8.37 ± 0.3	8.41 (8.25 to 8.56)	0.136§ <0.590*
Mandibular length2	R	24.85 ± 0.85	24.87 (24.15 to 25.53)	25.06 ± 0.54	25.1 (24.73 to 25.27)	0.520
	L	24.75 ± 0.8	24.71 (24.19 to 25.33)	25.05 ± 0.46	25.03 (24.74 to 25.52)	0.311
	Total	24.8 ± 0.8	24.8 (24.15 to 25.53)	25.06 ± 0.49	25.06 (24.73 to 25.35)	0.618§ 0.391*

† Based on GEE considering the correlation in the responses; §Comparison of right and left; \* adjusted the effect of laterality; IQR: Inter-quartile range; SD: standard deviation; L: Left; R: Right

### III.II.IV. 3-D Visualisation

The results of the study include left and right three-dimensional virtual models of the 3-D deviation of LIPUS average hemi mandible from Control average hemi mandible. The colour map (legend to the right) indicates the magnitude of change (in mm) with dark red indicative of maximum positive change (bone apposition), dark blue maximum negative

change (bone resorption) and green almost no change. Figure 3-7 is the lateral view (side of sonication) of the left and right virtual models of the 3-D growth map.

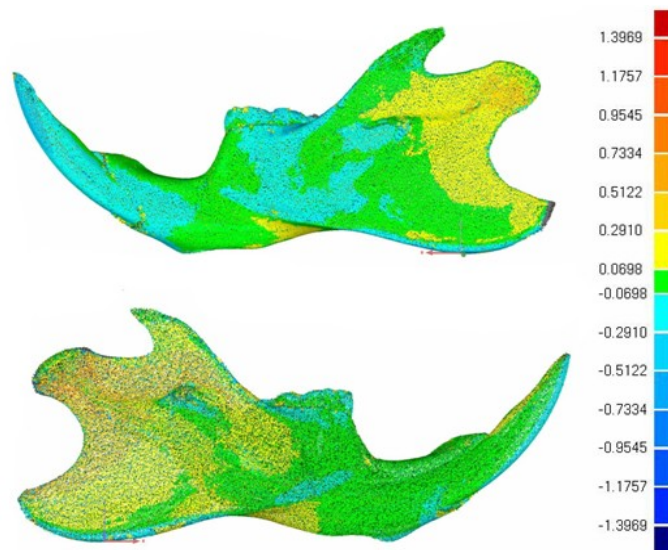


Figure 3-7; Lateral view of the virtual models of 3-D deviation map

The orange-yellow areas which can be seen in both left and right hemi-mandibles may suggest acceleration in periosteal bone apposition in the area of LIPUS application and its vicinity (Figure 3-7).

### III. III. Histological Observation and Histomorphometric Analysis

#### III. III. I. Condylar Cartilage

In general, the adult condylar cartilage was thinner compared to that of rapidly growing animals (Jiao K. et al., 2010) with marked reduction in the quantity of chondrocytes. A Hypertrophic layer was absent from the anterior region of the condyle of almost all animals and posterior region of some sections.

Mandibular condyle tissue response in the experimental animals varied. In the experimental group, three animals showed a visually significant thicker fibrocartilage (Figure 3-8-Am, Ap), five animals showed a moderate increase (Figure 3-8- Bm, Bp) and two (Figure 3-8- Cm Cp) showed almost similar features to that of control (Figure 3-8- Dm Dp). What was especially worthy to note in experimental animals was the increased thickness of the chondroblastic layer at the middle region of the condyles (Figure 2-8, 3-8, 3-9). Increased cellularity in prechondroblastic and chondroblastic layers in the experimental group in comparison to the control group was noteworthy (Figure 3-8). At the middle region the cellularity of chondroblastic layer in six animals showed an increase that control animal while this was the case in posterior region merely in 3 animals.

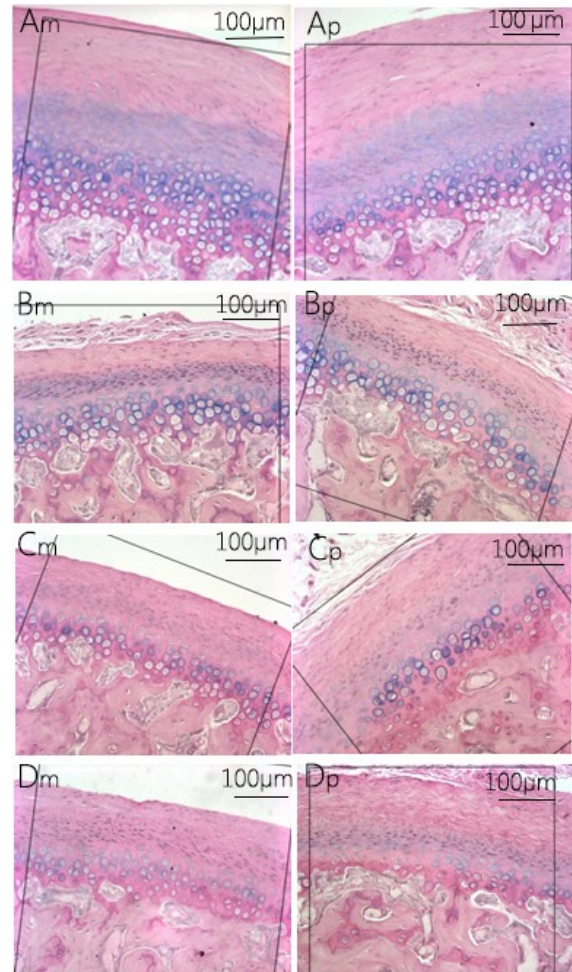
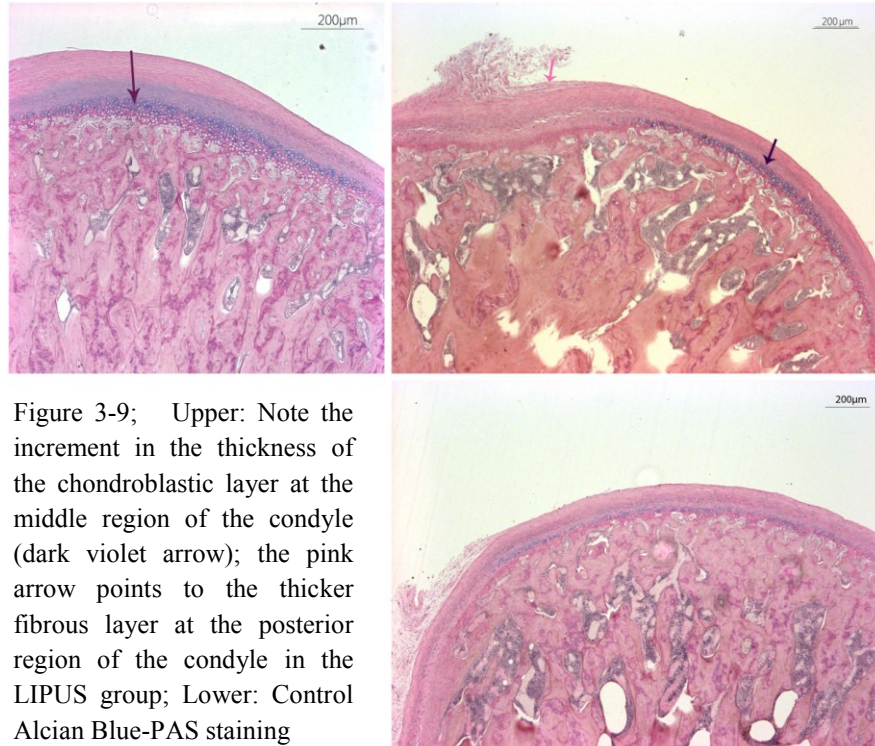


Figure 3-8; varied responses of mandibular condyle in experimental animals (A-C), Comparison to Control (dominant feature) (D); m: middle region, p: posterior region; Alcian Blue-PAS staining

In the proliferative layer such an increase in cellularity was observed in eight animals in the posterior region and six animals in the middle region. In addition, LIPUS treated condyles

showed more pronounced positive staining for Alcian Blue especially within the pericellular of chondroblastic region, which is consistent with increased proteoglycan synthesis. Moreover, chondroblasts were more hypertrophic in the LIPUS group compared to that of the control.

Based on histomorphometric analysis, in both evaluated regions (middle and posterior) the thickness of total fibrocartilage was slightly but significantly affected by LIPUS application. The thickness of all the layers in the middle region of the condyle was significantly higher in the experimental group compared to that of the control group. Even though the increase in thickness happened in all layers in the posterior region, it did not reach to a significant level in the chondroblastic layer. In contrast, the prechondroblastic and fibrous layers in the posterior region showed respectively similar and larger augmentation compared to the middle region. Likewise, a significant increment of cell population has been observed in the prechondroblastic layer in both evaluated regions while in chondroblastic layer it was observed only in the middle region (Table 3-3; Figure 3-9; 3-12). When the analysis was performed for both regions together (Total) all the above mentioned parameters showed significantly higher values for the LIPUS group compared to that of the control (Table 3-3; Figure 3-12).



One additional finding in a number (4) of experimental animals was the emergence or augmentation of the chondroblastic layer at the anterior and especially posterior end of the cartilaginous cap, which may suggest a higher potential of growth or sensitivity to external stimuli in these regions (Manson J. D., 1968) (Figure 3-10). Even though this observation was restricted to LIPUS group, it might be merely sporadic distribution of chondroblastic layer in adult condyle which was reported in one previous study (Mc Namara J.A. et al., 1982).

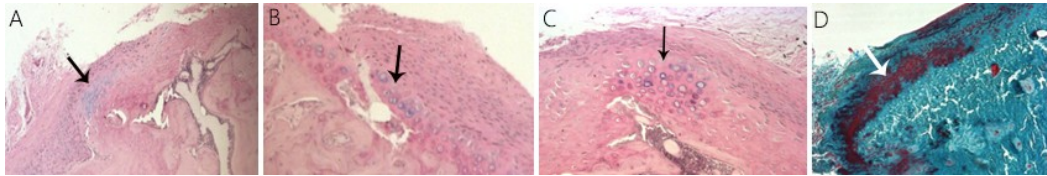


Figure 3-10; Potential emergence or augmentation of the chondroblastic layer in posterior (A, C, D) and anterior (B) end of the cartilaginous cap (arrows); Alcian Blue-PAS staining (A-C); Goldner's Trichrome staining (D)

### III. III. II. Subchondral Cancellous Bone

In the middle region, the percentage of bone area of subchondral trabecular bone/tissue area (bone volume fraction) was significantly lower and the percentage of remnants of calcifying cartilage and newly formed bone area was significantly higher in the experimental group compared to that of the control. However, in the posterior region the values for both parameters in the experimental group were slightly but not

significantly higher than that of the control (Table 3-3) (Figure 3-9, 3-11, 3-12). Combining the results for both regions together revealed significantly higher values for the percentage of remnants of calcifying cartilage and newly formed bone areas/ bone area in the LIPUS group when compared to that of the control group (Table 3-3).

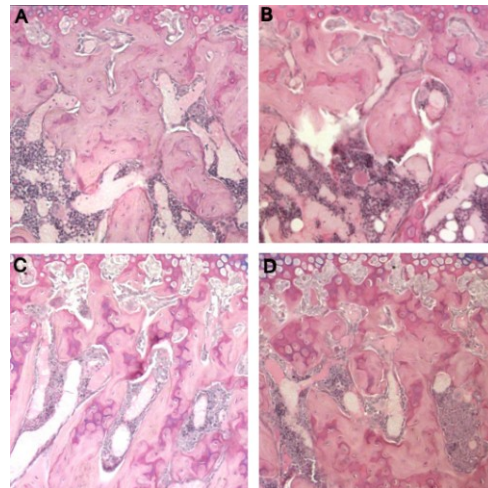


Figure 3-11; Subchondral cancellous bone; A: Control Middle region, B: Control Posterior region, C: LIPUS Middle region, D: LIPUS Posterior region; Alcian Blue PAS staining



Table 3-3; The comparison of histomorphometric parameters evaluated on decalcified sections stained with Alcian blue-PAS in experimental and control groups

Response	Location	Control		LIPUS		Mean Difference	P-Value
		Mean ± SD	Median (IQR)	Mean ± SD	Median (IQR)		
Total fibrocartilage thickness (µm)	Middle	170.981 ± 28.267	169.839 (158.8891 to 178.7308)	233.049 ± 63.7621	216.373 (182.690 to 265.357)	62.068	.004*
	Posterior	183.279 ± 16.892	186.222 (176.313 to 191.6072)	249.464 ± 69.5511	236.844 (185.188 to 273.110)	66.185	.002*
	Total	177.130 ± 23.375	178.730(162.806 to 186.235)	241.257 ± 65.483	227.014 (184.302 to 269.233)	64.157	<0.001†
Fibrous layer thickness (µm)	Middle	49.717 ± 9.893	49.804 (46.007 to 55.807)	70.642 ± 26.906	66.520 (50.534 to 78.106)	20.925	.016
	Posterior	62.108 ± 11.680	62.712 (57.372 to 68.658)	94.112 ± 38.676	79.358 (63.680 to 112.823)	32.004	.009
	Total	55.912 ± 12.258	57.372 (48.671to 63.464)	82.377 ± 34.590	72.551 (53.753 to 98.738)	26.465	<0.001
Proliferative layer thickness (µm)	Middle	41.928 ± 10.738	39.336 (33.245 to 50.189)	59.162 ± 15.986	56.130 (45.393 to 69.133)	17.234	.004
	Posterior	44.088 ± 7.914	45.1425 (36.255 to 50.1507)	61.692 ± 19.155	54.109 (50.135 to 78.579)	17.604	.005
	Total	43.008 ± 9.180	42.627 (35.794 to 50.150)	60.427 ± 17.220	54.109 (46.666 to 73.856)	17.419	<0.001
Chondroblastic layer thickness (µm)	Middle	86.613 ± 19.720	79.495(72.311 to 102.361)	110.836 ± 24.375	108.765 (98.837 to 111.250)	24.223	.013
	Posterior	81.820 ± 18.893	73.800 (65.955 to 100.733)	95.825 ± 17.488	90.438 (83.606 to 116.155)	14.005	.086
	Total	84.216 ± 18.820	76.985 (67.570 to 100.733)	103.331 ± 22.036	101.019 (85.385 to 113.702)	19.115	0.004
Cell population in Proliferative layer	Middle	165.125 ± 17.455	159 (151.5 to 180.5)	201.5 ± 32.694	203 (184 to 213)	36.375	.001
	Posterior	172.5 ± 11.880	175.5 (164 to 180.5)	229.3 ± 63.113	203.5 (196 to 218)	56.8	.003
	Total	168.812 ± 14.918	170 (154 to 180.5)	215.4 ± 50.956	203 (189 to 215.5)	46.588	<0.001
Cell population in Chondroblastic layer	Middle	138.5 ± 28.3196	131.5 (118.5 to 159.5)	185.5 ± 28.6327	185 (160 to 194)	47	.000
	Posterior	111.25 ± 32.8405	127.5 (84 to 133)	136 ± 45.77	125.5 (116 to 166)	24.75	.157
	Total	124.875 ± 32.796	127.5 (110.5 to 140.5)	160.75 ± 45.005	162.5 (125.5 to 188)	35.875	0.004
BV/TV (%)	Middle	69.986 ± 4.346	68.657 (67.255 to 71.599)	61.909 ± 8.183	63.197 (56.584 to 68.069)	-8.077	.005
	Posterior	58.880 ± 12.948	55.428 (53.274 to 63.793)	64.130 ± 10.291	64.007 (57.649 to 72.456)	5.25	.320
	Total	64.433 ± 10.952	67.255(55.428 to 70.545)	63.020 ± 9.120	64.007 (57.116 to 68.907)	-1.413	0.670
Remnants of calcifying cartilage &	Middle	15.473 ± 6.3341	14.379 (11.6795 to 17.2936)	24.702 ± 6.2691	24.745 (21.9933 to 31.3954)	9.229	.001
	Posterior	19.786 ± 6.9062	18.140 (14.0344 to 25.7808)	22.074 ± 4.933	22.164 (18.3767 to 26.1829)	2.228	.401
	Total	17.630 ± 6.777	16.082 (12.547 to 21.642)	23.388 ± 5.653	22.672 (18.592 to 27.119)	5.758	0.005

\*Based on GEE and adjusted for multiple comparison by Bonferroni method

§ Comparison of posterior and middle positions in LIPUS group based on GEE

† Based on GEE consider the correlation in the responses and adjusted the effect of position.

IQR: Inter-quartile range. SD: Standard Deviation

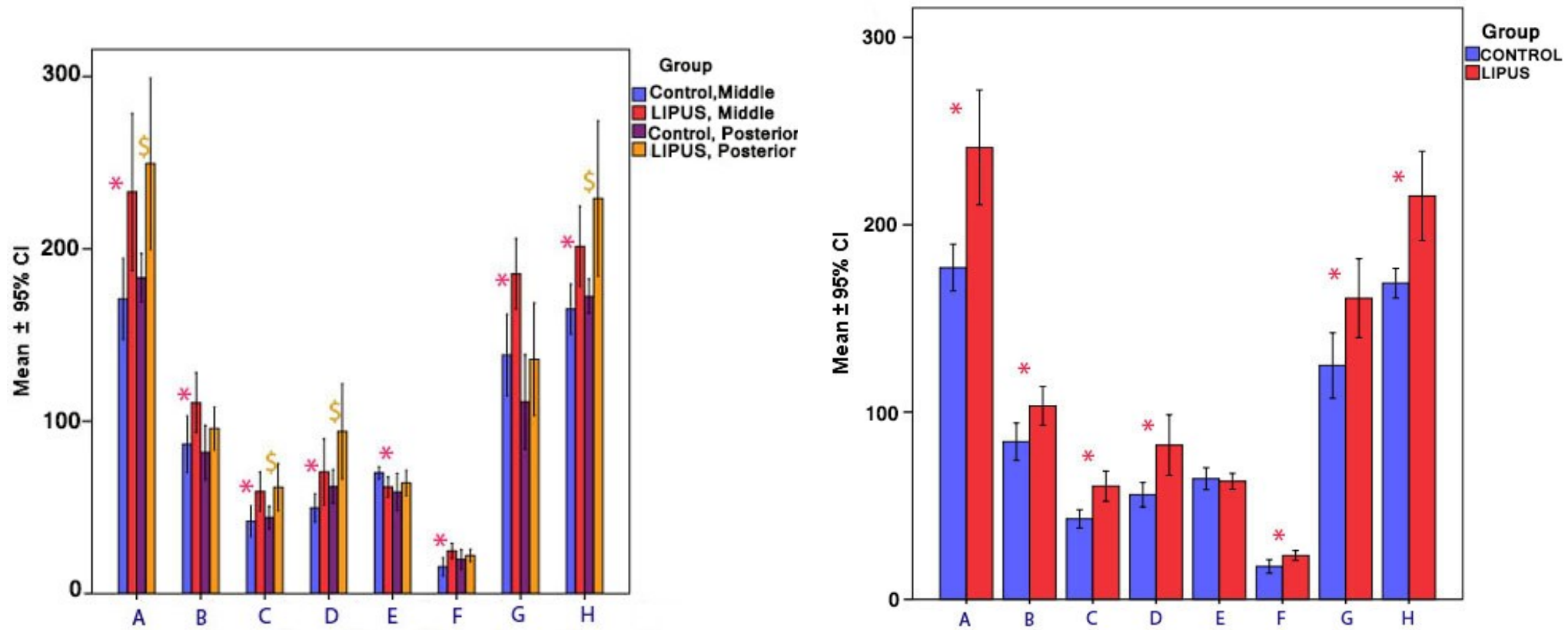


Figure 3-12; Histomorphometric Parameters: A: Total fibrocartilage thickness (μm), B: Chondroblastic layers thickness (μm), C: Proliferative layer thickness (μm), D: Fibrous layer thickness (μm), E: BV/ TV (%), F: Remnants of calcifying cartilage + newly formed bone area/ total bone area (%) G: Cell population in Chondroblastic layer, H: Cell population in Proliferative layer. LEFT: Region (location) specific comparison of groups (p < 0.05; middle \*); (p < 0.05; posterior \$); Right: Comparison of groups without considering different regions (p < 0.05\*)

The amount of endochondral bone growth after three weeks of treatment (determined by measuring the distance between the two fluorescent labels as previously explained in methods and materials) was moderately but significantly higher (mean difference= 53.7  $\mu\text{m}$ ) in the experimental group than that in the control group (Figure 3-13) (table 3-4). In three of the rats from the experimental group the

distance between the two labels was uncomparable to that of the control.

Table 3-4; The amount of endochondral bone growth ( $\mu\text{m}$ ) in experimental and control groups

	Control	LIPUS	P†
Mean $\pm$	264.894 $\pm$	318.594 $\pm$	0.002
SD	49.899	58.358	
Median	265.139	306.2744	
(IQR)	(223.146 to 307.233)	(272.071 to 369.756)	

† Based on Independent Sample T-Test  
SD: standard deviation; IQR: inter quartile range

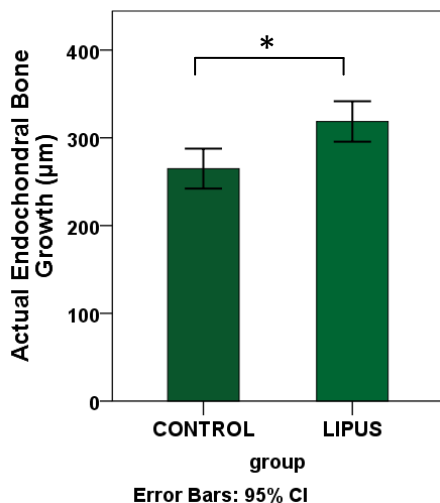
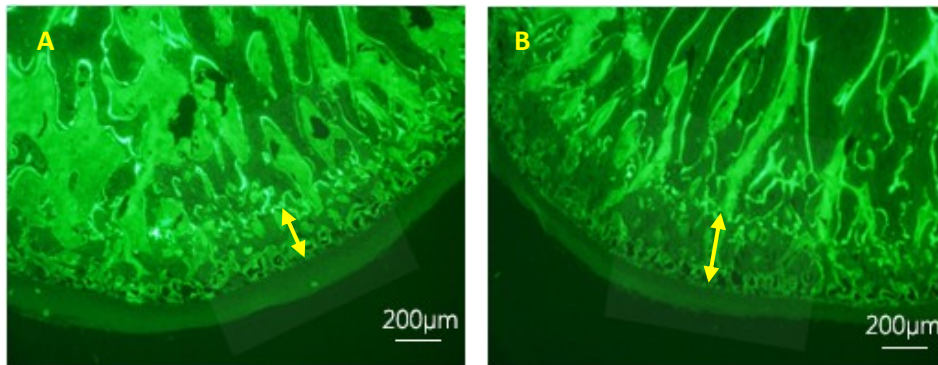


Figure 3-13; The amount of endochondral bone growth; The distance between two fluorescent labels echoes the amount of endochondral bone growth during three weeks of experimental period in Control (A) and LIPUS (B) groups. The bar chart demonstrates the same comparison (n=7 in control group) (n=9 in LIPUS group) \*  $p < 0.01$ .

Osteoid formation was greater and in some locations in a non organized fashion in subchondral cancellous bone compared to the centre (far from cartilage) of the condyle (fig 3-

15). This may point to the presence of woven bone and therefore active bone formation in this area. This feature manifests itself more in the LIPUS group. Osteoid thickness in trabecular bone subjacent to cartilage bone junction was 37% higher ( $p < 0.001$ ) in the LIPUS group than in the control group. This was more evident in the middle region (Figure 3-14, 3-15, Table 3-5). From the experimental group, five of the rats in the middle region and four of the animals in the posterior region revealed amounts of osteoid formation that could not be seen in any of the control animals.

Table 1-5; The comparison of Osteoid thickness ( $\mu\text{m}$ ) in experimental and control groups

location	LIPUS		Control		P <sup>†</sup>
	Mean $\pm$ SD	Median (IQR)	Mean $\pm$ SD	Median (IQR)	
Middle	8.38 $\pm$ 0.87	8.3 (7.62 to 9.16)	5.65 $\pm$ 0.99	5.36 (5.14 to 5.71)	<0.001
Posterior	8.06 $\pm$ 1.34	8.28 (6.74 to 9.15)	6.37 $\pm$ 0.97	6.59 (5.45 to 7.02)	0.002
Total	8.22 $\pm$ 1.11	8.3 (7.37 to 9.16)	6.01 $\pm$ 1.01	5.57 (5.34 to 6.65)	0.560 <sup>§</sup>
					<0.001*

<sup>†</sup> Based on GEE consider the correlation in the response

<sup>§</sup> Comparison of posterior and middle positions

\* Adjusted the effect of position; IQR: Inter-quartile range

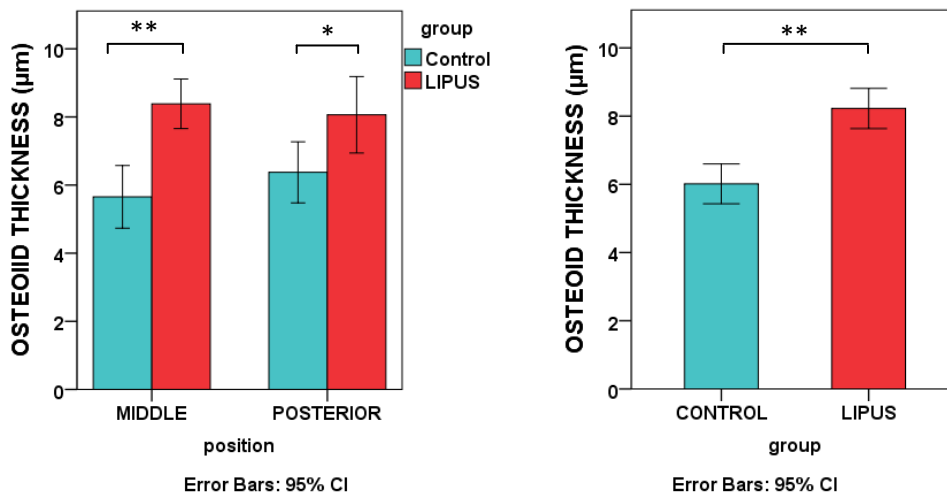


Figure 3-14; The comparison of osteoid thickness ( $\mu\text{m}$ ) in experimental and control groups; region specific comparison (LEFT), Total comparison without considering region (RIGHT) (n=7 in control group) (n=9 in LIPUS group) \*  $p < 0.01$ , \*\* $p < 0.001$

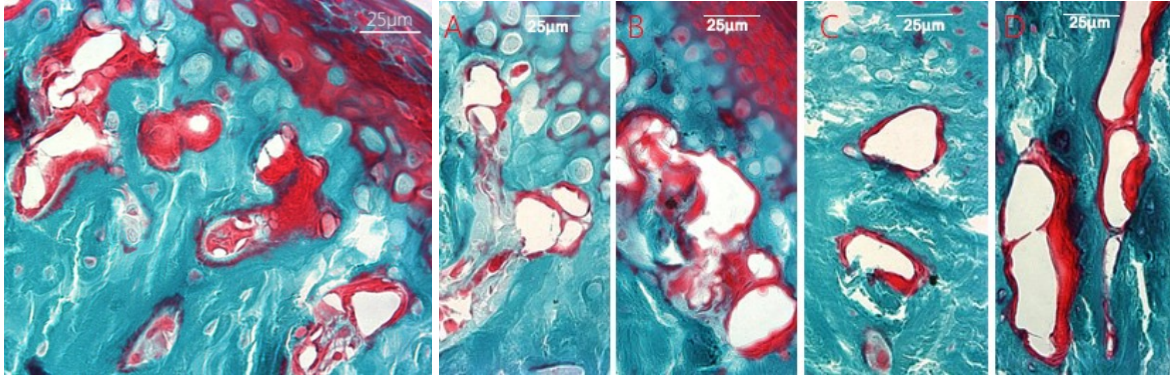
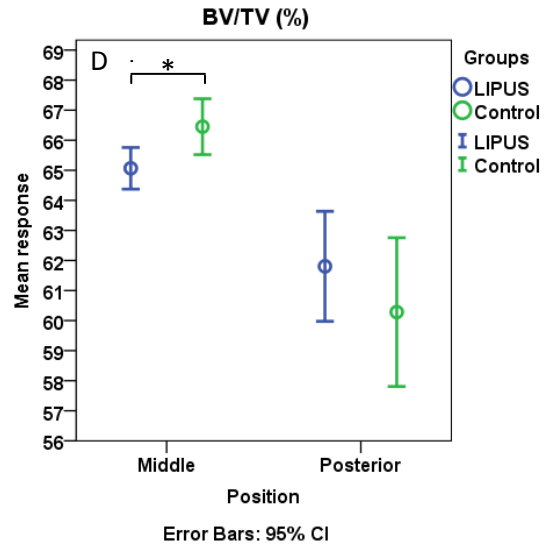
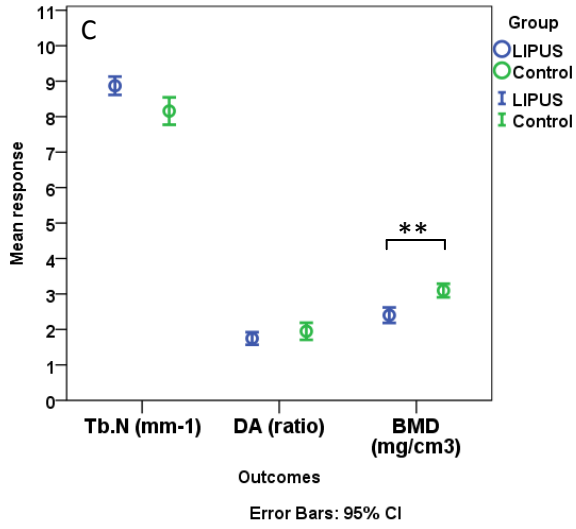
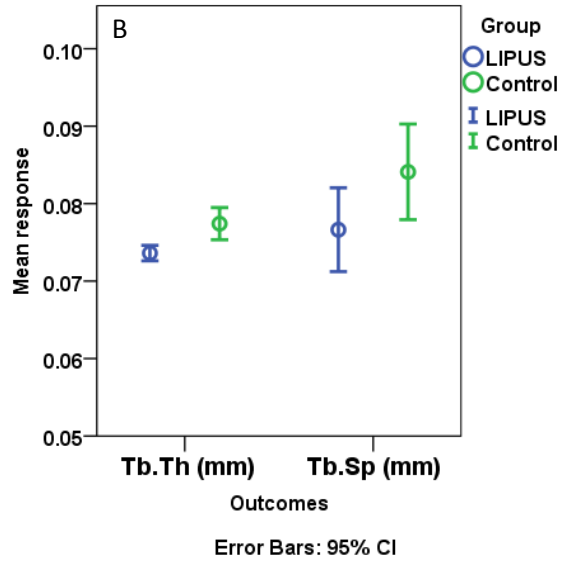
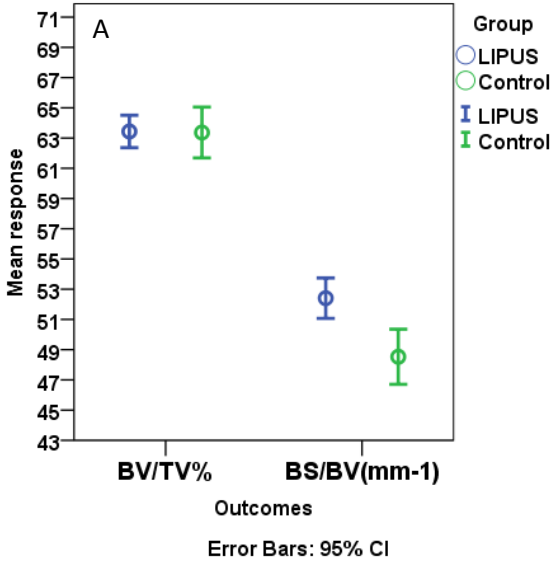


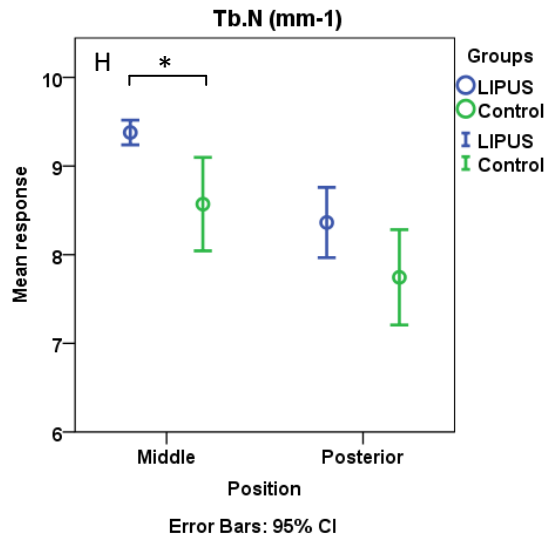
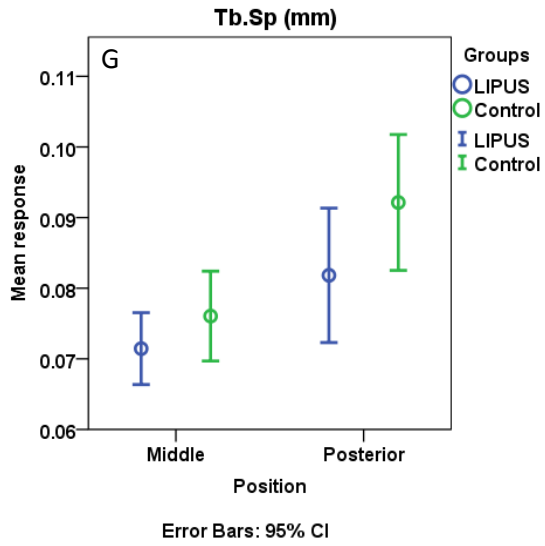
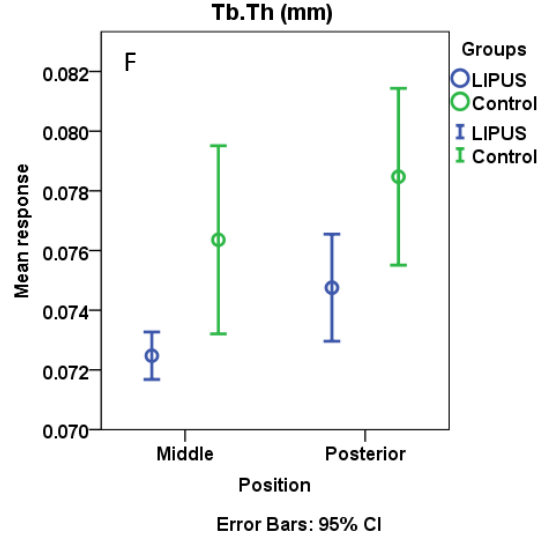
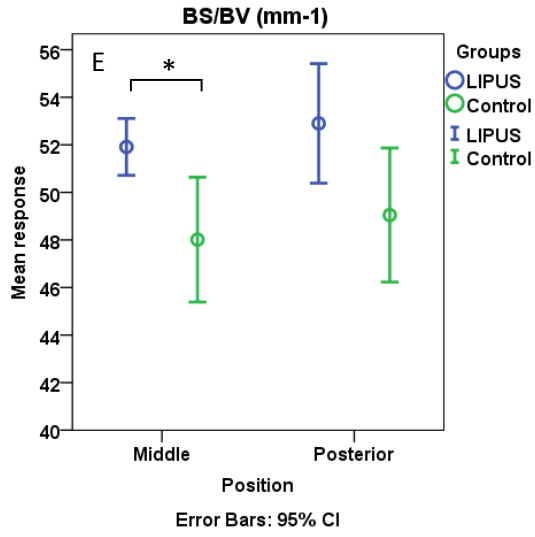
Figure 3-15; Osteoid structure in subchondral cancellous bone in 148 days old rats, LEFT: excessive osteoid formation subjacent to cartilage in the middle region of the condyle from the LIPUS group. RIGHT: comparison of osteoid formation in control (A: middle region, C: posterior region) and LIPUS (B: middle region, D: posterior region) groups. Goldner's Trichrome staining.

### III.IV. Micro-CT Analysis

As revealed by micro-CT analysis, the subchondral trabecular bone in the middle and posterior regions together showed no statistically significant difference between groups for static bone micro structural parameters. However, Bone Mineral Density (BMD) showed significantly ( $p < 0.01$ ) lower values for the LIPUS group ( $2.401 \pm 0.681$ ) compared to that of the control ( $3.096 \pm 0.534$ ). This lower degree of mineralization may point to a higher remodeling rate. Even though nonsignificant, higher BS/BV and Tb.N along with lower Tb.Th (larger trabecular surface area) (Renders J.A.P. et al., 2007) and DA values (characteristic of woven bone) (Daegling D.J. et al., 2007) may support the tendency towards higher remodeling rates and bone formation (Figure 3-16 (A-C)) (Table 3-6).

It seems that the mechanical stimulus of LIPUS treatment resulted in the more evident remodeling of subchondral cancellous bone in the middle region. BV/TV and Tb.Th showed respectively significant and marginally significant lower values in the LIPUS group compared to that of the control. The values of BS/BV and Tb.N were significantly higher and DA as well as BMD was significantly lower in the LIPUS group compared to that of the control group. Trabecular separation, however, remained almost unchanged which might be due to the higher impact of therapy on trabecular number rather than thickness. Apart from BV/TV, for all the parameters a similar trend has been observed in the posterior region. However, the differences between LIPUS and control groups for none of the outcome variables reach to a significant level in this region (Figure 3-16(D-J)) (Table 3-6).





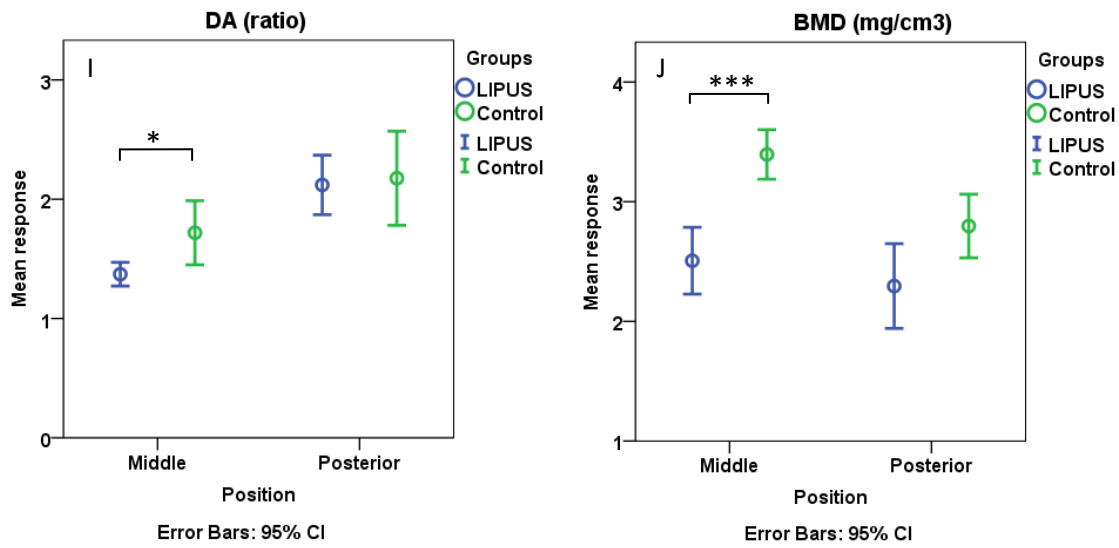


Figure 3-16; A comparison of densitometric and morphometric parameters of the condylar subchondral bone in evaluated regions between control and LIPUS groups; A-C: comparing the groups without considering regions .D-J: Region (Position) specific comparison of the groups \*p<0.05, \*\*p<0.01, \*\*\*p<0.001

Table 3-6; The comparison of densitometric and morphometric bone parameters of subcondral cancellous bone in experimental and control groups evaluated by  $\mu$ CT analysis

Response	Location	LIPUS		Control		Mean difference	P-value
		Mean $\pm$ SD	Median (IQR)	Mean $\pm$ SD	Median (IQR)		
BV/TV (%)	Middle	65.067 $\pm$ 1.479	64.867 (64.206 to 66.307)	66.452 $\pm$ 1.744	66.759 (65.38 to 67.554)	-1.453	0.046†
	Posterior	61.805 $\pm$ 3.91	62.772 (61.544 to 63.839)	60.283 $\pm$ 4.644	60.722 (59.066 to 63.956)	1.522	0.387†
	Total	63.436 $\pm$ 3.353	64.173 (62.621 to 65.23)	63.367 $\pm$ 4.661	64.801 (60.722 to 66.759)	0.069	< 0.001§
BS/BV (mm-1)	Middle	51.911 $\pm$ 2.552	52.461 (51.176 to 53.426)	48.013 $\pm$ 4.927	49.496 (44.744 to 51.499)	3.895	0.031
	Posterior	52.901 $\pm$ 5.369	53.491 (51.579 to 57.057)	49.046 $\pm$ 5.29	50.962 (44.514 to 52.099)	3.855	0.108
	Total	52.406 $\pm$ 4.179	52.711 (51.374 to 54.253)	48.529 $\pm$ 5.056	50.411 (44.514 to 51.695)	3.877	0.020
Tb.Th (mm)	Middle	0.072 $\pm$ 0.002	0.072 (0.072 to 0.073)	0.076 $\pm$ 0.006	0.074 (0.072 to 0.08)	-0.004	0.058
	Posterior	0.075 $\pm$ 0.004	0.074 (0.073 to 0.075)	0.078 $\pm$ 0.006	0.076 (0.075 to 0.081)	-0.003	0.088
	Total	0.074 $\pm$ 0.003	0.073 (0.072 to 0.074)	0.077 $\pm$ 0.006	0.075 (0.074 to 0.081)	-0.003	< 0.001
Tb.Sp (mm)	Middle	0.071 $\pm$ 0.011	0.067 (0.066 to 0.071)	0.076 $\pm$ 0.012	0.071 (0.067 to 0.085)	-0.005	0.188
	Posterior	0.082 $\pm$ 0.02	0.072 (0.07 to 0.082)	0.092 $\pm$ 0.018	0.084 (0.077 to 0.109)	-0.01	0.364
	Total	0.077 $\pm$ 0.017	0.07 (0.067 to 0.078)	0.084 $\pm$ 0.017	0.078 (0.071 to 0.093)	-0.007	0.229
Tb.N (mm-1)	Middle	9.378 $\pm$ 0.298	9.213 (9.163 to 9.69)	8.57 $\pm$ 0.99	8.985 (7.888 to 9.253)	0.808	< 0.001
	Posterior	8.363 $\pm$ 0.847	8.655 (8.269 to 8.806)	7.745 $\pm$ 1.009	7.904 (7.261 to 8.621)	0.618	0.134
	Total	8.871 $\pm$ 0.811	9.077 (8.655 to 9.218)	8.157 $\pm$ 1.069	8.574 (7.414 to 8.985)	0.714	0.131
DA (ratio)	Middle	1.371 $\pm$ 0.212	1.321 (1.252 to 1.412)	1.719 $\pm$ 0.505	1.539 (1.348 to 1.921)	-0.348	0.017
	Posterior	2.12 $\pm$ 0.533	1.991 (1.74 to 2.393)	2.176 $\pm$ 0.741	1.944 (1.683 to 2.622)	-0.056	0.797
	Total	1.745 $\pm$ 0.551	1.645 (1.321 to 1.991)	1.947 $\pm$ 0.665	1.769 (1.515 to 2.292)	-0.202	< 0.001
BMD (mg/cm <sup>3</sup> )	Middle	2.507 $\pm$ 0.596	2.158 (2.061 to 3.205)	3.395 $\pm$ 0.388	3.39 (3.221 to 3.717)	-0.808	< 0.001
	Posterior	2.295 $\pm$ 0.757	2.167 (1.629 to 2.851)	2.797 $\pm$ 0.499	2.763 (2.463 to 3.09)	-0.502	0.071
	Total	2.401 $\pm$ 0.681	2.158 (1.887 to 2.996)	3.096 $\pm$ 0.534	3.221 (2.71 to 3.469)	-0.695	0.636
							0.006

† Based on GEE considering the correlation in the responses. § Comparison of posterior and middle positions based on GEE \* Based on GEE considering the correlation in the responses and adjusted the effect of position and laterality. IQR: Inter-quartile range.

# CHAPTER IV: DISCUSSION

---

In this study, LIPUS was proposed as a therapeutic intervention for enhancing or reactivation of condylar remodelling in young adult rats based on its usefulness in previous *in vitro* and *in vivo* studies that depict its chondrogenic and osteogenic potential (please see section I.II.III.I. and II.). Additionally, previous studies demonstrated that LIPUS application in 3-4 weeks can efficiently enhance condylar and mandibular growth (please see section I.II.III.III.).

Our results from gross morphological evaluation<sup>1</sup> clearly demonstrated that 28 days LIPUS application, corresponding to a human equivalent period of 32 months (Panherz H. and Ruf S., 2008a), is not sufficient for statistically significant increase in condylar or mandibular size in adult rats. The linear and angular measurements were performed on two-dimensional photographs utilizing AutoCAD software with high accuracy and further confirmed by measurements on 3-D virtual models using Geomagic QUALIFY software. However, comparing the average 3-dimensional virtual models from experimental and control groups in the form of a 3-D deviation map was suggestive of enhanced periosteal bone apposition at the site of LIPUS application. This negligible response for longitudinal bone growth to short-term LIPUS treatment in non growing rats is in contrast with its reported effect on growing and even late adolescent animals (El-Bialy T. et al., 2003; Oyonarte R. et al., 2013; Kaur H. et al., 2014). Decreased or delayed tissue responsiveness in adult condyle (Ruf S. and Panherz H. et al., 1999a) along with differences in quantity and quality of covering soft tissues (Muller K. et al., 1995) that may affect LIPUS penetration in adult individuals are plausible reasons for this limited effect. However, these results are consonant with the effect of LIPUS (at the intensity of 30 mW/cm<sup>2</sup>) on long bones, i.e: absence of longitudinal bone growth and presence of periosteal bone growth (Spadaro J.A. et al., 1998; Korstjens C.M. et al., 2004; Nolte P.A. et al., 2001; Naruse K. et al., 2009; Perry M.J. et al., 2009).

It should be noted that the continuous bite-jumping in adult rats over 30 days (same species, gender and age as the present study) resulted in a marked increase in the length of condylar

---

<sup>1</sup>The degree of Alpha (Angle of condylar process axis to mandibular plane) was the only angular/linear parameter which was significantly more in the LIPUS group in comparison to the control group. This geometrically was attributed to more anterior inferior location of the most anterior-superior and posterior-inferior points of the condyle. A potential explanation for aforementioned observation could be progression of cartilaginous cap in perichondrial-periosteal junction. Histologic sections in a number of animals from the LIPUS group also demonstrated emergence or augmented chondroblastic layer in posterior and anterior end of the cartilaginous cap. These areas are more sensitive (Manson J. D., 1968) and are considered to be affected by the tensional force generated by mandibular movement (Hiiemae K., 1971; Weijs W.A., 1976). Thus, this observation could be the result of the cumulative effect of these tensional forces and LIPUS stimuli. However, this warrants further research.

process (0.51mm) as well as mandibular length (1.67 mm). This longitudinal growth was due to increased bone apposition in the posterior part of the condyle and superior part of the condylar head (Xiong H. et al., 2004).

Nevertheless, the following findings encourage us to conduct micro structural evaluations: 1. Minor non significant higher values in linear measurements ending in posterosuperior point of the condyle and at the direction of condylar growth (e.g.: condylar process length and mandibular length 2) in the LIPUS group compared to that of the control group. 2. The middle (superior) area of the condyle was consistently more translucent and thick in the LIPUS group compared to that of the control group. These findings suggested a potential increase in cartilage and/or bone in the middle region of the condylar head in experimental group.

Mandibular condyle grows mainly through endochondral ossification, which is a multistep process. This involves mesenchymal cell proliferation and differentiation to chondrocytes, cartilaginous matrix synthesis by chondrocytes, remodeling and calcification of matrix following hypertrophy of the chondrocytes and eventually resorption of the cartilage through neovascularization. Each step is controlled by different molecular regulators which expressed by chondrocytes (Rabie A.B. et al., 2002a and b). However, it is thought that by transition from adolescence to adult the role of the condyle will change from a growth site to an articular function. During this transformation, the hypertrophic layer disappears, endochondral ossification ceases and chondroid bone forms (Mizoguchi I. et al., 1993).

Evaluations in this study were restricted to middle and posterior areas of the condyle as the hypertrophic layer was totally absent from the anterior region of the condyle of the animals. In addition to our observation, previous studies showed cartilaginous matrices in the anterior region of the rat condyle are replaced by chondroid bone at 8 weeks of age (Mizoguchi I. et al., 1993; Takahashi I. et al., 1996). The animals in the present study were around 148 days old by the end of the experiment and thus there was little point to perform any analysis in this region. These evaluations encompass histomorphometric and histologic studies following various specialized staining to determine cartilage and bone formation. Micro-CT analysis was also performed for detecting micro structural as well as bone mineral density changes in subchondral cancellous bone. The regions of interest were placed as close to the interface of the cartilage and subchondral bone as possible to observe the changes of the trabecular bone subjacent to the condylar cartilage.

Based on histomorphometric results, the thickness of total fibrocartilage layer, the thickness of fibrous layer, and the thickness as well as cell population in the proliferative (prechondroblastic) layers in both evaluated regions (i.e: middle and posterior) showed slightly but significantly higher values in the LIPUS group. In the middle region, maturation and hypertrophic (chondroblastic) layer thickness and cell population were also significantly higher in the LIPUS group. In addition, cells in the hypertrophic layer were more hypertrophic and showed more pronounced positive staining for Alcian blue.

Similar histologic changes have been reported by previous studies in which the effect of LIPUS has been evaluated on mandibular condylar growth modification in growing (El-Bialy T. et al., 2003; Oyonarte R. et al., 2009; Oyonarte R. et al., 2013) as well as late adolescent (Kaur H et al., 2014) rodents. The stimulatory effect of LIPUS on fibroblast proliferation, activity, and collagen synthesis has been documented in in vitro studies (Zhou S. et al., 2004; Mendonca A.C. et al., 2006; Lai J. And Pittelkow D.M.P., 2007; Piers Oliveria D.A.A. et al., 2009). Numerous in vitro and in vivo studies as previously mentioned in detail (section I.II.III.II) suggest chondrogenic potential of the LIPUS.

Even though the stimulatory effect of LIPUS on cell proliferation of chondrocytes is still debated, which is mainly attributed to experimental conditions, a number of recent studies depict this effect even on chondrocytes isolated from elderly individuals (Miyamoto K. et al., 2005; Choi B.H. et al., 2006; Hsu S.H. et al., 2006; Korstjens C.M. et al., 2008). Takeuchi R. et al. (2008) demonstrated that LIPUS promoted the proliferation of cultured chondrocytes (from 6 month old pig's metatarso-phalangeal joints) and the production of type IX collagen (involved in promoting chondrocyte proliferation and cartilage layer expansion) in a three-dimensional culture using a collagen sponge following 14 days. The rate of increase in the cell number was significantly higher in the LIPUS group. Ki-67 index of the chondrocytes (a very reliable marker for cell proliferation) exposed to LIPUS was significantly higher compared to that of the control (Takeuchi R. et al., 2008). LIPUS increases integrin expression through mechanical stress, phosphorylates Focal Adhesion Kinase (FAK), activates phosphatidylinositol 3-kinase (PI3K) /Akt pathway which leads to the proliferation of chondrocytes (Korstjens C.M. et al., 2008; Takeuchi R. et al., 2008; Whitney N.P. et al., 2012). There is no supportive data of stimulatory effect of LIPUS at low intensities on proliferative activity of chondrocytes in long bones (Naruse K. et al., 2009). Nonetheless, there are fundamental differences between the primary cartilage of

epiphysis and secondary cartilage of mandibular condyle (please see section I.II.II). This includes but is not limited to the fact that epiphysis lack fibrocartilaginous cap (Voudouris J.C. and Kufnec M.M., 2000) and prechondroblasts are surrounded by an intracellular matrix which isolates them from local factors; whereas, this intracellular matrix is absent in MCC (Kantomma T. and Ronning O., 1997). In addition, secondary cartilage of mandibular condyle is covered by a fully developed mesenchymal tissue layer which is responsible for an essential characteristic of the condylar cartilage: adaptive remodeling to external stimuli (e.g: condylar repositioning, articular functioning, and mechanical loading) during or after natural growth (Delatte M. et al., 2005; Nakano H. et al., 2003; Shen G. et al., 2003; Rabie A.B. et al., 2003e; Chayanupatkul A. et al., 2003; Rabie A.B. et al., 2004a). Another interesting point is that the mandibular condylar cartilage, in contrast to primary cartilages, originates from alkaline phosphatase-positive cells of periosteum (Shibata S. et al., 2002). These relatively undifferentiated cells are responsible for the growth of the mandibular condylar cartilage by their proliferation and differentiation (Carlson D.S. et al., 1980). In vitro and in vivo studies in young tissues as well as adult bone demonstrated the stimulatory effect of LIPUS on periosteum and induction of bone growth (Naruse K. et al., 2009; Perry M.J. et al., 2009).

It has been demonstrated by previous studies that mechanical stimuli produced by mandibular advancement can increase expression of IHH, the mechanotransduction mediator in the condyle (Tang G.H. et al., 2005) and hence increase in the rate of cellular proliferation in both growing and adult individuals (Xiong H. et al., 2005a). This starts the cascade of cellular and molecular events that lead to enhance chondrogenesis and finally endochondral ossification (please see section I.II.I). Mechanotransduction is one of the main suggested mechanisms of action of LIPUS (Oyonarte R. et al., 2009) and the same scenario might happen as a result of US therapy in mandibular condyle. However, currently there is no evidence on up regulation of IHH following LIPUS application (please see section I.II.III.III.). Thus, this could be investigated in future studies.

Here we should mention that mechanical stimuli produced by forward mandibular positioning (continuous bite-jumping) in the same species, gender and age as in the present study led to an increment in mesenchymal cell population in proliferative layer and thickness of different cartilaginous layers that was 2 to 6 fold of the control groups over 21 days (Xiong H. et al., 2005a). The amount of increase in abovementioned parameters as a result of functional therapy

in this previous study was far greater than that following LIPUS application in the present study. This could be due to the fact that we might have missed the peak of increment by the end of the experiment or more possibly the mechanical stimuli produced by LIPUS and its subsequent effect is much lower than that of functional therapy and we have yet to reach to that stage.

In the present study the cell population as well as the thickness of hypertrophic layer was more in the middle (superior) region in the control group compared to the posterior region and its increment as a result of LIPUS application reached a significant level in this region but not in the posterior area. In addition, in the middle region, the percentage of bone area of subchondral trabecular bone/ tissue area (bone volume fraction) was significantly lower and the percentage of remnants of calcifying cartilage and newly formed bone area/ bone area was significantly higher in the experimental group compared to that of the control, which is indicative of higher bone remodeling activity and active bone formation respectively. However, in the posterior region none of these two parameters showed significant changes even though a tendency was present. Moreover, micro-CT analysis of subchondral cancellous bone in the middle region was suggestive of higher remodeling rate and bone formation. This could be understood from significantly higher BS/BV and Tb.N along with, respectively, marginally significant and significant lower values for Tb. Th and BV/TV which shows larger trabecular surface area (Renders J.A.P. et al., 2007) and significant lower DA (characteristic of woven bone) (Daegling D.J. et al., 2007) and BMD. Again, evaluation of these static bone micro structural and densitometric parameters in the posterior area represents merely a similar tendency.

In the mandibular condyle, the disappearance of hypertrophic cartilage which is accompanied by the cessation of endochondral ossification and the formation of a compact subchondral bone plate occurs gradually (Luder H.U. et al., 1998). With gradual transition from adolescence (growth) to adulthood this process begins from the periphery of the condyle (Lei J. et al., 2013). The hypertrophic layer slowly disappears from the posterior slope of the condyle, for instance at 16 weeks of age in rats (Takahashi I. et al., 1996),<sup>2</sup> and decreases in cellularity occurs last at the top of the condyle (Luder H.U. et al., 1998). Thus, it is possible that the middle region of the condyle (superior /top /posterosuperior point in anthropometric measurements) maintains growth cartilaginous appearance, i.e.: presence of maturative and hypertrophic cell layers, into later stages. This temporal difference in the phenotype change could be due to regional variations

---

<sup>2</sup> In the present study also hypertrophic layer was absent from the posterior regions in some sections.

between these regions, and on whether or not they contribute to resist articulating loads caused by mastication (Takahashi I. et al., 1996). Therefore, it can be suggested that this region's specific response to LIPUS probably is due to difference in intrinsic maturity of the condylar cartilage in different regions (Middle versus Posterior). It should be noted that the condylar cartilage of 32-week old rats is articular cartilage with no hypertrophic cell layer on compact bone in all regions of the condyle (Takahashi I. et al., 1996).

Hypertrophic chondrocytes are at the terminal stage of differentiation, but are still metabolically active for the maintenance of cellular morphology and protein synthesis (Hickok N.J. et al., 1998). Therefore, it can be hypothesized that hypertrophic chondrocytes should be capable of responding to physical stimuli such as LIPUS. In the present experiment, the increased cell population and thickness of matured and hypertrophic cell layer as well as increased proteoglycan synthesis (as can be understood from pronounced Alcian blue staining in the LIPUS group compare to that of the control) is in agreement with this hypothesis. In a previous study in which LIPUS was applied to proximal sternum, type X collagen (marker of hypertrophic cells) was seen to increase as compared with the controls in certain regions (Zhang Z.J. et al., 2002). In addition, it has previously been reported that LIPUS increased the number of hypertrophic chondrocytes around the callus of healing femoral fracture in rats (Azuma Y. et al., 2001). The increase in the amount of matured /hypertrophic chondrocytes could be due to higher mitosis of these cells themselves as hypertrophic cells still preserve their proliferation capability (Suda N. et al., 1999) or accelerated transition of proliferating chondrocytes to the hypertrophic phenotype (Dibbets J.M.H., 1990; Zhang Z.J. et al., 2002).

Hypertrophic chondrocytes appear during the maturation of cartilage. It is generally agreed that the hypertrophy of chondrocytes is a crucial step in endochondral bone formation. Even though the above mentioned effect might be transient, it could be the basis for the acceleration of bone formation by LIPUS when used as an ongoing therapy. In fact, hypertrophic chondrocytes produce calcified cartilaginous matrix and angiogenic stimulators, thus becoming a target for capillary invasion and neovascularization which marks the onset of ossification (Alini M. et al., 1996). VEGF is an essential mediator of neovascularization and has a major role in cartilage maturation and resorption. It is produced by hypertrophic chondrocytes and promotes endochondral ossification by recruiting and/or differentiating osteoclastic cells that resorb cartilage and by attracting osteoblasts (Colnot C. et al, 2003). LIPUS can up regulate VEGF in a

variety of cells both in vitro and in vivo (please see section I.II.III.III.), and it is well documented that LIPUS can accelerate endochondral ossification through neovascularization (Lu H. et al., 2008; Katano M. et al., 2011).

Subchondral cancellous bone in adults is composed of dense and compact trabecular bone with high bone mineral density, while the growing condyle, in which endochondral bone formation is actively progressing, has a low BMD, BV/TV (small bone area), Trabecular thickness, and more trabecular number with larger trabecular surface area (BS/BV) (Jiao K. et al., 2010). Moreover, the degree of anisotropy in woven bone, which forms under conditions of rapid turnover like normal growth, is low while by maturation its increases (Daegling D.J. et al., 2007). Thus, the abovementioned changes in the subchondral cancellous layer which were more prominent in the middle region of the condyle could be due to reactivation of or increased bone remodeling and active bone formation in this area. Even though the underlying reason is not clear, proliferation of chondroblasts, accumulation of hypertrophic chondrocytes, and increased secretion of regulatory factors like VEGF from these cells that are induced by local application of LIPUS may have an effect on bone remodeling in adjacent subchondral bone.

It should be mentioned here that the magnitude of changes in the above mentioned parameters following LIPUS application were lower compared to similar evaluations in the posterior area of the condyle in the same population subsequent to continuous bite-jumping. However, the trend was relatively similar (Xiong H. et al., 2005b).

In the present study the percentage of remnants of calcifying cartilage with newly deposited bone areas/bone area showed a 59% increase in the LIPUS group compared to that of the control. In comparison, the amount of increase in new bone formation was 318.91% as a result of forward mandibular positioning (continuous bite jumping) over 30 days (Rabie A.B. et al., 2004b).

The more pronounced response at the middle region of the condyle reported in the present study resembles one previous bite jumping study of adult rhesus monkeys in which adaptive response was more in the superior and postero superior region (Mc Namara J.A., 1982). In addition, condylar cartilage enhancement mostly occurred in the middle and postero superior region following mandibular advancement in 7 and 15 month old mice (Tagliaro M.L. et al., 2009).

We also attempted to determine the amount of endochondral bone growth in 3 weeks of treatment by using the technique of vital staining (calcein green). However, the course of the fluorescent lines was very irregular which makes measuring difficult. Further, even though the second label was distinguishable, it was palish and less prominent compared to the first label. One possible reason for the latter is the loss of label due to dissolution into the fixative (Galen S.M.V. et al., 2010). 24 hrs might not be enough time between the last injection and sacrifice. Thus, for similar studies in future two different fluorescent injections and at least two consecutive days for each time point to have more distinct labels is highly recommended.

Nevertheless, within these limitations we performed the measurements in the middle region of the condyle. The values obtained for the control animals were quite close to a previous study (Suzuki et al., 2004) on mature rats with the same marker interval and hence we decided to report the results. The results suggested slightly but significantly higher (mean difference = 53.7  $\mu\text{m}$ ) endochondral bone growth in the LIPUS group compared to that of the control.

In this preceding study the treatment was 3 times local administration of IGF-I (0.02 ml at the concentration of 50  $\mu\text{g}/\text{ml}$ ) into the condyle of adult (15 (at the beginning of the experiment) +3 (experimental period) weeks) male rats. The treatment in 21 days led to 157  $\mu\text{m}$  thicker total fibrocartilage layer compared to that of the control, which is less than three times higher than the effect of LIPUS on fibrocartilage thickness in the present study. However, a decline in the percentage of bone area in the subchondral cancellous bone as a result of this treatment was only 4% more than that of the present study and the amount of endochondral bone growth merely 12  $\mu\text{m}$  higher. This could be relevant as the IGF-I was injected into the condyle and should have a more profound effect on cartilage with merely an indirect effect on subchondral cancellous bone. In contrast, even though LIPUS has a lower stimulatory effect on both structures, it might have a direct effect on osteogenic cells of subchondral cancellous bone as well. In addition, it is worthy to note that IGF-pathway is an important mechanism for cells to respond to LIPUS stimulation (please see section I.II.III.III.) and IGF-I is known to have a profound chondrogenic and also osteogenic effect (Patil A.S. et al., 2012) (please see section I.II.I).

Further support can be provided from the study by Nolte et al. (2001) in which daily LIPUS stimulation was applied for 7 days to 17-day-old mouse metatarsal rudiments developed via endochondral ossification. In the LIPUS treated group, the growth of the metatarsal diaphysis

was increased and reached to an eventual size of approximately 3 times that of the controls (Nolte P.A. et al., 2001).

Lastly, we performed Goldner's Trichrom staining for osteoid as a gold standard to estimate the amount of newly formed bone which had yet to be mineralized. LIPUS treatment resulted in a significant increase in osteoid thickness in subchondral cancellous bone subjacent to cartilage bone junction. This increase in osteoid thickness (37%) as a result of increased osteoid apposition suggests an anabolic effect of LIPUS on the activity of osteoblasts. The significant increment in osteoid thickness happened in both middle and posterior areas but was more prominent in the middle region. This might again suggest that rather than an indirect effect, through a stimulatory effect on hypertrophic cells, LIPUS has a direct effect on osteogenic cells of subchondral cancellous bone. In a previous study LIPUS application led to a 47% increase in osteoid thickness in the area of fracture healing in patients with a delayed union of the osteotomized fibula (Rutten S. et al., 2008). Cultured mouse bone-marrow-derived ST2 cells have been shown to respond to LIPUS. This is through increased levels of IGF, osteocalcin, and bone sialoprotein mRNA, suggesting that LIPUS induces a direct anabolic reaction of osteogenic cells leading to bone matrix formation (Naruse K. et al., 2000). The target osteoblasts of LIPUS are cells at a relatively early stage in the osteoblastic lineage (Naruse K. et al., 2003); only relatively young osteoblasts responded to LIPUS by up regulating message and protein levels of immediate-early genes as well as those of osteocalcin and insulin-like growth factor I. The osteogenic potential of LIPUS is the most studied aspect of this treatment and was partially mentioned in section I.II.III.I. However, we should further note the fact that mandibular osteoblasts and osteocytes response to LIPUS is different from that of long bones or calvarial bone. This different response could be because mandibular osteoblasts should be mechanically loaded to maintain their capability to promote remodeling and to insure osteoblast survival and hence to preserve intact mandibular bone tissue (Watabe H. et al., 2011).

## Limitations

Several limitations should be considered when interpreting the results of this study.

- The interpretation of histomorphometric analysis due to two main issues should be performed with caution: first, the standard deviations in the majority of parameters were large and second the cells especially in the proliferative zone were not labeled with appropriate markers such as H-thymidin, PCNA, or Anti ki-67 to report the percentage of truly proliferative cells in a representative field. This results because not all condyles, even in rats, are at the same size. More over tissue responsiveness of animals also might be different.
- In our study, a single time point in the time course of ultrasound treatment has been depicted. Future studies should take benefit of in vivo micro-CT imaging technology and histology in different time points to allow for the measurement of changes throughout the treatment period.
- In the present study it is unclear for us how the ultrasound wave transmits through the skin, fat, muscle, tendons, cartilage and cortical bone to act on cartilage and cancellous bone addressed in the present study.
- The purpose of the current experiment was to determine whether US could stimulate an in vivo cartilage and bone forming response in young adult individuals. Thus, the molecular mechanism underlying the observed US effect was not investigated.

## Conclusions and Recommendations for Future Works

- LIPUS may stimulate both chondrogenesis and osteogenesis in adult rat mandibular condyle and enhance endochondral bone formation and subcondral trabecular bone remodeling.
- This response is region specific, probably due to difference in intrinsic maturity of the condylar cartilage in different regions (Middle versus Posterior). The middle region maintains growth cartilaginous appearance into later stages and so probably is more responsive to LIPUS stimuli. Thus, LIPUS may enhance the residual growth potential of the condyle rather than the reactivation of mandibular condylar growth/remodeling.
- Among the biomolecules that are known or assumed to play a role in mandibular condylar growth, in vitro and in vivo studies revealed that LIPUS can up regulate expression of Runx2/Cbfa1, Osterix, Sox9, VEGF, IGF, FGF, TGF $\beta$ , PDGFS; CTGF, BMPs, Cyclin D1, type II and X collagen, and activate Wnt/  $\beta$  catenin, PI3K/Akt pathways in a variety of cells. Thus, any of these biomolecules could be appropriate candidates for investigating the molecular mechanism of LIPUS on mandibular condylar growth/remodeling modification. IHH is the critical mechanotransduction mediator of the condylar growth and mechanotransduction is one of the main mechanisms of action of LIPUS. Thus, IHH could be another suitable candidate for this purpose.
- However, it is less likely that this biological effect would be of any clinical significance. Even though the present study showed the ability of LIPUS application in enhancing cartilage and bone formation, this potential is limited and far below that of fixed bite-jumping appliances. If the applied loading stimulus by fixed bite jumping appliances is enough to induce a maximal chondrogenic and osteogenic response, then it would be unlikely that the slight effects of this ultrasound regimen would increase the response.
- It is of course possible that the dose of ultrasound i.e. any relevant ultrasound parameters such as burst rate, intensity, frequency, or duration was less than the

amount needed to induce a maximal response. Thus, changing any of these parameters might result in more profound results.

- No statistically significant changes in condylar process length, ramus height, and mandibular length were detected while remarkable increases in these linear parameters have been reported when LIPUS was applied to the TMJ area of growing and even late adolescent animals. Considering biological responses have been observed in the present study, this limited effect might be attributed to delayed onset of response and remodeling in adult condyle.
- Among the available non invasive treatments for adults with underdevelopment of the lower jaw, stepwise mandibular advancement using fixed bite jumping appliances clinically seems to be more promising. However, in this protocol each step should be elongated for 6 months to let the newly formed bone (with type III collagenous matrix) mature to a more stable type I collagenous matrix (Chaiyongsirisern A. et al., 2009). It is suggested that LIPUS can enhance bone maturation and may accelerate type I collagen maturation (Saito M et al., 2004; Hsu SK et al., 2011; Gu X.Q. et al., 2014). Thus, concurrent LIPUS application and fixed functional therapy in a stepwise manner may decrease the treatment time in each step and may provide stability in a shorter time. This could be investigated in future research.
- In 3-D visualisation, a potential increase in periosteal bone apposition in the side of sonication has been demonstrated and supports the findings of previous histologic and micro-CT evaluations in long bones (Naruse K et al., 2009; Perry MJ et al., 2009). This aspect may have little clinical relevance; nonetheless, to increase the amount of knowledge in sciences related to LIPUS' effect on intact bone, future histologic and micro-CT analysis could be conducted to compare the treatment effect on the side of sonication and the opposite side in mandible or mandibular condyle.
- In tissue engineering of the mandibular condyle, it is challenging to bioengineer the bone and cartilage concurrently. However, it has been observed that following transplantation of the bony tissue engineered condyle and subsequent to jaw movement (when condyle is located in a function environment) the MCC which is a secondary cartilage forms but not to a substantial degree (Personal communication with Prof. G. Novacovik, April 29, 2013). Based on the findings of the present study,

in vivo LIPUS application especially following finding optimal settings might be promising for further cartilage and bone formation in such tissue engineered transplants and relieve the need of producing a separate tissue engineered cartilage.

## REFERENCES

1. Abtahi M, Poosti M, Saghravanian N, Sadeghi K, Shafae H (2012 Feb). The effect of low level laser on condylar growth during mandibular advancement in rabbits. *Head Face Med* 23;8:4.
2. Adams CD, Meikle MC, Norwick KW, Turpin DI (1972). Dentofacial remodelling produced by intermaxillary forces in *Macaca mulatta*. *Arch Oral Biol* 17:1519-35.
3. Aidar LA, Abrahao M, Yamashita HK, Dominguez GC (2006). Herbst appliance therapy and temporomandibular joint disc position: a prospective longitudinal magnetic resonance imaging study. *Am J Orthod Dentofacial Orthop* 129 (4): 486-96.
4. Akiyama H, Kim J-E, Nakashima K, Balmes G, Iwai N, Deng JM, Zhang Z, Martin JF, Behringer RR, Nakamura T, de Crombrughe B (2005). Osteochondroprogenitor cells are derived from Sox9 expressing precursors. *Proc Natl Acad Sci USA* 102:14655–14670.
5. Alini M, Marriott A, Chen T, Abe S, Poole AR (1996). A novel angiogenic molecule produced at the time of chondrocyte hypertrophy during endochondral bone formation. *Dev Biol* 176:124–32.
6. Al-kalaly A, Charlene Wu, Wong R, Rabie ABM (2009). The assessment of cell cycle genes in the rat mandibular condyle. *Arch Oral Biol* 54: 470-478.
7. Andre T (1956). Studies on the distribution of titanium-labelled dihydrostretomycin and tetracycline in the body, *Acta Radiol Suppl* 1.
8. Angers S, Moon RT (2009). proximal events in Wnt signal transduction. *Nat Rev Mol Cell Biol* 10(7):468-77.
9. Angle SR, Sena K, Sumner DR, Virkus WW, Viridi AS (2014 Jan 23). Combined Use of Low Intensity Pulsed Ultrasound and rhBMP-2 to Enhance Bone Formation in a Rat Model of Critical-Size Defect. *J Orthop Trauma*[Epub ahead of print]
10. Anthwal N, Chai Y, Tucker AS (2008). The role of transforming growth factor- $\beta$  signaling in the patterning of the proximal processes of the murine dentary. *Dev Dyn* 237:1604-1613.

11. Azagra-Calero E, Espinar-Escalona E, Barrera-Mora JM, Lamas-Carreras JM, Solano-Reina E (2012 Nov 1). Obstructive Sleep Apnea Syndrome (OSAS). Review of the literature. *Med Oral Pathol Oral Cir Bucal*. 17(6): e925-9.
12. Azuma Y, Ito M, Harada Y, Takagi H, Ohta T, Jingushi S (2001). Low-intensity pulsed ultrasound accelerates rat femoral fracture healing by acting on the various cellular reactions in the fracture callus. *J Bone Miner Res* 16:671-80.
13. Bacabac RG, Smit TH, Van Loon JJWA, Zandieh Doulabi B, Helder MN, Klein-Nulend J (2006). Bone cell responses to high-frequency vibration stress: does the nucleus oscillate within the cytoplasm? *FASEB J*. 20:858-64.
14. Baker KG, Robertson VJ, Duck FA (2001). A review of therapeutic ultrasound: *bio-physical effects Phys Ther*. 81: 1351-1358.
15. Bandow K, Nishikawa Y, Ohnishi T, Kakimoto K, Soejima K, Iwabuchi S, Kuroe K, Matsuguchi T (2007). Low-intensity pulsed ultrasound (LIPUS) induces RANKL, MCP-1, and MIP-1beta expression in osteoblasts through the angiotensin II type 1 receptor. *J. Cell. Physiol*. 211, 392–398.
16. Barnouti ZP, Owtad P, Shen G, Petocz P, Dareendeliler MA (2011). The biological mechanisms of PCNA and BMP in TMJ adaptive remodeling. *Angle Orthod*. 81:91-99.
17. Bashardoust Tajali S, Houghton P, MacDermid JC, Grewal R (2012). Effects of low-intensity pulsed ultrasound therapy on fracture healing (A systematic review and meta-analysis). *Am J Phys Med Rehabil*. 91:349-367.
18. Bathia SN, Leighton BC (1993). *A manual of facial growth. A computer analysis of longitudinal cephalometric growth data*. Oxford: Oxford University Press. p:57.
19. Behrents RG (1985). *Growth of the aging craniofacial skeleton: Monograph 17, Craniofacial growth series*. Ann Arbor: Center for Human Growth and Development, The University of Michigan.
20. Bemenderfer TB, Harris J S, Condon K W, Kacena M A (2014). *Tips and Techniques for Processing and Sectioning Undecalcified Murine Bone Specimens*. In Hilton MJ editor. *Skeletal Development and Repair Methods and Protocols* University of Rochester Medical Center, Rochester, NY, USA, Human Press P: 129,130,136,137.

21. Blackwood HJJ (1966). Adaptive changes in the mandibular joints with function. *Dent Clin North Am.* 559-66.
22. Bock NC, Bremen JV, Ruf S (2010). Occlusal stability of adult class II division 1 treatment with the Herbst appliance. *Am J Orthod Dentofacial Orthop.* 138:146-51.
23. Bremaen J V, Bock N, Ruf S (2009). Is Herbst-Multibracket appliance treatment more efficient in adolescents than in adults? A dental cast study. *Angle Orthod.* 79:173-177.
24. Bremaen JV, Bock N, Ruf S (2009). Is Herbst-multibracket appliance treatment more efficient in adolescents than in adults? A dental cast study. *Angle Orthod.* 79:173-177.
25. Buxton PG, Hall B, Archer CW, Francis-WestP (2003 Oct). Secondary chondrocyte-derived Ihh stimulates proliferation of periosteal cells during chick development. *Development.* 130(19):4729-39.
26. Carlson DS, McNamara JA Jr, Graber LW, Hoffman DL (1980). *Experimental studies of growth and adaptation of TMJ.* In: Irby WB, editor. Current advances in oral surgery. St. Louis: Mosby; p 28–77.
27. Carlson DS, McNamara JA Jr, Jial DH (1978). Histological analysis of the growth of the mandibular condyle in the rhesus monkey (*Macaca mulatta*). *Am J Anat.* 151:103-18.
28. Carvalho DC, Cliquet Junior A (2004). The action of low-intensity pulsed ultrasound in bones of osteopenic rats. *Artif Organs.* 28:114-8.
29. Chaiyongsirisern A, Rabie AB, Wong RWK (2009). Stepwise advancement herbst appliance versus mandibular sagittal split osteotomy. Treatment effects and long-term stability of adult class II patints. *Angle Orthod* 79:1084-1094.
30. Chayanupatkul A, Rabie AB, Hagg U (2003). Temporomandibular response to early and late removal of bite-jumping devices. *Eur J Orthod* 25:465-470.
31. Chen Y, Ke J, Long X, Meng Q, Deng M, Fang W, Li J, Cai H, Chen S (2012). Insulin-like growth factor-1 boosts the developing process of condylar hyperplasia by stimulating chondrocytes proliferation. *Osteoarthritis and Cartilage* 20: 279-287.

32. Chen YJ, Wang CJ, Yang KD, Chang PR, Huang HC, Huang YT, Sun YC, Wang FS (2003). Pertussis toxin-sensitive Gai protein and ERK-dependent pathways mediate ultrasound promotion of osteogenic transcription in human osteoblasts. *FEBS Letters* 554:154-158.
33. Cheng K, Xia P, Lin Q, Shen S, Gao M, Ren S, Li K (2014 Jul). Effects of low-intensity pulsed ultrasound on integrin-FAK-PI3K/Akt mechanochemical transduction in rabbit osteoarthritis chondrocytes. *Ultrasound Med Biol* 40(7): 1609-18.
34. Chiu R, Boyle WJ, Meek J, Smeal T, Hunter T, Karin M (1988). The c-fos protein interacts with c-Jun/AP-1 to stimulate transcription of AP-1 responsive gene. *Cell* 54(4):541-52.
35. Choi BH, Woo JI, Min BH, Park SR (2006). Low intensity ultrasound stimulates the viability and matrix gene expression of human articular chondrocytes in alginate bead culture. *J Biomed Mater Res A* 79:858-864.
36. Chu FT, Tang GH, Hu Z, Qian YF, Shen G (2008). Mandibular functional positioning only in vertical dimension contributes to condylar adaptation evidenced by concomitant expression of L-Sox5 and typeII collagen. *Arch Oral Biol* 53: 567-574.
37. Claes L, Willie B (2007). The enhancement of bone regeneration by ultrasound. *Prog Biophys Mol Biol* 93:384-98.
38. Colnot C, Thompson Z, Miclau T, Werb Z, Helms JA (2003). Altered fracture repair in the absence of MMP9. *Development* 130: 4123–4133.
39. Cook SD, Ryaby JP, McCabe J, Frey JJ, Heckman JD, Kristiansen TK (1997). Acceleration of tibia and distal radius fracture healing in patients who smoke. *Clin Orthop Relat Res* 198-207.
40. Cook SD, Salkeld SL, Patron LP, Whitecloud TS (2001a). Low-intensity pulsed ultrasound improves spinal fusion. *Spine J.* 1: 246-54.
41. Cook SD, Salkeld SL, Patron LP, Doughty ES, Jones DG (2008). The effect of low-intensity pulsed ultrasound on autologous osteochondral plugs in a canine model. *Am J Sports Med.* 36: 1733-1741.

42. Cook SD, Salkeld SL, Popich-Patron LS, Ryaby JP, Jones DG, Barrack RL (2001b). Improved cartilage repair after treatment with low-intensity pulsed ultrasound. *Clin Orthop*. 391: S231-s243.
43. Coords M, Breitbart E, Paglia D, Kappy N, Gandhi A, Cottrell J, Cedeno N, Pounder N, O'Connor JP, Lin SS (2011). The effects of low-intensity pulsed ultrasound upon diabetic fracture healing. *J Orthop Res* 29:181-8.
44. Cozza P, Baccetti T, Franchi L, De Toffol, McNamara JA (2006). Mandibular changes produced by functional appliances in Class II malocclusion: A systematic review. *Am J Orthod Dentofacial Orthop* 129:599. e1-599.e12.
45. Cui JH, Park SR, Park K, Choi BH, Min BH (2007). Preconditioning of mesenchymal stem cells with low-intensity ultrasound for cartilage formation in vivo. *Tissue Eng* 13:351-360.
46. Daegling DJ And Grine FE (2007). *Mandibular Biomechanics and the paleontological evidenc for the evolution of human diet*. In Ungar P.S. editor. Evolution of the human diet. The known, the unknown, and the unknowable. New York. New York. USA. Oxford University Press Inc. P:84
47. Dahlberg G (1940). *Statistical Methods for Medical and Biological students*. London: Gorge Allen &Unwin LTD:122-132.
48. De Albornoz PM, Khanna A, Longo UG, Forriol F, Maffuli N (2011). The evidence of low-intensity pulsed ultrasound for in vitro, animal and human fracture healing. *Br Med Bull* 100:39-57.
49. De Gusmao CVB, Pauli JR, Abdalla Saad MJ, Alves JM, Beangero WD (2010). Low-intensity ultrasound increase FAK, ERK-1/2, and IRS-1 expression of intact rat bones in a noncumulative manner. *Clin Orthop Relat Res* 468:1149-1156.
50. Dee C, Shim J, Rubin C, McLeod K (1996). Modulation of osteoblast proliferation and differentiation by subtle alterations in temperature. *Trans Orthop Res Soc* 21:341.
51. Delatte M, Von den Hoff JW, Nottet SJ, De Clerck HJ, Kuijpers-Jagtman AM (2005). Growth regulation of the rat mandibular condyle and femoral head by transforming growth factor- $\beta$ 1, fibroblast growth factor-2 and insulin-like growth factor-I. *Eur J Orthod* 27:17–26.

52. Deng Z, Liu Y, Wang C, Fan H, Ma J, Yu H (2014). Involvement of P13K/Akt pathway in rat condylar chondrocytes regulated by PTHrP treatment. *Arch Oral Biol* 59:1032-1041.
53. Dibbets JMH (1990). *Introduction to the temporomandibular joint*. In: Facial growth. Enlow DH, editor. Philadelphia: Saunders, pp. 149-163.
54. Doan N, Reher P, Meghji S, Harris M (1999). In vitro effects of therapeutic ultrasound on cell proliferation, protein synthesis and cytokine production by human fibroblasts, osteoblasts and monocytes. *J Oral Maxillofac Surg* 57:409-19.
55. Durate LR (1983). The stimulation of bone growth by ultrasound. *Arch Orthop Trauma Surg* 101:153-159.
56. Durkin J, Heeley J, Irving JT (1973). The cartilage of the mandibular condyle. *Oral Sci Rev* 2:29-99.
57. Dyson, M (1987). Mechanisms involved in therapeutic ultrasound. *Physiotherapy* 73: 116-120.
58. Edlund J, Hansson T, Willmar K (1979). Sagittal splitting of the mandibular ramus. *Scand J Plast Reconstr Surg* 13:437-43.
59. El-Bialy T, Alhadlaq A, Felemban N, Yeung J, Ebrahim A, Hassan A (2014 Jul 14). The effect of light-emitting diode and laser on mandibular growth in rats. *Angle Orthod* Epub ahead of print.
60. El-Bialy T, Alhadlaq A, Lam B (2012). Effects of therapeutic ultrasound on human periodontal ligament cells for dental and periodontal tissue engineering. *Open Dent J* 6(suppl 1:M5):235-239.
61. El-Bialy T, El-Shamy I, Graber TM (2003). Growth modification of the rabbit mandible using therapeutic ultrasound: Is it possible to enhance functional appliance results? *Angle Orthod* 73: 631-639.
62. El-Bialy T, Hassan A, Albaghdadi T, Fouad HA, and Maimani AR (2006). Growth modification of the mandible with ultrasound in baboons: A preliminary report. *Am J Orthop Dentofacial Orthop* 130:435.e7-435.e14.

63. El-Bialy T, Hassan A, Janadas A, Albaghdadi T (2010). Non surgical treatment of hemifacial microsomia by therapeutic ultrasound and hybrid functional appliance. *Open Access J Clin Trials* 2; 29-36.
64. El-Bialy T, Uludag H, Jomha N, and Badylak SF (2010). In vivo ultrasound-assisted tissue-engineered mandibular condyle: a pilot study in rabbits. *Tissue Eng part C* 16(6): 1315-1322.
65. El-Mowafi H, Mohsen M (2005). The effect of low-intensity pulsed ultrasound on callus maturation in tibial distraction osteogenesis. *Int Orthop* 29:121-4.
66. Erdogan O and Esen E (2009 Jun). Biological aspects and clinical importance of ultrasound therapy in bone healing. *J Ultrasound Med* 28:765-76.
67. Farias-Neto A; Martins APVB ; Figueroba SR ; Francisco; Groppo C; Maria de Almeida S ; Rizzatti-Barbosa CM (2012). Altered mandibular growth under functional posterior displacement in rats. *Angle Orthod* 82:3-7.
68. Ferreri SL, Talish R, Trandafir T, Qin Y-X (2011). Mitigation of bone loss with ultrasound induced dynamic mechanical signals in an OVX induced rat model of osteopenia. *Bone* 48: 1095-1102.
69. Flores-Mir C, Korayem M, Heo G, Witmans M, Major MP, Major PW (2013). Craniofacial morphological characteristics in children with obstructive sleep apnea syndrome: a systematic review and meta-analysis. *J Am Dent Assoc* 144(3):269-77.
70. Frost, H.M (1969). Tetracycline labelling of bone and the zone of demarcation of osteoid seams. *Can J Biochem Physiol* 41:31.
71. Frye L, Diedrich PR, Kinzinger GSM (2009). Class II treatment with fixed functional orthodontic appliances before and after the pubertal growth peak- a cephalometric study to evaluate differential therapeutic effects. *J Orofac Orthop* 70:511-27.
72. Gaalen SMV, Kruyt MC, Geuze RE, Bruijn JD, Alblas J, and Dhert WJA (2010). Use of Fluorochrome Labels in In Vivo Bone Tissue Engineering Research. *Tissue Eng: Part B* 16(2): 209-217.
73. Gebhard A, Pancherz H (2003). The effect of anabolic steroids on mandibular growth. *Am J Orthod Dentofacial Orthop* 123:435-40.

74. Giancotti FG, Ruoslahti E(1999). *Integrin signaling*. Science 285 1028–1032.
75. Gleizal A, Ferreira S, Lavandier B, Simon B, Beziat JL, Bera JC (2010). The impact of low intensity pulsed ultrasound on mouse skull bone osteoblast cultures. *Rev Stomatol Chir Maxillofac* 111(5-6):280-5.
76. Gong FF, Feng J, Hu Z, Shen G, Chen RJ, You QL (2011). Effect of semifixed Twin-block appliance on temporomandibular joint remodeling. *Shanghai Kou Qiang Yi Xue*. 20:409-412.
77. Gu S, Wei N, Yu L, Fei J, Chen YP (2008). Shox-2-deficiency leads to dysplasia and ankylosis of the temporomandibular joint in mice. *Mech Dev* 125:729–742.
78. Gu XQ, Li YM, Guo J, Zhang LH, Li D, Gai XD (2014). Effect of low intensity pulsed ultrasound on repairing the periodontal bone of Beagle canines. *Asian Pac J Trop Med* 17:325-328.
79. Gurkan I, Ranganathan A, Yang X, Horton WE Jr, Todman M, Huckle J, Pleshko N, Spencer RG (2010). Modification of osteoarthritis in the guinea pig with pulsed low-intensity ultrasound treatment. *Osteoarthritis Cartilage* 18:724-733..
80. Hagg U and Panchez H (1988). Dentofacial orthopedics in relation to chronological age, growth period and skeletal development. An analysis of 72 male patients with Class II division 1 malocclusion treated with the Herbst appliance. *Eur J Orthod* 10: 169-179.
81. Haijar D, Santos MF, Kimura ET (2003). Propulsive appliance stimulates the synthesis of insulin-like growth factors I and II in the mandibular condylar cartilage of young rats. *Arch Oral Biol* 48:635–42.
82. Hall BK (1972). Immobilization and cartilage transformation into bone in the embryonic chick. *Anat Rec* 173:391–404.
83. Hanson T, Nordström B (1977). Thickness of the soft tissue layer and the articular disc in the temporomandibular joint with deviations in form. *Acta Odontol Scand* 35:281-8.
84. Hayton MJ, Dillon JP, Glynn D, Curran JM, Gallagher JA, Buckley KA (2005). *Ultrasound Med Biol* 31:1131-8.

85. Heckman JD, Sarasohn-Khan J (1997). The economics of treating tibia fractures. The cost of delayed unions. *Bull Hosp Jt Dis* 56:63-72.
86. Hellsing G, Hollender LG, Carlsson GE, Johansson B (1985). Temporomandibular joint adaptation to mandibular repositioning in adult occlusal rehabilitation. *J Craniomand Pract* 3:273-9.
87. Hickok NJ, Haas AR, Tuan RS (1998). Regulation of chondrocyte differentiation and maturation. *Micros Res Tech* 43:174-90.
88. Hiiemae K (1971). The structure and function of the jaw muscles in the rat (*Rattus norvegicus* L.) III. The mechanics of the muscles. *Zool J Linn Soc* 50:111-132.
89. Hildebrand, T., A. Laib, R. Muller, J. Dequeker and P. Ruegsegger (1999). Direct three-dimensional morphometric analysis of human cancellous bone: microstructural data from spine, femur, iliac crest, and calcaneus. *J Bone Miner Res* 14: 1167-1174.
90. Hiniker JJ, Ramfjord SP (1966). Anterior displacement of the mandible in adult rhesus monkeys. *J Prosthet Dent* 16:503-12.
91. Hinton RJ and McNamara JA Jr (1984a). Effect of age on the adaptive response of the adult temporomandibular joint. A study of induced protrusion in *Macaca mulatta*. *Angle Orthod* 54(2):154-162.
92. Hinton RJ and McNamara JA Jr (1984b). Temporomandibular bone adaptation in response to protrusive function in juvenile and young adult rhesus monkeys (*Macaca mulatta*). *Eur J Orthod* 6:155-74.
93. Hinton RJ, Serrano M, So S (2009). Differential gene expression in the perichondrium and cartilage of the neonatal mouse temporomandibular joint. *Orthod Craniofac Res* 12:168–177.
94. Hinton RJ (2014). Genes that regulate morphogenesis and growth of the temporomandibular joint: a review. *Dev Dyn* 243:864-874.
95. Hinton RJ (1988). Response of the intermaxillary suture cartilage to alterations in masticatory function. *Anat Rec* 220:376–387.
96. Hiyama A, Mochida J, Iwashina T et al (2007). Synergistic effect of low-intensity pulsed ultrasound on growth factor stimulation of nucleus pulposus cells. *J Orthop Res* 25: 1574-1581.

97. Hollender L, Ridell A (1974). Radiography of the temporomandibular joint after oblique sliding osteotomy of the mandibular rami. *Scand J Dent Res* 82:466-9.
98. Hou CH, Hou SM, Tang CH (2009). Ultrasound increased BMP-2 expression via PI3K, Akt, c-Fos/c-Jun, and AP-1 pathways in cultured osteoblasts. *J Cel Biochem* 106:7-15.
99. Hsu SH, Kuo CC, Whu SW, Lin CH, Tsai CL (2006). The effect of ultrasound stimulation versus bioreactors on neocarilage formation in tissue engineering scaffolds seeded with human chondrocytes in vitro. *Biomol Eng* 23: 259-264.
100. Hsu SK, Husng WT, Liu BS, Li SM, Chen HT, and Chang CJ (2011). Effect of near-field ultrasound stimulation on new bone formation and osseointegration of dental titanium implants in vitro and in vivo. *Ultrasound in Med & Biol* 37(3):403-416.
101. Huang M, Ding H, Chai C, Huang Y, Yang R (1997). Effects of sonication on articular cartilage in experimental osteoarthritis. *J. Rheumatol* 24:1978-1984.
102. Huang MH, Chen TW, Weng MC, Wang MC, Wang YL (2001). *Effects of pulse sonication on functional status of patients with knee osteoarthritis*. In: Peek WJ, Lankhrst GJ, editors. International society of Physical and Rehabilitation Medicine Jul 7-13; Amesterdam (The Netherlands). Bologna: Monduzzi; P: 297-300.
103. Hynes RO (2002). Integrins: bidirectional, allosteric signaling machines. *Cell* 110:673-87.
104. Ikeda K, Takayama T, Suzuki N, Shimada K, Otsuka K, Ito K (2006). Effects of low-intensity pulsed ultrasound on the differentiation of C2C12 cells. *Life Sci*. 79: 1936-1943.
105. Ingber DE (2003). Mechanosensation through integrins: cells act locally but think globally. *Proc Natl Acad Sci. USA*. 5:1472-1474.
106. Ingervall B, Carlsson GE, Thilander B (1976). Postnatal development of the human temporomandibular joint II: a microradiographic study. *Acta Odontol Scand* 34:133-9.
107. Irrechukwu ON, Lin PC, Fritton K, Doty S, Pleshko N, Spencer RG (2011). Magnetic resonance studies of macromolecular content in engineered cartilage treated with pulsed low-intensity ultrasound. *Tissue Eng: Part A*. 17: 407-415.

108. Ishihara Y, Uei K, Sotobori M, Marukawa K, Moroi A (2014). Bone regeneration by statin and low-intensity pulsed ultrasound (LIPUS) in rabbit nasal bone. *J Craniomaxillofac Surg.* 42: 185-193.
109. Ito M, Azuma Y, Ohta T (2000). Effects of ultrasound and 1, 25-dihydroxyvitamin D3 on growth factor secretion in co-cultures of osteoblasts and endothelial cells. *Ultrasound Med Biol.* 26:161-6.
110. Iwashina T, Mochida J, Sakai D, Yamamoto Y, Miyazaki T, Ando K, Holta T (2006). Feasibility of using a human nucleus pulposus cell line as a cell source in cell transplantation therapy for intervertebral disc degeneration. *Spine (Phila Pa 1976),* 31(11): 1177-86.
111. Jacobsen PU, Lund K (1972). Unilateral overgrowth and remodeling processes after fracture of the mandibular condyle. *Scand J Dent Res* 80:68-74.
112. Jang KW, Ding L, Seol D, Lim TH, Buckwalter JA, Martin JA (2014). Low-intensity pulsed ultrasound promotes chondrogenic progenitor cell migration via focal adhesion kinase pathway. *Ultrasound Med Biol* 40(6):1177-1186.
113. Jia XL, Chen WZ, Zhou K, Wang ZB (2005). Effects of low-intensity pulsed ultrasound in repairing injured articular cartilage. *Chin J Traumatol* 28: 175-178.
114. Jiao K, Dai j, Wang M-Q, Niu L-N, Yu Sb, Liu X-D (2 0 1 0). Age- and sex-related changes of mandibular condylar cartilage and subchondral bone: A histomorphometric and micro-CT study in rats. *Arch Oral Biol* 55: 1 55 – 1 63.
115. Jinguishi S, Mizuno K, Matsushita T (2007). low intensity pulsed ultrasound treatment for postoperative delayed union or non-union of long bone fractures. *J Orthop Sci* 12:35-41.
116. Johnston LE Jr. A comparative analysis of class II treatments. In: Vig PS, Ribbens KA, editors. Science and clinical judgement in orthodontics. Ann Arbor: Centre for Human Growth and Development; 1986 p. 103-48.
117. Kabbur KJ, Hemanth M, Patil GS, Sathyadeep V, Shamnur N, Hariyesha KB, Praveen GP (2012). An esthetic treatment outcome of orthognathic surgery and dentofacial orthopedics in Class II treatment: A cephalometric study. *J contemp dent pract* 13(5): 602-606.

118. Kaneyama K, Segami N, and Hatta T (2008). Congenital deformities and developmental abnormalities of the mandibular condyle in the temporomandibular joint. *Congenital Anomalies* 48, 118–125.
119. Kaneyama K, Segami N, and Hatta T (2008). Congenital deformities and developmental abnormalities of the mandibular condyle in the temporomandibular joint. *Congenital Anomalies* 48, 118-125.
120. Kantomma T, Ronning O (1997). *Growth mechanisms of the mandible*. In: Fundamentals of craniofacial growth. Dixon AD, Hoyte DA, Ronning O, editors. New York: CRC Press. pp. 189-204.
121. Kaplan RG (1989). Induced condylar growth in a patient with hemifacial microsomia. *Angle Orthod* 59(2):85-90.
122. Kasturi G, Adler RA (2011). Mechanical means to improve bone strength: ultrasound and vibration. *Curr Rheumatol Rep* 13:251-256.
123. Katano M, Naruse K, Uchida K, Mikuni-Takagaki Y, Takaso M, Itoman M, Urabe K (2011). Low intensity pulsed ultrasound accelerates delayed healing process by reducing the time required for the completion of endochondral ossification in the aged mouse femur fracture model. *Exp Anim*. 60(4):385-95.
124. Kaur H, Uludag H, El-Bialy T (2014). Effects of nonviral plasmid delivered basic fibroblast growth factor and low intensity pulsed ultrasound on mandibular condylar growth: a preliminary study. *Biomed Research International* 426710.
125. Kersey ML, Nebbe B, Major PW (2003). Temporomandibular Joint morphology changes with mandibular advancement surgery and rigid internal fixation: a systematic literature review. *Angle Orthod* 73: 79-85.
126. Khan I, El-Kedi AO, El-Bialy T (2013). Effects of growth hormone and ultrasound on mandibular growth in rats: microCT and toxicity analysis. *Arch Oral Biol* 58(9):1217-1224.
127. Khan RS and Horrocks EN (1991). A study of adult orthodontic patients and their treatment. *Br J Orthod* 18(3): 183-194.
128. Khanna A, Nelmes RTC, Gougoulas N, Maffulli N, Gray J (2009). The effects of LIPUS on soft-tissue healing: a review of literature. *Br Med Bull* 89:169-182.

129. Kiliaridis S (1989). Muscle function as a determinant of mandibular growth in normal and hypocalcaemic rat. *Eur J Orthod* 11:298-308.
130. Kinzinger G, Frye L, Diedrich P (2009). Class II treatment in Adults: Comparing camouflage orthodontics, dentofacial orthopedics and orthognathic surgery- a cephalometric study to evaluate various therapeutic effects. *J Orofac Orthop* 69:63-91.
131. Kinzinger G. and Diedrich P (2005). Skeletal effects in class II treatment with the functional mandibular advancer (FMA). *J Orofac Orthop* 66: 469-90.
132. Klug W, Frane WG, Knoch HG (1986). Scintigraphic control of bone fracture healing under ultrasonic stimulation: an animal experimental study. *Eur J Nucl Med* 11:494-7.
133. Kobayashi Y, Saai D, Iwashina T, Iwabushi S, Mchida J (2009). Low-intensity pulsed ultrasound stimulates cell proliferation, proteoglycan synthesis and expression of growth factor-related genes in human nucleus pulposus cell line. *Eur Cell Mater* 30(17):15-22.
134. Kokubu T, Matsui N, Fujioka H, Tsunoda M, Mizuno K (1999). Low intensity pulsed ultrasound exposure increases prostaglandin E<sub>2</sub> production via the induction of cyclooxygenase-2 mRNA in mouse osteoblasts. *Biochem Biophys Res Commun* 256:284-7.
135. Konick M, Pancherz H, Hansen K (1997 Jul). The mechanism of class II correction in the late Herbst treatment. *Am J Orthod Dentofacial Orthop* 112 (1):87-91.
136. Kopakkala-Tani M, Leskinen JJ, Karjalainen T, Hynynen K, Toyras J, Jurvelin JS, Lammi MJ (2006). Ultrasound stimulates proteoglycan synthesis in bovine primary chondrocytes. *Biorheology* 43:271-282.
137. Korstjens CM, Nolte PA, Burger EH, Albers GH, Semeins CM, Aartman IH, et al (2004). Stimulation of bone cell differentiation by low-intensity ultrasound-a histomorphometric in vitro study. *J Orthop Res* 22:495-500.
138. Korstjens CM, van der Rijt RHH, Albers GHR, Semeins CM, Klein-Nulend J (2008). Low-intensity pulsed ultrasound affects human articular chondrocytes in vitro. *Med Biol Eng Comput* 46:1263-1270.

139. Kosaka T, Masaoka T, Yamamoto K (2011). Possible molecular mechanism of promotion of repair of acute Achilles tendon rupture by low intensity-pulsed ultrasound treatment in a rat model. *West Indian Med J* 60(3):263-8.
140. Lai CH, Chen SC, Chiu LH, Yang CB, Tsai YH, Zuo CS, Chang WHS, , and Lai WF (2010). Effects of low intensity pulsed ultrasound , dexamethasone/TGF- beta 1 and/or BMP-2 on the transcriptional expression of genes in human mesenchymal stem cells: chondrogenic vs. Osteogenic differentiation. *Ultrasound Med Biol* 36: 1022-1033.
141. Lai J and Pittelkow DPM (2007). Physiological effects of ultrasound mist on fibroblasts. *Int J Dermatol* 46:587-593.
142. Lee HJ, Choi BH, Min BH, and Park SR (2007). Low-intensity ultrasound inhibits apoptosis and enhances viability of human mesenchymal stem cells in three-dimensional alginate culture during chondrogenic differentiation. *Tissue Eng* 13: 1049–1057.
143. Lei J, Liu MQ, Yap AUJ, Fu KU (2013). Condylar subchondral formation of cortical bon in adolescents and young adults. *Br J Oral Maxillofac Surg* 51: 63-68.
144. Leng KS. Qin Y-X. Cheng WH, Qin L (2008). *A practical manual for musculoskeletal research*. World Scientific publishing Co, p 228-271
145. Leskinen JJ, Karjalainen HM, Olkku A, Hynynen K, Mahonen A, Lammi MJ (2008).Genome-wide microarray analysis of MG-63 osteoblastic cells exposed to ultrasound. *Biorheology* 45, 345–354.
146. Leung KS, Cheung WH, Zhang C, Lee KM, Lo HK (2004a). Low intensity pulsed ultrasound stimulates osteogenic activity of human periosteal cells. *Clin Orthop Relat Res* 418:253-259.
147. Leung KS, Lee WS, Tsui HF, Liu PP, Cheung WH (2004b). Complex tibial fracture outcomes following treatment with low-intensity pulsed ultrasound. *Ultrasound Med Biol* 30:389-95.
148. Levrini L, Deli R, Sfondrini MF, Pantanali F (2003). Consistency of diet and its effects on mandibular morphogenesis in the young rat. *Prog Orthod.* 4:3-7.
149. Li JG, Chang WH, Lin JC, Sun JS (2002). Optimum intensities of ultrasound for PGE2 secretion and growth of osteoblasts. *Ultrasound Med Biol.*;28:683-690.

150. Li JK, Chang WH, Lin JC, Ruaan RC, Liu HC, Sun JS (2003). Cytokine release from osteoblasts in response to ultrasound stimulation. *Biomaterials*;24:2379-2385.
151. Li XJ, Jee WSS, Ke HZ, Mori S, Akamine T (1991). Age related changes of cancellous and cortical bone histomorphometry in female Sprague-Dawley rats. *Cells Mater; suppl.* 1:25-35
152. Li L, Yang Z, Zhang H, Chen W, Chen M, Zhu Z (2012). Low-intensity pulsed ultrasound regulates proliferation and differentiation of osteoblasts through osteocytes. *Biochem Biophys Res Commun.*; 418: 296–300.
153. Lim D, Ko CY, Seo DH, Woo DG, Kim JM, Chun KJ, Kim HS (2011). Low-intensity ultrasound stimulation prevents osteoporotic bone loss in young adult ovariectomized mice. *J Orthop Res.*; 29(1):116-25.
154. Lindahl L, Hollender L (1977). Condylar fractures of the mandible. II: a radiographic study of remodeling processes in the temporomandibular joint. *Int J Oral Surg.*;6:153-65.
155. Litsas G, Ari-Demirkaya A (2010). Growth indicators in orthodontic patients. Part 1: comparison of cervical vertebral maturation and hand-wrist skeletal maturation. *Eur J Paediatr Dent.* 11(4):171-175.
156. Liu J, Zou L, Zhao Z, Welburn N, Yang P, Tang T, Li Y (2009). Successful treatment of postpeak stage patients with class II division I malocclusion using non-extraction and multiloop edgewise archwire therapy: a report on 16 cases. *Int J Oral Sci.*; 1(4):207-216.
157. Liu Q, Wan Q, Yang R, Zhou H, Li Z (2012 Jul 20). Effects of intermittent versus continuous parathyroid hormone administration on condylar chondrocyte proliferation and differentiation. *Biochem Biophys Res Commun.* 424(1):182-8.
158. Loeser RF, Sadiev S, Tan L, Goldring MB (2000). Integrin expression by primary and immortalized human chondrocytes evidence of differential role for alpha 1 beta 1 and alpha 2 beta1 integrins in mediating chondrocyte adhesion to types II and VI collagen. *Osteoarthritis Cartilage.* 8(2):96-105.
159. Losken A, Mooney MP, Siegel MI (1992). A comparative study of mandibular growth patterns in seven animal models. *J Oral Maxillofac Surgery.* 50: 490-495.

160. Loyola-Sanchez A, Richardson J, Beattie KA, Otero-Fuentes C, Adachi JD, MacIntyre NJ (2012). Effects of low-intensity pulsed ultrasound on the cartilage repair in people with mild to moderate knee osteoarthritis: A double-blinded, randomized, placebo-controlled pilot study. *Arch Phys Med Rehabil.*93:35-42.
161. Lu H, Qin L, Cheung W, Lee K, Wong W, Leung K (2008). Low intensity pulsed ultrasound accelerated bone-tendon junction healing through regulation of vascular endothelial growth factor expression and cartilage formation. *Ultrasound Med Biol.* 34:1248-1260.
162. Lu H, Qin L, Le K, Cheung W, Chan K, Leung K (2009). Identification of genes responsive to low-intensity pulsed ultrasound stimulations. *Biomed Biophys Res Commun.* 375: 569-573.
163. Lubbert PH, van der Rijt RH, Hoorntje LE et al (2008). Low intensity pulsed ultrasound (LIPUS) in fresh clavicle fractures: a multi-centre double blind randomised controlled trial. *Injury.*39:1444-52
164. Lubsen CC, Hansson TL, Nordstrom BB, Solberg WK (1985). Histomorphometric analysis of cartilage and subchondral bone in mandibular condyles of young human adults at autopsy. *Arch Oral Biol.*30:129-136.
165. Luder HU, Schroeder HE (1992). Light and electron microscopic morphology of the temporomandibular joint in growing and mature crab-eating monkeys (*Macaca fascicularis*): the condyle calcified cartilage. *Anat Embryol (Berlin).*185:189-99.
166. Luder HU (1998). Age changes in the articular tissue of human mandibular condyles from adolescence to old age: a semi quantitative light microscopic study. *Anat Rec.*; 251:439-447.
167. Luder HU (1996). *Comparative skeletal maturation, somatic growth, and aging.* In Luder H-U, editor. Postnatal Development, Aging, and Degeneration of the Temporomandibular Joint in Humans, Monkeys, and Rats. Monograph 32. Craniofacial growth Series. Ann Arbor, Mich: The Centre for Human Growth and Development, The University of Michigan, Ann Arbor, MI, USA;:111-127.MC
168. Lyon R, Liu XC, Meier J (2003). The effect of therapeutic vs. high-intensity ultrasound on the rabbit growth plate. *J Orthop Res.*; 21: 865-871.

169. Maia S, Raveli DB, Santos-Pinto AD, Raveli TB, Gomes SP (2010). Computer Tomographic evaluation of a young adult treated with the Herbst appliance. *Dental Press J Orthod.* 15(5):130-6.
170. Maki RG (2010). Small is beautiful: insulin-like growth factors and their role in growth, development, and cancer. *J Clin Oncol.* 28:4985-95.
171. Manson J D (1968 a). *A comparative study of the postnatal growth of the mandible.* Henry Kimpton, London, P: 87.
172. Manson J D. (1968 b) *A comparative study of the postnatal growth of the mandible.* Henry Kimpton, London, P:36.
173. Mavropoulos A, Bresin A, Kiliaridis S (2004). Morphometric analysis of the mandible in growing rats with different masticatory functional demands: adaptation to an upper posterior bite block. *Eur J Oral Sci.* 112:259-266.
174. Mc Namara JA Jr, Connelly TG, McBride MC (1982). *Histological studies of temporomandibular joint adaptability.* In: McNamara JA Jr, editor. Determinants of mandibular form and growth. Monograph No. 4, Craniofacial growth series. Ann Arbor (MI) 1975: Centre for Human Growth and Development, The University of Michigan.
175. Mc Namara JA Jr, Hinton RJ, Hoffman DL (1975). Histological analysis of temporomandibular joint adaptation to protrusive function in young adult rhesus monkey (*Macaca mulatta*). *Am J Orthod.* 82: 288-98.
176. Mc Namara JA Jr, Peterson JE, Pancherz H (2003). Histologic changes associated with the Herbst appliance in adult rhesus monkeys (*Macaca mulatta*). *Semin Orthod.*9:26-40.
177. Mc Namara JA Jr (1981). Components of class II malocclusion in children 8-10 years of age. *Angle orthod.* 51:177-202.
178. Mc Namara JA Jr. (1973) Neuromuscular and skeletal adaptation to altered function in the orofacial region. *Am J Orthod.*; 64:578-607.
179. Mc Namara JA Jr (1972). *Neuromuscular and skeletal adaptations to altered orofacial function.* Monograph No 1, Craniofacial growth series. Ann Arbor (MI):Centre for Human Growth and Development, The University of Michigan.

180. McCormick SM, Saini V, Yazicioglu Y, Demou ZN, and Royston TJ (2006). Interdependence of pulsed ultrasound and shear stress effects on cell morphology and gene expression. *Ann Biomed Eng.*34(3): 436-45.
181. Meikle MC (2007). Remodeling the dentofacial skeleton: the biological basis of orthodontics and dentofacial orthopedics. *J Dent Res.*5: 12-24.
182. Mendonca C, Ferreira AS, Barbieri CH, Thomazine JA, and Mazzer N (2006). Efeitos do ultra-som pulsado de baixa intensidade sobre a cicatrizacao por segunda intencao de lesoes cutaneas totais em rotos. *Acta Ortop Bras.* 14: 152-157
183. Meng Q, Long X, Deng M, Cai H, Li J (2011). The expressions of IG-1, BMP-2, and TGF-beta 1 in cartilage of condylar hyperplasia. *J Oral Rehabil.*38:34-40.
184. Miyabe M, Urabe K, Naruse K, Uchida K, Mikuni Takagaki Y, Minehara H, and Itoman M (2010). Accelerated fracture healing using low-intensity pulsed ultrasound in an aged rat closed femoral fracture model. *Kitasato Med.* 40: 20–26.
185. Miyamoto K, An HS, Sah RL et al (2005). Exposure to pulsed low intensity ultrasound stimulates extracellular matrix metabolism of bovin intervertebral disc cells cultured in alginate beads. *Spine.* 30: 2398-2405.
186. Mizoguchi I, Nakamura M, Takahashi I, Kagayama M, Mitani H (1990). An immunohistochemical study of localization of type I and type II collagens in mandibular condylar cartilage compared with tibial growth plate. *Histochemistry.* 93:593–599.
187. Mizoguchi I, Nakamura M, Takahashi I, Sasano Y, Kagayama M, Mitani H (1993). Prsence of chondroid bone on rat mandibular condylar cartilage, An Immunohistochemical study. *Anat mbryol.* 187: 9-15.
188. Montalibt A, Jossinet J, Matias A, Cathignol D (2001). Electric current generated by ultrasonically induced Lorentz force in biological media. *Med Biol Eng Comput.*39:15-20.
189. Mukai S, Ito H, Nakagawa Y, Akiyama H, Miyamoto M, Nakamura T (2005). Transforming growth factor-beta 1 mediates the effects of lowintensity pulsed ultrasound in chondrocytes. *Ultrasound Med Biol.*31:1713-1721.

190. Muller K, Roth S, Fischer DC, Walther S, Dannhauer KH (1996). The soft tissue cover of the mandibular condyle: age-related changes in high byoant density proteoglycans, free tissue water and remodelling activity. *J Orofac Orthop.* 57:310-21.
191. Naito K, Watari T, Muta T, Furuhashi A, Iwase H, Igarashi M, Kurosawa H, Nagaoka I, Kaneko K (2010). Low-intensity pulsed ultrasound(LIPUS) increases the articular cartilage type II collagen in a rat osteoarthritis model. *J Orthop Res.*, 28(3):361-369.
192. Nakano H, Watahiki J, Kubota M, Maki K, Shibasaki Y, Hatcher D, et al (2003). Micro x-ray computed tomography analysis for the evaluation of asymmetrical condylar growth in the rat. *Orthod Craniofac Res.* 6(Suppl 1):168-172; discussion 179-182.
193. Nalbantgil D., Arun T, Sayinsu K, Isik F(2005). Skeletal, dental and soft-tissue changes induced by the Jasper Jumper appliance in late adolescence. *Angle Orthod.*75:426-436.
194. Naruse K, Mikuni-Takagaki Y, Urabe K, Uchida K, Itoman M (2009). Therapeutic ultrasound induces periosteal ossification without apparent changes in cartilage. *Connect Tissue Res.* 50:55-63.
195. Naruse K, Miyauchi A, Itoman M, and Mikuni-Takagaki Y (2003). Distinct anabolic response of osteoblast to low-intensity pulsed ultrasound. *J Bone Miner Res.* 18: 360-369.
196. Naruse K, Sekiya H, Harada Y, Iwabuchi S, Koazai Y, Kawamata R, Kashima I, Uchida K, Urabe K, Seto K, Itoman M, and Mikuni-Takagaki Y (2010). Prolonged endochondral bone healing in senescence is shortened by low-intensity pulsed ultrasound in a manner dependent on COX-2. *Ultrasound Med Biol.* 36: 1098–1108.
197. Naruse K, Mikuni-Takagaki Y, Azuma Y, Ito M, Oota T, Kameyama K, Itoman M (2000). Anabolic response of mouse bone-marrow-derived stromal cell clone ST2 cells to low-intensity pulsed ultrasound. *Biochem Biophys Res Commun.* 268, 216–220.
198. Ng TC, Chiu KW, Rabie AB, Hagg U (2006 a). Factors regulating condylar cartilage growth under repeated load application. *Front Bioscience.* 11:943-8.

199. Ng TCS, Chiu WK, Rabie ABM, Hagg U (2006 b). Repeated mechanical loading enhances the expression of Indian hedgehog in condylar cartilage. *Front Bioscience*. 11:943-948.
200. Nishikori T, Ochi M, Uchio Y et al (2002). Effects of low-intensity pulsed ultrasound on proliferation and chondroitin sulfate synthesis of cultured chondrocytes embedded in atelocollagen gel. *J Biomed Mater Res*. 59,201-206.
201. Nolte PA, Klein-Nulend J, Albers GH, Marti RK, Smeins CM, Goei SW, et al (2001). Low intensity ultrasound stimulates endochondral ossification in vitro. *J Orthop Res*.19:301-7.
202. O'Brien Jr, WD (2007). Ultrasound biophysics mechanisms Prog. Biophys. *Mol. Biol.* 93, 212-255.
203. Olkku A, Leskinen JJ, Lammi MJ, Hynynen K, Mahonen A (2010). Ultrasound-induced activation of Wnt signaling in human MG-63 osteoblastic cells. *Bone*. 47: 320-330.
204. Omi H, Mochida J, Iwashina T et al (2008). Low-intensity pulsed ultrasound stimulation enhances TIMP-1 in nucleus pulposus cells and MCP-1 in macrophages in the rat. *J Orthop Res*. 26: 865-871.
205. Orton RJ, Sturm OE, Vyshemirsky V, Calder M, Gilbert DR, Kolch W (2005). Computational modelling of the receptor-tyrosine-kinase-activated MAPK pathway. *Biochem J*. 392 (Pt 2): 249–61.
206. Oswald F, Tauber B, Dobner T, Bourtede S, Kostezka U, Adler G, Liptay S, Schmid RM (2001). P 300 acts as a transcriptional coactivator formation. *Mol Cell Biol*.2(22): 7761-74.
207. Ow ATC and Cheung LK (2009). Skeletal stability and complications of bilateral sagittal split osteotomies and mandibular distraction osteogenesis: an evidenced-based review. *J Oral Maxillofac Surg*. 67:2344-2353.
208. Ow ATC and Cheung LK (2008). Meta-analysis of mandibular distraction osteogenesis: clinical applications and functional outcomes. *Plast Reconstr Surg*.121:54e.
209. Owtad P, Park JH, Shen G, Potres Z, Darendeliler MA (2013). The biology of TMJ growth modification: a review. *J Dent Res*. 92(4):315-321.

210. Owtad P, Potres Z, Shen G, Petož P, Darendeliler MA (2011). A histochemical study on condylar cartilage and glenoid fossa during mandibular advancement. *Angle Orthod.* 81:270-276.
211. Oyonarte R, Becerra D, Diaz-Zuniga J, Rojas V, Carrion F (2013). Morphological effects of mesenchymal stem cells and pulsed ultrasound on condylar growth in rats: a pilot study. *Aust Orthod J.* 29(1):3-12.
212. Oyonarte R, Zarate M, Rodriguez F (2009). Low-intensity pulsed ultrasound stimulation of condylar growth in rats. *Angle Orthod.* 79:964-970.
213. Panchez H. and Ruf S (2008 a). *The Herbst Appliance. Research-based Clinical Management.* Quintessence Publishing Co, Ltd. Grafton Road, Nw Malden, Surrey, Great Britain. p: 31-41.
214. Panchez H. and Ruf S (2008 b). *The Herbst Appliance. Research-based Clinical Management.* Quintessence Publishing Co, Ltd. Grafton Road, Nw Malden, Surrey, Great Britain. p: 225-243.
215. Panchez H (2000). Dentofacial orthopedics or orthognathic surgery: is it a matter of age? *Am J Orthod Dentofac Orthop.* 117:571-574.
216. Papatheodorou LK, Malizos KN, Poullysidis LA, Hantes ME, Grafanaki K, Giannouli S, Loannou MG, Koukoulis GK, Protopappas VC, Fotiadis DI, Stathopoulos C (2009 Apr). Effect of transosseous application of low-intensity ultrasound at the tendon graft-bone interface healing gene expression and histological analysis in rabbits. *Ultrasound Med Biol.* 35: 576-84.
217. Park SR, Choi BH, Min BH (2007). Low-intensity ultrasound as an innovative tool for chondrogenesis of mesenchymal stem cells (MSCs). *Organogenesis.*;3:74-78.
218. Parvizi J, Wu CC, Lewallen DG, et al. (1999): Low intensity ultrasound stimulates proteoglycan synthesis in rat chondrocytes by increasing aggrecan gene expression. *J Orthop Res.* 17: 488-94.
219. Patil AS, Sable RB, Kotari RM (2012). Role of Insulin-like Growth Factors (IGFs), Their Receptors and Genetic Regulation in the Chondrogenesis and Growth of the Mandibular Condylar Cartilage. *Cell Physiol.* 227: 1796–1804.

220. Paulsen HU, Karle A, Bakke M, Herslink A (1995). CT-scanning and radiographic analysis of temporomandibular joints and cephalometric analysis in a case of Herbst treatment in laterd. puberty. *Eur J Orthod.*17 (3): 165-75.
221. Paulsen HU, Karle A (2000 Dec). Computer tomographic and radiographic changes in the temporomandibular joints of two young adults with occlusal asymmetry, treated with the Herbst appliance. *Eur J Orthod.* 22(6):649-56
222. Paulsen HU, Rabol A, Sarensen SS (1998). Bone scintigraphy of human temporomandibular joints during Herbst treatment:a case report. *Eur J Orthod.* 20(4): 369-74.
223. Paulsen HU, Thomsen JS, Hougen HP, Moskilde L (1999). A histomorphometric and scanning microscopy study of human condylar cartilage and bone tissue changes in relation to age. *Clin Orthod Res.* 2:67-78.
224. Perry MJ, Parry LK, Burton VJ, Gheduzzi S, Beresford JN, Humphrey VF, Skerry TM (2009). Ultrasound mimics the effect of mechanical loading on bone formation *in vivo* on rat ulnae. *Medical Engineering & Physics.* 31: 42–47
225. Piers Oliveria DAA, De Oliveria RF, Magini M, Zangaro RA, Soares CP (2009). Assesment of cytoskeleton and endoplasmic reticulum of fibroblast cells subjected to low-level laser therapy and low-intensity pulsed ultrasound. *Photomed Laser Surg.*27(3): 461-466.
226. Pilla AA, Figueiredo M, Nasser P, Alves JM, Ryaby JT, Klein M, Kaufman JJ, Siffert RS (1990). Non-invasive low-intensity pulsed ultrasound accelerates bone healing in the rabbit. *J Orthop Trauma.*4:246-53.
227. Pilla AA (2002). Low-intensity electromagnetic and mechanical modulation of bone growth and repair: are they equivalent? *J Orthop Sci.* 7:420-8.
228. Pirttiniemi P, Peltomäki T, Müller L and Luder HU (2009). Abnormal mandibular growth and the condylar cartilage. *European Journal of Orthodontics*; 31: 1-11.
229. Pounder NM and Harrison AJ (2008). *Low intensity pulsed ultrasound for fracture healing: A review of the clinical evidence and the associated biological mechanism of action Ultrasonics.* 48(4):330-8.

230. Proffit W, Fields H, Moray L (1998). Prevalence of malocclusion and orthodontic treatment need in the united states: estimates from the NHANES III survey. *Int J Adult Orthod Orthognath Surg.* 13:97-106.
231. Proffit WR (2013 a). *Concepts of growth and development in Proffit WR, Fiels H W, Sarver DMeditors, Contemporary Orthodontics. Fifth Ed.* Louis, MO: Mosby El-sevier Inc. p. 39-40.
232. Proffit WR (2013 b). *Later stages of development in Proffit WR, Fiels H W, Sarver DM,editors Contemporary Orthodontics. Fifth Ed.* Louis, MO: Mosby El-sevier Inc. p.97-98.
233. Proffit WR (2013 c) *Malocclusion and dentofacial deformity in contemporary society, in Proffit WR, Fiels H W, Sarver DM editors, Contemporary Orthodontics. Fifth Ed.* Louis, MO: Mosby El-sevier Inc. p.5-8
234. Pukayastha SK, Rabie ABM, Wong R (2008). Treatment of skeletal class II malocclusion in adults: stepwise vs single-step advancement with the Herbst appliance. *World J Orthod.* 9:233-243.
235. Purcell P, Joo BW, Hu JK, Tran PV, Calicchio ML, O'Connell DJ, Maas RL, Tabin CL (2009). temporomandibular joint formation requires two distinct hedgehog-dependent steps. *Proc Natl Acad Sci U S A.* 106:18297–18302.
236. Puricelli E, Ponzoni D, Munaretto JC, Corsetti A, Leite M.G.T (2012). Histomorphometric analysis of the temporal bone after change of direction of force vector of mandible: an experimental study in rabbits. *J Appl Oral Sci.* 20(5):526-30.
237. Rabie AB and Hagg U (2002a) . Factors regulating mandibular condylar growth. *Am J Orthod Dentofacial Orthop.* 122: 401-9.
238. Rabie AB, Chayanuptkul A, Hagg U (2003a). Stepwise advancement using fixed functional appliances: experimental perspectives. *Semin Orthod* 9:41-46.
239. Rabie AB, Dai J, Xu R (2007). Recombinant AAV-mediated VEGF gene therapy induces mandibular condylar growth. *Gene Ther.* 14:972-980.
240. Rabie AB, Leung FY, Chayanupatkul A, Hägg U (2002b). The correlation between neovascularization and bone formation in the condyle during forward mandibular positioning. *Angle Orthod.* 72:431-438.

241. Rabie AB, She TT, Hagg U (2003b). Functional appliance therapy accelerates and enhances condylar growth. *Am J Orthod Dentofacial Orthop.* 123:40-48.
242. Rabie AB, She TT, Harley VR (2003c). Forward mandibular positioning up-regulates SOX9 and type II collagen expression in the glenoid fossa. *J Dent Res.* 82:725-730.
243. Rabie AB, Tang GH, Hagg U (2004a). Cbfa1 couples chondrocytes maturation and endochondral ossification in rat mandibular condylar cartilage. *Arch Oral Biol.* 49:109-118.
244. Rabie AB, Tang GH, Xiong H (2003d). PTHrP regulates chondrocyte maturation in condylar cartilage. *J Dent Res.* 82:627-631.
245. Rabie AB, Wong L, Tsai M (2003e). Replicating mesenchymal cells in the condyle and the glenoid fossa during mandibular forward positioning. *Am J Orthod Dentofacial Orthop.* 123:49-57.
246. Rabie AB, Xiong H, Hagg U (2004b). Forward mandibular positioning enhances condylar adaptation in adult rats. *Eur J Orthod.* 26: 353-358.
247. Rabie AB, Zhao Z, Shen G, Hagg E U, Robinson W (2001). Osteogenesis in the glenoid fossa in response to mandibular advancement. *Am J Orthod Dentofacial Orthop.* 119: 390-400.
248. Ramfjord SP, Blankenship JR (1981). Increased occlusal vertical dimension in adult monkeys. *J Prosthet Dent.* 45:74-83.
249. Ramfjord SP, Enlow RD (1971). Anterior displacement of the mandible in adult rhesus monkeys: long-term observations. *J Prosthet Dent.* 26:517-31.
250. Ramfjord SP, Walden JM, Enlow RD (1971). Unilateral function and the temporomandibular joint in rhesus monkeys. *Oral Surg.* 32:236-47.
251. Randerath W.J., Verbraecken J, Andreas S, Bettega G, Boudewyns A et al (2011). Non-CPAP therapies in obstructive sleep apnoea. *Eur Respir J.* 37: 1000-1028.
252. Rawool NM, Goldberg BB, Forsberg F, Winder AA, Hume E (2003). Power Doppler assessment of vascular changes during fracture treatment with low-intensity ultrasound. *J Ultrasound Med.* 22:145-53.

253. Reher P, Doan N, Bradnock B, et al (1999). Effect of ultrasound on the production of IL-8, basic FGF and VEGF. *Cytokines*. 11:416-23.
254. Renders GAP, Mulder L, van Ruijven LJ and van Eijden TMGJ (2007). Porosity of human mandibular condylar bone. *J Anat*. 210: 239–248
255. Reynolds M, Reynolds M, Adeeb S, El-Bialy T (2011). 3-D Volumetric Evaluation of Human Mandibular growth. *Open Biomed Eng J*. 5: 83-89.
256. Riveline D, Zamir E, Balaban NQ, Schwarz US, Ishizaki T, Narumiya S, Kam Z, Geiger B, Bershadsky AD (2001). Focal contacts as mechanosensors: externally applied local mechanical force induces growth of focal contacts by an mDia1- dependent and ROCK-independent mechanism, *J Cell Biol*. 153: 1175–1180.
257. Rubin C, Turner AS, Mallinckrodt C, Jerome C, McLeod K, Bian S (2002). Mechanical strain, induced noninvasively in the high-frequency domain, is anabolic to cancellous bone, but not cortical bone. *Bone*. 30:445-52.
258. Rubin CT, Lanyon LE (1984). Regulation of bone formation by applied dynamic loads. *J Bone Jt Surg Am*. 66:397-402.
259. Rubin CT, Lanyon LE (1985). Regulation of bone mass by mechanical strain magnitude. *Calcif Tissue Int*. 37:411-7.
260. Ruf S and Pancherz H (2006). Herbst/multibracket appliance treatment of Class II, Division 1 malocclusions in early and late adulthood. A prospective cephalometric study of consecutively treated subjects. *Eur J Orthod*. 28:352-360.
261. Ruf S. and Pancherz H (1999a). Dentoskeletal effects and facial profile changes in young adults treated with the Herbst appliance. *Angle Orthod*. 69:239-246.
262. Ruf S. and Pancherz H (2004). Orthognathic surgery and dentofacial orthopedics in adult Class II, Division 1 treatment: mandibular sagittal split osteotomy versus Herbst appliance. *Am J Orthod Dntofac Orthop*. 126:140-152.
263. Ruf S. and Pancherz H (1999b). Temporomandibular joint remodeling in adolescents and young adults during Herbst treatment: a prospective longitudinal magnetic resonance imaging and cephalometric radiographic investigation. *Am J Orthod Dentofac Orthop*. 115:607-18.

264. Rutten S, Nolte PA, Korstjens C M, Duin MA, Klein-Nulend J (2008). Low-intensity pulsed ultrasound increases bone volume, osteoid thickness and mineral apposition rate in the area of fracture healing in patients with a delayed union of the osteotomized fibula. *Bone*. 43:348-354.
265. Ryaby JT , Matthew J, Duarte-Alves P (1989). Low intensity pulsed ultrasound increases calcium incorporation in both differentiating cartilage and bone cell cultures. *Trans Orthop Res Soc*. 14:15.
266. Saito M., Soshi S, Tanaka T, Fujii K (2004). Intensity-related differences in collagen post-translational modification in MC3T3-E1 osteoblasts after exposure to low- and high-intensity pulsed ultrasound. *Bone*. 35:644-55.
267. Sant'Anna EF, Leven RM, Viridi AS, Sumner DR (2005). Effect of low intensity pulsed ultrasound and BMP-2 on rat bone marrow stromal cell gene expression, *J Orthop Res*. 23:646–652
268. Santana LA, Alves JA, Andrade TAM, Kajiwara JK, Garcia SB, Gomes FG, Frade MAC (2013). Clinical and immunohistopathological aspects of venous ulcers treatment by low-intensity pulsed ultrasound (LIPUS). *Ultrasonics*. 53: 870-879.
269. Sato H, Fujii T, Uetani M, Kitamori H (1997). Anterior mandibular repositioning in a patient with temporomandibular disorders: a clinical and tomographic follow-up case report. *J Craniomand Pract*. 15:84-8.
270. Sawai Y, Murata H, Koto K, Matsui T, Horie N, Ashihara E, Maekawa T, Fushiki S, Kubo T(2012 Aug). Effects of low-intensity pulsed ultrasound on osteosarcoma and cancer cells. *Oncol Rep*. 28(2):481-6
271. Schlaepfer DD, Hunter T(1998). Integrin signalling and tyrosine phosphorylation: just the FAKs? *Trends Cell Biol*. 8: 151–157.
272. Schumann D, Kujat R, Zellner J, Angele MK, Nerich M, Mayr E, Angele P(2006). Treatment of human mesenchymal stem cells with pulsed low intensity ultrasound enhances the chondrogenic phenotype in vitro. *Biorheology*. 43(3-4):431-43.
273. Seehra J, Fleming PS, Newton T, DiBiase AT (2011). Bullying in orthodontic patients and its relationship to malocclusion, self-esteem and oral health-related quality of life. *J Orthod*. Dec;38(4):247-56; quiz 294.

274. Seifi M, Maghzi A, Gutknecht N, Mir M and Asna-Ashari M (2010). The effect of 904 nm low level laser on condylar growth in rats. *Lasers Med Sci.* 25:61–65.
275. Sena K, Angle SR, Kanaji A, Aher C, Karwo DG, Sumner DR, Viridi AS (2011). Low-intensity pulsed ultrasound (LIPUS) and cell-to-cell communication in bone marrow stromal cells. *Ultrasonics.* 51: 639–644.
276. Serrano MJ, So S, Hinton RJ (2014). Roles of Notch signaling in mandibular condylar cartilage. *Arch Oral Biol.* 59(7):735-40.
277. Serrano MJ, So S, Svoboda KK, Hinton RJ (2011). Cell fate mediators Notch and Twist in mouse mandibular condylar cartilage. *Arch Oral Biol.* 56: 607-613.
278. Shakouri K, Eftekharsadat B, Oskuie MR et al (2010). Effect of low-intensity pulsed ultrasound on fracture callous mineral density and flexural strength in rabbit tibial fresh fracture. *J Orthop Sci.* 15:240-4.
279. Shen G, Rabie B, Hägg U (2003). Neovascularization in the TMJ in response to mandibular protrusion. *Chin J Dent Res.* 6:28-38.
280. Shen G. and Darendeliler MA (2006). Cephalometric evaluation of condylar and mandibular growth modification: a review. *Orthod Craniofac Res.* 9:2-9.
281. Shen G. and Darendeliler A (2005). The adaptive remodeling of condylar cartilage- A transition from chondrogenesis to osteogenesis. *J Dent Res.* 84(8):691-699.
282. Shen G, Zhao Z, Kaluarachchi K, Bakr Rabi A (2006). Expression of type X collagen and capillary endothelium in condylar cartilage during osteogenic transition-a comparison between adaptive remodeling and natural growth. *Eur J Orthod.* 28:210-216.
283. Shibata S, Fukada K, Suzuki S, Ogawa T, Yamashita Y (2002). In situ hybridization and immunohistochemistry of bone sialoprotein 1 (osteopontin) in the developing mouse mandibular condylar cartilage compared with limb bud cartilage. *J Anat.* 309-320.
284. Shibata S, Fukada K, Suzuki S, Yamashita Y (1997). Immunohistochemistry of collagen types II and X, and enzyme-histochemistry of alkaline phosphatase in the developing condylar cartilage of the fetal mouse mandible. *J Anat.* 191:561-570.

285. Shibata S, Suda N, Suzuki S, Fukoka H, Yamashita Y (2006). An in situ hybridization study of Runx2, Osterix, and Sox9 at the onset of condylar cartilage formation in fetal mouse mandible. *J Anat.* 208:169–177.
286. Shibata S, Yokohama-Tamaki T(2008). An in situ hybridization study of Runx2, Osterix, and Sox9 in the anlagen of mouse mandibular condylar cartilage in the early stages of embryogenesis. *J Anat.* 213:274-83.
287. Shibukawa Y, Young B, Wu C, Yamada S, Long F, Pacifici M, Koyama E (2007). Temporomandibular joint formation and condyle growth require Indian hedgehog signaling. *Dev Dyn.* 236: 426–434.
288. Shirashi R, Masai C, Toshinaga A, Okinaga T, Nishihara T, Yamanaka N, Nakamoto T, Hosokawa R (2011 October). *J Periodontol.* 62(10): 1496-503.
289. Sood S (2010). Treatment of class II division 1 malocclusion in a non growing patient. A case report with review of literature. *Virtual Journal of Orthodontics [Serial Online]*.
290. Spadaro JA, Albanese SA (1998). Application of low-intensity pulsed ultrasound to growing bone in rats. *Ultrasound Med Biol.* 24:567-73.
291. Speed CA (2001).Therapeutic ultrasound in soft tissue lesions. *Rheumatology (Oxford)*, 40:1331-1336.
292. Sperber GH, Sperber SM, Guttman GD (2010). *Mandible in Craniofacial Embryogenetics and Development*. Second edition. People’s Medical Publishing house, USA, Shelton, Connecticut, Section II, Chapter 12, P:15.
293. St-John Brown B (1984). How safe is diagnostic ultrasonography? *Can Md Assoc J* 131:307-311.
294. Suda N, Shibata S, Yamazaki K, Kuroda T, Senior PV, Beck F, et al (1999). Parathyroid hormone-related protein regulates proliferation of condylar hypertrophic chondrocytes. *J Bone Miner Res.* 14:1838-41.
295. Sun JS, Hong RC, Chang W H-S, Chen LT, Lin FH, Liu HC (2001). In vitro effects of low-intensity ultrasound stimulation on the bone cells. *J Biomed Mater Res.* 57: 449-456.

296. Suzuki A, Takayama T, Suzuki N, Kojima T, Ota N, Asano Sh and Ito K (2009). Daily low intensity pulsed ultrasound stimulates production of bone Morphogenic protein in ROS 17/2.8 cells. *J Oral Sci.* 51: 29-36.
297. Suzuki S, Itoh K, and Ohayama K (2004). Local administration of IGF-I stimulates the growth of mandibular condyle in mature rats. *J Orthod.* 31: 138-143.
298. Tabuchi Y, Sugahara Y, Ikegame M, Suzuki N, Kitamura K, Kondo T (2013). Genes responsive to low-intensity pulsed ultrasound in MC3T3-E1 preosteoblast cells. *Int J Mol Sci.* 14: 22721-22740.
299. Tabuchi Y, Takasaki I, Zhao QL, Wada S, Hori T, Feril LB Jr, Tachibana K, Nomura T, Kondo T (2008). Genetic networks responsive to low-intensity pulsed ultrasound in human lymphoma U937 cells. *Cancer Lett.* 270, 286–294.
300. Tagliaro ML, De Oliveria RM, Pereira Padilha DM, Callegari Jacques SM, Jeckel-Neto EA (2009). Morphological changes in the mandible of male mice associated with aging and biomechanical stimulus. *Anat Rec.* 292:431-438.
301. Tagliaro ML, Rassi Guimaraes ML, Pereira Padilha DM, Callegari Jacques SM, Jeckel-Neto EA (2006). Mandibular advancement and morphological changes in the mandibles of female mice of different ages. *Exp Gerontol.* 41:1157-1164.
302. Taira K, Iino Sh, Kubota T, Fukunaga T, Miyawaki Sh (2009). Effects of mandibular advancement plus prohibition of lower incisor movement on mandibular growth in rats. *Angle Orthod.* 79: 1095–1101.
303. Tajima Y, Kawasaki M, Kurihara K, Ueha T, Yokose S (1998). Immunohistochemical profile of basic fibroblast growth factor and heparan sulphate in adult rat mandibular condylar cartilage. *Arch Oral Biol.* 43:873–877.
304. Takahashi I, Mizoguchi I, Sasano Y, Saitoh S, Ishida M, Kagayama M et al (1996). Age-related changes in the localization of glycosaminoglycans in condylar cartilage of the mandible in rats. *Anat Embryol.* 194:489-500.
305. Takayama T, Suzuki N, Ikeda K, Shimada T, Suzuki A, Maeno M, Ostuka K, Ito K (2007). Low-intensity pulsed ultrasound stimulates osteogenic differentiation in ROS 17/2.8 cells. *Life Sci.* 80: 965-971.

306. Takeuchi R, Ryo A, Komitsu N, Mikuni-Takagaki Y, Fukui A, Takagi Y, Shiraishi T, Morishita S, Yamazaki Y, Kumagai K et al (2008). Low-intensity pulsed ultrasound activates the phosphatidylinositol 3 kinase/Akt pathway and stimulates the growth of chondrocytes in three-dimensional cultures: a basic science study. *Arthritis Res Ther.* 10, R77.
307. Tang CH, Lu DY, Tan TW, Fu WM, Yang RS (2007). Ultrasound induces hypoxia-inducible factor-1 activation and inducible nitric-oxide synthase expression through the integrin/ integrin-linked kinase/Akt/ mammalian target of rapamycin pathway in osteoblasts. *J Biol Chem.* 282:25406-15.
308. Tang CH, Yang RS, Huang TH, Lu DY, Chuang WJ et al (2006). Ultrasound stimulates cyclooxygenase-2 expression and increases bone formation through integrin, focal adhesion kinase, phosphatidylinositol 3-kinase, and Akt pathway in osteoblasts. *Mol Pharmacol.* 69:2047-2057.
309. Tang GH, Rabie AB (2005). Runx2 regulates endochondral ossification in condyle during mandibular advancement. *J Dent Res.* 84:166–71.
310. Tanzer M, Harvey E, Kay A, Morton P (1996). Effect of non invasive low intensity ultrasound on bone growth into porous-coated implants. *J Orthop Res.* 14: 901-906.
311. Teo JCM, Si-Heo KM, Keh JEL, Teoh SH (2006). Relationship between CT intensity, microarchitecture and mechanical properties of porcine vertebral cancellous bone. *Clin Biomech.* 21:235-244.
312. Testori T, Wallance SS, Trisi P, Capelli M, Zuffetti F, Del Febbro M (2013). Effect of Xenograft (ABBM) particle size on vital bone formation following maxillary sinus augmentation: a multicentre, randomized, controlled, clinical histomorphometric trial, *Int J Periodontics Restorative dent.* 33(4):467-75
313. Tien YC, Lin SD, Chen CH, Lu CC, Su SJ, Chih TT (2008). Effects of pulsed low-intensity ultrasound on human child chondrocytes. *Ultrasound Med Biol.* 34: 1174-1181.
314. Tsumaki N, Kakiuchi M, Sasaki J, Ochi T, Yoshikawa H (2004 Nov). Low intensity pulsed ultrasound accelerates maturation of callus in patients treated with

- opening-wedge high tibial osteotomy by hemicallotaxis. *J Bone Joint Surg Am.* 86-A (11): 2399-405.
315. Tucker MR and Farrell BB (2014). *Correction of Dentofacial Deformities.* In Hupp JR, Ellis III E, Tucker M.R. Contemporary Oral and Maxillofacial Surgery. Sixth Ed. St. Louis, MO: Mosby El-sevier Inc. p. 520-563.
316. Uddin SM, Qin YX (2013 Sep 12). Enhancement of osteogenic differentiation and proliferation in human mesenchymal stem cells by a modified low intensity ultrasound stimulation under simulated microgravity. *PLoS One.* 8(9):e73914.
317. Uenaka K, Imai S, Ando K, and Matsusue Y (2010). Relation of low-intensity pulsed ultrasound to the cell density of scaffold-free cartilage in a high-density static semi-open culture system. *J Orthop Sci.* 15:816-824.
318. Vanarsdall RL, Musich DR (2005). *Adult Interdisciplinary Therapy, Diagnosis and Treatment.* In: Graber T, Vanarsdall R, Vig K. Orthodontics: Current principles and techniques. 4<sup>th</sup> ed. Philadelphia, PA: Elsevier; 8:937-992.
319. Vinkka H (1982). Secondary cartilages in the facial skeleton of the rat. *Proc Finn Dent Soc.* 78(suppl 7): 1-137.
320. Visnapuu V (2001). Growth hormone and insulin-like growth factor I receptors in the Temporo mandibular joint of the rat. *J Dent Res.* 80:1903-7.
321. Von den Hoff JW and Delatte M (2008). Interplay of mechanical loading and growth factors in the mandibular condyle. *Arch Oral Biol.* 53:709 – 715.
322. Voudouris JC and Kufninec MM (2000). Improved clinical use of twin-block and herbst as a result of radiating viscoelastic tissue forces on the condyle and fossa in treatment and long-term relation: growth relativity. *Am J Orthod Dentofacial Orthop* 117:247-66.
323. Walsh WR, Langdown AJ, Auld JW, Stephens P, Yu Y, Vizesi F, Bruce WJM, Pounder N (2008). Effect of low intensity pulsed ultrasound on healing of an ulna defect filled with a bone graft substitute. *J Biomed Mater Res Part B:Appl Biomater.* 86b:74-81.
324. Wana Q, Li Z-B (2010). Intra-articular injection of parathyroid hormone in the temporomandibular joint as a novel therapy for mandibular asymmetry. *Medical Hypotheses.* 74: 685–687.

325. Wang L and Detamore MS (2007). Tissue engineering the mandibular condyle. *Tissue Eng.* 13:1955-1971.
326. Wang SJ, Lewallen DG, Bolander ME, Chao EY, Ilstrup DM, Greenleaf JF (1994). Low intensity ultrasound treatment increases strength in a rat femoral fracture model. *J Orthop Res.* 12:40-7.
327. Wang W, Wang YG, Reginato AM, Glotzer DJ, Fukai N, Plotkina S et al (2004). Groucho homologue Grg5 interacts with the transcription factor Runx2-Cbfa1 and modulates its activity during postnatal growth in mice. *Dev Biol.* 270:364-381.
328. Warden SJ, Bennel KL, Forwood MR, McLeen JM, Wark JD (2001a). Efficacy of low-intensity pulsed ultrasound in the prevention of osteoporosis following spinal cord injury. *Bone.* 29:431-6.
329. Warden SJ, Bennel KL, Forwood MR, McLeen JM, Wark JD (2001b). Skeletal effects of low-intensity pulsed ultrasound on the ovariectomized rodent. *Ultrasound Med Biol.* 27:989-98.
330. Warden SJ, Favaloro JM, Bennell KM, McMeeken JM, Ng Kong-Wah, Zajac JD, and Wark JD (2001c). Low-Intensity pulsed ultrasound stimulates a bone-forming response in UMR-106 cells. *Biochemical and Biophysical research communications.* 286: 443-450.
331. Warden SJ, Fuchs RK, Kessler CK, Avin KG, Cardinal RE, Stewart RL (2006). Ultrasound produced by a conventional therapeutic ultrasound unit accelerates fracture repair. *Phys Ther.* 86:1118-27.
332. Watabe H, Furuhashi T, Tani-Ishii N, Mikuni-Takagaki Y (2011 Nov 1). Mechanotransduction activates  $\alpha_5\beta_1$  integrin and PI3K/Akt signaling pathways in mandibular osteoblasts. *Exp Cell Res.* 317(18):2642-9.
333. Webster DF, Havery W, Dyson M, Pond JB (1980). The role of cavitation in the 'in vitro' stimulation of collagen synthesis in fibroblasts. *Ultrasonics.* 18:33-37.
334. Webster DF, Pond JB, Dyson M et al (1978). The role of cavitation in the in vitro stimulation of protein synthesis in human fibroblasts by ultrasound, *Ultrasound Med Biol.* 4: 343-351.

335. Weijs WA (1976). Morphology of the muscles of mastication in the albino rat, *Rattus norvegicus*. *Acta Morphol Neerl-Scand*. 11: 321-340.
336. Welgus HG, Jeffrey JJ, Eisen AZ (1981). Human skin fibroblast collagenase. Assessment of activation energy and deuterium isotope effect with collagenous substrates. *J Biol Chem*. 256:9516-9521.
337. Wells PNT(1985). *Surgical applications of ultrasound*. In: Nyborg WL, Zisin MC, editors. Biological effects of ultrasound. New York: Churchill livingstone; P 157-167.
338. Westesson PL, Lundh H (1988). Temporomandibular joint disk displacement: arthrographic and tomographic follow-up after 6 months treatment with disk-repositioning onlays. *Oral Surg Oral Med Oral Pathol* 66:271-8.
339. Whitney NP, Lamb AC, Louw TM, Subramanian A (2012). Integrin-mediated mechanotransduction pathway of low-intensity continuous ultrasound in human chondrocytes. *Ultrasound Med Biol*. 38(10):1734-43.
340. Witlink A, Nijweide PJ, Oosterbaan WA, et al (1995). Effect of therapeutic ultrasound on endochondral ossification. *Ultrasound Med Biol*. 21:121-127.
341. Woodside DG, Altuna G, Harvold E, Herbert M, Metaxas A (1983). Primate experiments in malocclusion and bone induction. *Am J Orthod*. 83:460-8.
342. Woodside DG, Metaxas A, Altuna G (1987). The influence of functional appliance therapy on glenoid fossa remodeling. *Am J Orthod Dentofacial Orthop*. 92:98-108.
343. Wu CC, Lewallen DG, Bolander ME, et al (1996). Exposure to low intensity ultrasound stimulates proteoglycan synthesis in rat chondrocytes by increasing aggrecan gene expression. *Trans Orthop Res Soc*. 21:622.
344. Wu S, Fadoju D, Rezvani G, De Luca F (2008). Stimulatory effects of insulin-like growth factor-1 on growth plate chondrogenesis are mediated by nuclear factor-kappa B P65. *J Biol Chem*. 283:34037-44.
345. Xavier CAM, Duarte LR (1983). Stimulation of bone callus by ultrasound. *Clinical Rev Brasileira Orthop* 18:73-80.

346. Xiong H, Hagg U, Tang GH, Rabie AB, Robinson W (2004). The effect of continuous bite-jumping in adult rats: a morphological study. *Angle Orthod* 74:86-92.
347. Xiong H, Rabie AB, Hagg U (2005a). Mechanical strain leads to condylar growth in adult rats. *Front Biosci* 10:67-73.
348. Xiong H, Rabie AB, Hagg U (2005b). Neovascularization and mandibular condylar bone remodeling in adult rats under mechanical strain. *Front Biosci* 10:74-82.
349. Xue H, Zheng J, Cui Z, Bai X, Li G, Zhang C, He S, Li W, Lajud SA, Duan Y, Zhou H (2013). Low-intensity pulsed ultrasound accelerates tooth movement via activation of the BMP-2 signaling pathway. *Plos ONE* 8(7): e68926.
350. Yang KH, Park S (2001). Stimulation of fracture healing in a canine ulna full-defect model by low-intensity pulsed ultrasound. *Yonesi Med J (Korea)* 42:503-508.
351. Yang KH, Parvizi J, Wang SJ, Lewallen DG, Kinnick RR, Greenleaf JF, Bolander ME (1996). Exposure to low-intensity ultrasound increases aggrecan gene expression in a rat femur fracture model. *J Orthop Res* 14:802-9.
352. Yang KH, Wang SJ, Lewallen DG, Greenleaf J, Oles K, Bronk J, Bolander ME (1994). Low intensity ultrasound stimulates fracture healing in rat model: biomechanical and gene expression analysis. *Trans Orthop Res Soc.* 19:519.
353. Yang RS, Lin WL, Chen YZ, Tang CH, Huang TH et al (2005). Regulation by ultrasound treatment on the integrin expression and differentiation of osteoblasts. *Bone* 36:276-283.
354. Yang SW, Kuo CL, Chang SJ, Chen PC, Lin PC, Lin YT, Manouskas L, and Kuo SM (2014). Does low-intensity pulsed ultrasound treatment repair articular cartilage injury? A rabbit model study. *Musculoskeletal Disorders.* 15:36.
355. Yang Y, Topol L, Lee H, Wu J (2003). Wnt5a and Wnt5b exhibit distinct activities in coordinating chondrocyte proliferation and differentiation. *Development.* 130:1003-15.
356. Yasuda T, Mundy C, Kinumatsu T, Shibukawa Y, Shibutani T, Grobe K, Minugh-Purvis N, Pacific M, Koyama E (2010). Sulfotransferase Ndst1 is needed for mandibular and TMJ development. *J Dent Res.* 89:1111-1116.

357. Yuan LJ, Niu CC, Lin SS, Yang CY, Chan YS, Chen WJ and Ueng SWN (2014). Effects of low-intensity pulsed ultrasound and hyperbaric oxygen on human osteoarthritic chondrocytes. *J Orthop Surg Res.* 9:5.
358. Yue Y, Yang X, Wei X, Chen J, Fu N, Fu Y, Ba K, Li G, Yao Y, Liang C, Zhang J, Cai X, and Wang M (2013). Osteogenic differentiation of adipose-derived stem cells prompted by low-intensity pulsed ultrasound. *Cell Prolif.* 46: 320-327.
359. Zhang X, Hu Z, Hao J, Shen J (2013 Jan). Low-intensity pulsed ultrasound stimulates the extracellular matrix synthesis of human degenerative nucleus pulposus cells via PI3K/Akt pathway. *Xi Bao Yu Fen Zi Mian Yi Xue Za Zhi.* 29(1):34-8.
360. Zhang ZJ, Huckle J, Francomano CA, Spencer RG (2003). The effects of pulsed low-intensity ultrasound on chondrocyte viability, proliferation, gene expression and matrix production. *Ultrasound Med Biol* 29: 1645-1651.
361. Zhang ZJ, Huckle J, Francomano CA, Spencer RG (2002). The influence of pulsed low intensity ultrasound on matrix production of chondrocytes at different stages of differentiation: an explant study. *Ultrasound Med Biol.* 28:1547-1553.
362. Zhou S, Schmelz A, Seufferlein T, Li Y, Zhao J, Bachem MG (2004). Molecular mechanisms of low intensity pulsed ultrasound in human skin fibroblasts. *J Biol Chem.* 279: 54463–54469.
363. Ziskin MC (1987). *Applications of ultrasound in medicine-comparison with other modalities.* In: Repacholi, MH, Grandolfo M, Rindi A, editors. *Ultrasound: medical applications, biological effects, and hazard potential.* New York: Plenum; P 49-59.

## APPENDIX 1

The size of method error (ME) based on Dahlberg's formula and degree of absolute agreement (single measure values (r)) for intra rater reliability based on ICC test for linear and angular 2-dimensional measurements:

Linear & angular measurements	ME	r
i	0.013	1
ii	0.014	0.997
iiia	0.018	0.989
iii	0.023	0.995
iv	0.028	0.996
v	0.021	0.99
vi	0.023	0.989
vii	0.022	0.996
viii	0.016	0.993
iiia	0.007	1
ix	0.032	0.995
x	0.005	0.999
xi	0.007	0.999
xia	0.007	0.998
xii	0.015	0.998
$\alpha$	0.28	0.989
w	0.021	0.957